Tauopathy in the *APP*$_{swe}$/*PS1*$_{\Delta E9}$ mouse model of familial Alzheimer's disease

Athanasios Metaxas[1*], Camilla Thygesen[1,2†], Stefan J. Kempf[2], Marco Anzalone[1], Ramanan Vaitheeswaran[1], Sussanne Petersen[1], Anne M. Landau[3,4], Hélène Audrain[3], Jessica L. Teeling[5], Sultan Darvesh[6,7], David J. Brooks[3,8], Martin R. Larsen[2], Bente Finsen[1]

Affiliations:

[1]Institute of Molecular Medicine, University of Southern Denmark, Odense C, Denmark.

[2]Department of Biochemistry and Molecular Biology, University of Southern Denmark, Odense M, Denmark.

[3]Department of Nuclear Medicine and PET Centre, Aarhus University and Hospital, Denmark.

[4]Translational Neuropsychiatry Unit, Aarhus University and Hospital, Denmark.

[5]Biological Sciences, University of Southampton, United Kingdom.

[6]Department of Medical Neuroscience, Dalhousie University, Halifax, NS, Canada.

[7]Department of Medicine (Neurology and Geriatric Medicine), Dalhousie University, Halifax, NS, Canada.

[8]Division of Neuroscience, Department of Medicine, Newcastle University, United Kingdom.

[†]Shared first authorship

*To whom correspondence should be addressed:
ametaxas@health.sdu.dk; a.metaxas@hotmail.com

One Sentence Summary: Neurofibrillary tangles in amyloidosis mice

Abstract

Despite compelling evidence that the accumulation of amyloid-beta (Aβ) promotes cortical MAPT (tau) aggregation in familial and idiopathic Alzheimer's disease (AD), murine models of cerebral amyloidosis are not considered to develop tau-associated pathology. The absence of neurofibrillary lesions in amyloidosis mice remains a challenge for the amyloidocentric paradigm of AD pathogenesis. It has resulted in the generation of transgenic mice harboring mutations in their *tau* gene, which may be inappropriate for studying a disease with no known *TAU* mutations, such as AD. Here, we have used $APP_{swe}/PS1_{\Delta E9}$ mice to show that tau pathology can develop spontaneously in murine models of familial AD. Tauopathy was abundant around Aβ deposits, with Gallyas- and thioflavin-S-positive perinuclear inclusions accumulating in the $APP_{swe}/PS1_{\Delta E9}$ cortex by 18 months of age. Age-dependent increases in Gallyas signal correlated positively with binding levels of the paired helical filament (PHF) ligand [^{18}F]Flortaucipir, in all brain areas examined. Sarkosyl-insoluble PHFs were visualized by electron microscopy. Tandem mass tag proteomics identified sequences of hyperphosphorylated tau in transgenic mice, along with signs of RNA missplicing, ribosomal dysregulation and disturbed energy metabolism. Human frontal gyrus tissue was used to validate these findings, revealing primarily quantitative differences between the tauopathy observed in AD patient vs. transgenic mouse tissue. Levels of *tau* mRNA were not different between $APP_{swe}/PS1_{\Delta E9}$ and littermate control animals. As physiological levels of endogenous, 'wild-type' tau aggregate secondarily to Aβ in transgenic mice, this study demonstrates that amyloidosis is both necessary and sufficient to drive tauopathy in experimental models of familial AD.

Introduction

Genetically-inherited and sporadic forms of Alzheimer's disease (AD) are characterized by a common set of hallmark brain lesions, which include the accumulation of amyloid-β (Aβ) peptides into plaques, neuroinflammation, aggregation of hyperphosphorylated MAPT (tau) into neurofibrillary tangles (NFTs), and neurodegeneration. Transgenic mouse models that reproduce aspects of the aforementioned lesions have been generated based on mutations in the amyloid precursor protein (*APP*) and presenilin 1 (*PSEN1*) and 2 (*PSEN2*) genes, which are known to cause familial AD (*1*). Despite playing important roles in evaluating APP processing, Aβ toxicity, and amyloid-targeting therapeutic strategies, transgenic mice are not being regarded as models that can replicate the full spectrum of AD histopathology (*2*). In particular, while the overexpression of mutant *APP* and *APP*/*PSEN1* has been shown to yield amyloidosis (*3*), neuroinflammation (*4*) and neurodegeneration (*5*) in mice, it is generally not considered to promote the conversion of endogenous tau into neurofibrillary structures (*6*).

To address the *in vivo* role of tau hyperphosphorylation and NFT formation in AD pathogenesis, human *MAPT* (*TAU*) has been introduced into the mouse genome, either mutated or non-mutated, on a *Tau*-knockout background (*7, 8*). *TAU* overexpressing mice demonstrate progressive neurofibrillary pathology, albeit in the marked absence of cerebral amyloidosis, which is required for a neuropathological diagnosis of AD. Moreover, mutations in *TAU* have been linked to non-AD tauopathies, most commonly frontotemporal lobar degeneration [FTLD; (*9*)], a condition with neuropathological hallmarks distinct from AD. Thus, murine models of amyloidosis and combined amyloidosis-tauopathy models have been widely criticized for their translational relevance to the human condition. It has been argued that virtually all existing

murine models would be considered as 'not' AD (*10*) according to the ABC scoring system of neuropathology (*11*). The inability of amyloidosis mice to develop neurofibrillary lesions is thought to contribute to the poor translation of preclinical research into clinical benefits (*12*), and has raised concern about the amyloidocentric model of AD pathogenesis (*13*).

Two principal explanations have been put forward for the lack of tau-associated pathology in amyloidosis mice (*14*). First, adult mice express fewer isoforms of the tau protein than humans (three vs. six), which might render them less liable to the post-translational modifications (PTMs) that are associated with the accumulation of tau into NFTs, such as phosphorylation (*15*). However, murine tau has been shown to readily fibrillize *in vitro* upon treatment with polyanionic factors, including RNA (*16*), and there is ample evidence of tau hyperphosphorylation in the transgenic mouse brain [(*17*), Table S1], indicating that no differences exist in the propensity of murine and human tau for aggregation and PTMs. A second reason that is often cited for the absence of tauopathy in amyloidosis models is that the murine lifespan may be too short for the complete sequence of neurofibrillary pathology to unfold in transgenic mice. Although age scaling studies suggest otherwise (*18*), the aging factor has been neglected in the design of preclinical studies.

Transgenic Fischer rats (TgF344-AD), expressing human *APP* harboring the Swedish double mutations (KM670/671NL) and *PSEN1* lacking exon 9 ($APP_{swe}/PS1_{\Delta E9}$), both under control of the mouse prion protein promoter, develop progressive neurofibrillary pathology (*19*). In this study, transgenic $APP_{swe}/PS1_{\Delta E9}$ mice that were constructed in an identical manner as TgF344-AD rats were used to demonstrate neurofibrillary pathology in aging amyloidosis mice.

Results

Neurofibrillary pathology in aging $APP_{swe}/PS1_{\Delta E9}$ mice

Fresh-frozen brain sections from 3-, 6-, 12-, 18- and 24-month-old $APP_{swe}/PS1_{\Delta E9}$ transgenic (TG) mice and their wild-type (WT) counterparts were processed for the detection of neurofibrillary alterations with the Gallyas silver stain (n=6/group). Thioflavin-S and DAPI (4',6-diamidino-2-phenylindole) were used to detect perinuclear β-pleated structures. Co-staining for amyloid and Gallyas was used to probe the relationship between amyloidosis and tau-associated pathology in aging TG animals. Fresh-frozen sections of the middle frontal gyrus from a patient with definite AD were processed in parallel with sections from $APP_{swe}/PS1_{\Delta E9}$ mice, to compare Gallyas-positive structures in mouse vs. human tissue.

Aβ deposition was the predominant lesion in the 6-month-old $APP_{swe}/PS1_{\Delta E9}$ brain (Fig. 1A&B), with age-dependent increases in argyrophilic density observed exclusively in TG mice (Fig. 1C-F). Only mild and diffuse silver staining was observed in the neocortex of 6-month-old animals (Fig. 1G). Densely-labeled, round structures, surrounded by a halo of argyrophilic staining, constituted the majority of Gallyas-positive signal in the neuropil of the neocortex and hippocampus at 12-24 months of age (Fig. 1H&I). In addition, diffuse and compact argyrophilic staining was observed surrounding red-stained nuclei in the neocortex of 18- and 24-month-old $APP_{swe}/PS1_{\Delta E9}$ mice (Fig. 1J&K). The perinuclear structures were positive for thioflavin-S (Fig. 1L-N), which colocalized with nuclear DAPI (Fig. 1O) and was further detected in cell-sized structures lacking a stainable nucleus (Fig. 1P). There were no apparent differences in morphology between the argyrophilic structures in brain tissue from 24-month-old TG mice (Fig 1Q-U) and AD-confirmed patient material (Fig. 1V-Z), although neuropil threads were detected

exclusively in AD tissue (Fig. 1Q-Z). Coronal brain sections of 20-month-old Tg2576 mice, harboring the Swedish double mutations, were used to examine 6E10- and Gallyas-positive pathology in a second mouse model of amyloidosis (Fig. 1AA-AD). Amorphous argyrophilic signal (AC) and perinuclear lesions (AD) were also present in the Tg2576 mouse brain, albeit at lower levels compared to 18-month-old *APP*$_{swe}$/*PS1*$_{\Delta E9}$ mice.

The fraction of brain tissue occupied by Gallyas-positive staining in aging *APP*$_{swe}$/*PS1*$_{\Delta E9}$ mice is shown in Fig. S1A. Conformationally-altered tau was detected with the MC-1 monoclonal antibody (Fig. S1B). Vascular and meningeal lesions were present in 18- and 24-month-old animals (Fig. S1C).

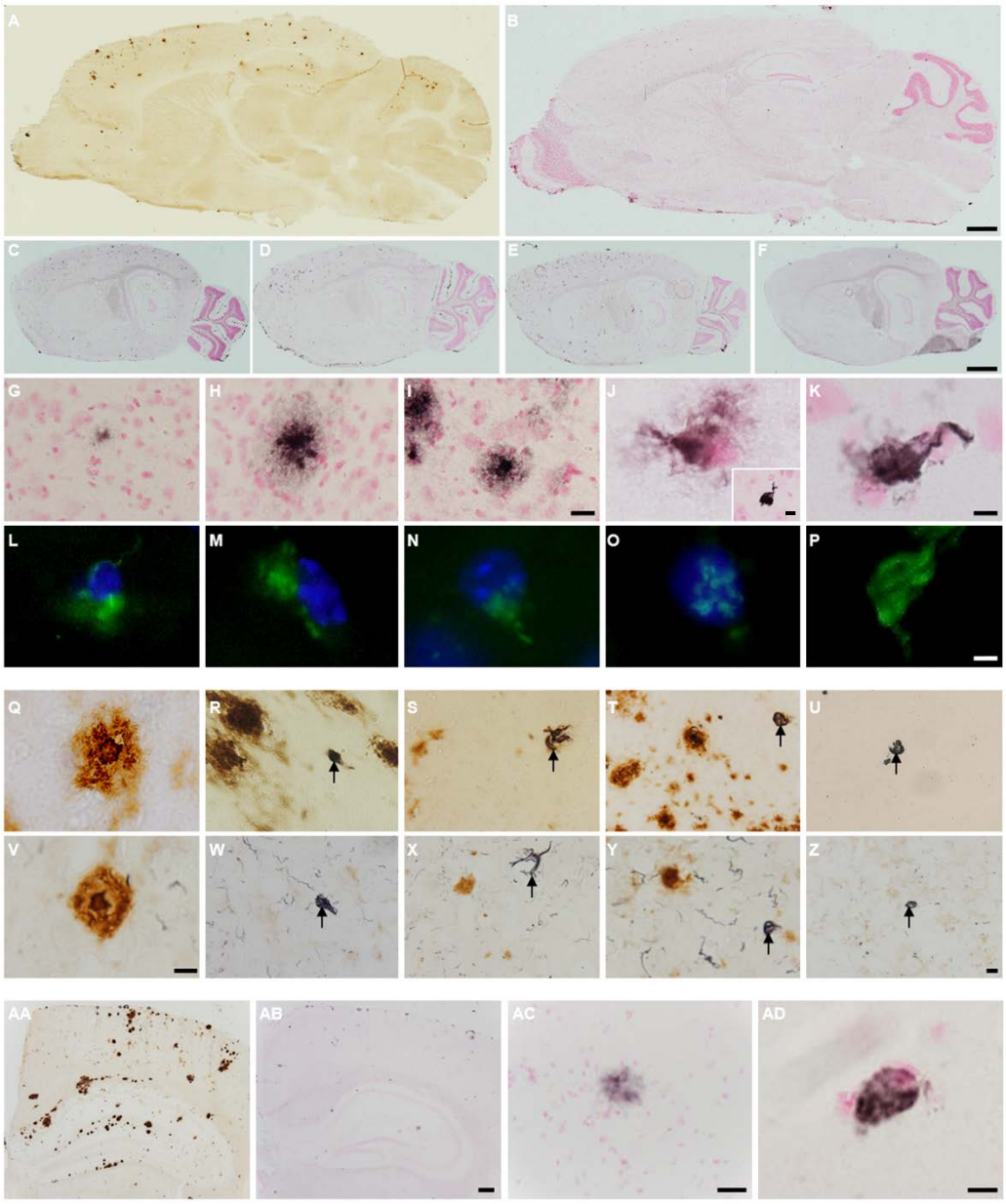

Fig. 1. Neurofibrillary alterations in amyloidosis mice. (A&B) Sagittal brain sections of 6-month-old *APP*$_{swe}$/*PS1*$_{\Delta E9}$ mice, processed for 6E10 immunohistochemistry (A) and the Gallyas silver stain (B). Silver-labeled sections were counterstained with nuclear fast red. β-amyloidosis dominates over argyrophilic pathology in 6-month-old *APP*$_{swe}$/*PS1*$_{\Delta E9}$ mice. **(C-F)** Progressive increase in Gallyas-positive signal in 12- (C), 18- (D), and 24-month-old transgenic mice (E). Wild-type animals showed no silver deposition up to 24 months of age (F). **(G-P)** All photomicrographs are from the neocortex of *APP*$_{swe}$/*PS1*$_{\Delta E9}$ mice. Argyrophilic signal was scarce in 6-month-old TG animals (G). Gallyas-positive structures in 18- (H) and 24-month-old animals (I), likely of neuritic nature. Gallyas silver (J & K) and thioflavin-S stainings (L-P), showing perinuclear and intranuclear signal in 18- and 24-month-old transgenic mice. The insert in J shows compact Gallyas staining in the absence of nuclear fast red. Note potential fragmented nuclei in (M) and (N), intranuclear signal in (O), and absence of DAPI signal in (P). **(Q-Z)** Gallyas/6E10 doubly-labeled sections from a 24-month-old transgenic mouse (Q-U) and an AD patient (V-Z),

showing dense-core plaques (Q & V), teardrop-shaped structures (R & W, arrows), tuft-shaped filaments (S & X, arrows), and globose structures in close proximity (T & Y) and over 200 µm afar from Aβ deposits (U & Z). **(AA-AD)** 6E10/Gallyas- (AA) and Gallyas-labeled (AB-AD) sections of 20-month-old Tg2576 mice. Scale bar is 2 mm for A&B, 1 mm for C-F, 10 µm for G-I, 5 µm for J-K, L-P, 10 µm for Q & V, 20 µm for R-U & W-Z, 200 µm for AA&AB, 20 µm for AC, and 5 µm for AD.

[^{18}F]Flortaucipir autoradiography

The paired helical filament (PHF) ligand [^{18}F]Flortaucipir ([^{18}F]AV-1451, [^{18}F]T807) was used to quantify tau pathology in aging *APP*$_{swe}$/*PS1*$_{\Delta E9}$ TG mice by autoradiography (Table 1). Increased binding was observed in the neocortex, hippocampus, amygdala and the cerebellum of 12-month-old *APP*$_{swe}$/*PS1*$_{\Delta E9}$ mice, compared to age-matched WT, 3- and 6-month-old TG animals (P<0.001 for all regions; Bonferroni *post-hoc* tests). [^{18}F]Flortaucipir binding was further elevated in the visual (P<0.001), somatosensory (P<0.001), motor cortex (P<0.001), and the amygdala (P<0.05) of 18- vs. 12-month-old *APP*$_{swe}$/*PS1*$_{\Delta E9}$ TG mice. Increased binding over age-matched WT mice was first observed in the thalamus of TG animals at 18 months of age (P<0.001). In 24-month-old *APP*$_{swe}$/*PS1*$_{\Delta E9}$ mice, [^{18}F]Flortaucipir signal had increased in all brain regions examined compared to age-matched controls. Three-way ANOVA confirmed genotype- [$F_{(1,476)}$=2603.1, P<0.001], age- [$F_{(4,476)}$=457.3, P<0.001] and brain region-specific increases in the binding levels of [^{18}F]Flortaucipir [$F_{(9,476)}$=42.9, P<0.001], as well as significant age x genotype x region interaction effects [$F_{(36,476)}$=5.5, P<0.001].

Within each brain area analyzed, there was a positive correlation between the age-dependent increase in the binding levels of [^{18}F]Flortaucipir and the progressive increases in the density of Gallyas-positive lesions (Pearson r for all brain regions: 0.92, P<0.001; Fig. S2).

Brain region	3 months		6 months		12 months		18 months		24 months		Correlation with Gallyas-positive fraction
Cortical	**WT**	***APP/PS1***	**WT**	***APP/PS1***	**WT**	***APP/PS1***	**WT**	***APP/PS1***	**WT**	***APP/PS1***	**Pearson r (Significance)**
Frontal	**2.2 ± 0.7**	**3.6 ± 1.3**	**2.3 ± 0.9**	**10.0 ± 1.6**	**4.0 ± 1.0**	**46.7 ± 2.7*****	**4.7 ± 1.1**	**53.2 ± 3.0**	**4.2 ± 1.0**	**55.2 ± 5.7**	**0.74 (*P*<0.001)**
Motor	**2.5 ± 0.5**	**2.8 ± 0.8**	**2.5 ± 0.7**	**7.3 ± 1.3**	**3.2 ± 0.7**	**31.0 ± 1.3*****	**3.2 ± 0.8**	**45.1 ± 2.0**	**4.3 ± 1.1**	**55.7 ± 2.9**	**0.90 (*P*<0.001)**
Somatosensory	**5.2 ± 1.3**	**5.0 ± 2.0**	**4.0 ± 0.9**	**11.6 ± 1.9**	**6.7 ± 4.5**	**34.9 ± 2.6*****	**6.5 ± 1.8**	**50.3 ± 1.5**	**5.8 ± 1.6**	**57.8 ± 2.7**	**0.93 (*P*<0.001)**
Visual	**6.8 ± 2.4**	**4.7 ± 1.4**	**2.4 ± 1.1**	**11.8 ± 2.5**	**8.2 ± 1.8**	**35.5 ± 3.2*****	**6.3 ± 1.9**	**52.9 ± 2.8**	**5.0 ± 1.3**	**56.4 ± 2.9**	**0.92 (*P*<0.001)**
Entorhinal	**3.2 ± 1.0**	**2.9 ± 1.0**	**3.3 ± 0.8**	**8.8 ± 1.1**	**6.7 ± 1.5**	**29.8 ± 1.9*****	**4.1 ± 2.6**	**40.6 ± 3.8**	**6.3 ± 1.7**	**42.8 ± 4.0**	**0.84 (*P*<0.001)**
Subcortical											
Hippocampus	**3.1 ± 1.3**	**2.8 ± 0.8**	**3.0 ± 0.7**	**7.5 ± 1.3**	**4.3 ± 1.3**	**31.3 ± 2.4*****	**4.3 ± 1.2**	**40.9 ± 2.5**	**5.6 ± 1.5**	**49.1 ± 3.1**	**0.86 (*P*<0.001)**
Striatum	**2.6 ± 1.4**	**3.1 ± 1.0**	**3.1 ± 0.7**	**4.8 ± 0.9**	**4.4 ± 1.1**	**10.9 ± 2.4**	**5.1 ± 1.5**	**17.2 ± 1.2**	**5.4 ± 1.5**	**19.7 ± 2.8****	**0.64 (*P*<0.001)**
Amygdala	**1.8 ± 1.5**	**2.9 ± 0.9**	**3.1 ± 0.7**	**7.4 ± 1.0**	**4.2 ± 1.1**	**27.8 ± 2.9*****	**5.2 ± 1.5**	**40.0 ± 2.5**	**5.2 ± 1.1**	**47.7 ± 4.8**	**0.79 (*P*<0.001)**
Thalamus	**2.6 ± 0.6**	**2.2 ± 0.6**	**3.3 ± 1.0**	**3.5 ± 0.5**	**3.6 ± 0.9**	**11.2 ± 3.2**	**3.9 ± 1.3**	**17.5 ± 2.0*****	**4.1 ± 1.0**	**27.2 ± 4.5**	**0.87 (*P*<0.001)**
Cerebellum	**4.2 ± 0.8**	**3.1 ± 1.1**	**4.1 ± 1.2**	**10.3 ± 1.1**	**3.3 ± 1.0**	**23.0 ± 3.1*****	**4.5 ± 1.5**	**31.2 ± 3.6**	**5.8 ± 1.6**	**32.4 ± 3.7**	**0.83 (*P*<0.001)**
Mean binding levels **(all brain regions)**	**3.4 ± 1.1**	**3.3 ± 1.1**	**3.1 ± 0.9**	**8.3 ± 1.3**	**4.9 ± 1.5**	**28.2 ± 2.6**	**4.8 ± 1.5**	**38.9 ± 2.5**	**5.2 ± 1.3**	**44.4 ± 3.7**	**0.92 (*P*<0.001)**

Table 1. Autoradiography of [^{18}F]Flortaucipir binding sites in aging *APP*$_{swe}$/*PS1*$_{\Delta E9}$ mice. Fresh-frozen brain sections from *APP*$_{swe}$/*PS1*$_{\Delta E9}$ and age-matched wild-type (WT) animals were incubated with 38.4±9.6 MBq [^{18}F]Flortaucipir for a period of 60 min (specific activity: 145±68 GBq/µmol). Autoradiography data are presented as the mean specific binding of [^{18}F]Flortaucipir (kBq/mL) ± standard error of the mean in brain regions of 5-6 animals/group. By 24 months of age, [^{18}F]Flortaucipir binding in *APP*$_{swe}$/*PS1*$_{\Delta E9}$ mice had increased across all brain areas examined vs. age-matched WT animals. The age-dependent increase in [^{18}F]Flortaucipir binding levels was positively correlated with the progressive increase in Gallyas-positive argyrophilic signal, in all TG brain areas examined. ***P*<0.01, ****P*<0.001 vs. age-matched littermate control mice, Bonferroni *post-hoc* tests. Symbols of significant differences between groups of 24 & 18 vs. 3-, 6- and 12-month-old-mice were omitted from the table for clarity of presentation.

Representative autoradiograms of [^{18}F]Flortaucipir binding sites are shown in Fig. 2. Binding was decreased in the presence of 50 µM unlabeled flortaucipir but was not reversed by 1 µM of the amyloid-preferring Pittsburgh compound B (PIB).

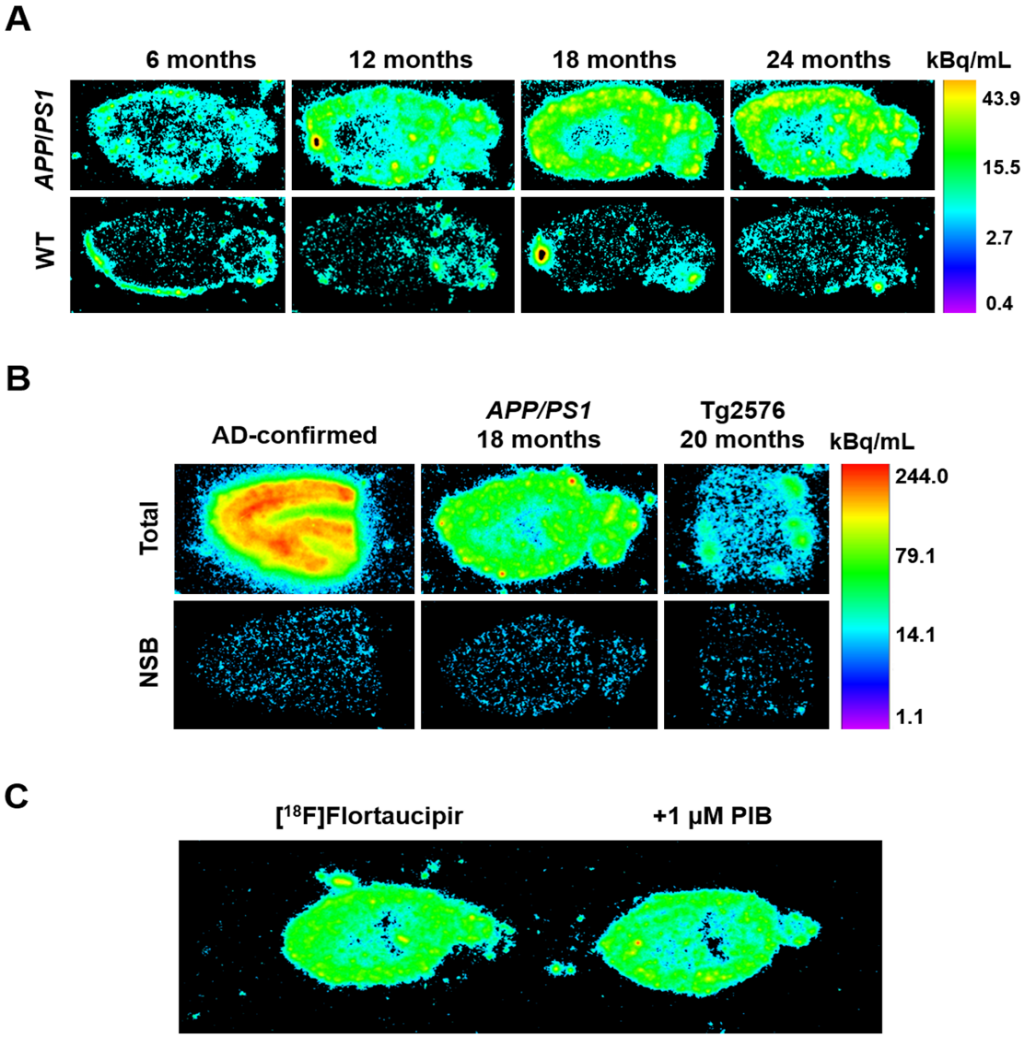

Fig. 2. Representative autoradiograms of [^{18}F]Flortaucipir binding sites. (A) Sagittal brain sections of aging transgenic (top panel) and wild-type mice (WT, lower panel), taken at the level of the entorhinal cortex [lateral 2.88±0.12 mm of the Paxinos and Franklin mouse atlas (74)]. Images were analyzed on a black & white display mode, and presented as a pseudocolor interpretation of black & white pixel intensity, calibrated in kBq/mL of [^{18}F]Flortaucipir solution. Age-dependent increases in binding levels were observed exclusively in $APP_{swe}/PS1_{\Delta E9}$ mice. **(B)** [^{18}F]Flortaucipir binding in sections from the middle frontal gyrus of AD-confirmed patients, 18-month-old $APP_{swe}/PS1_{\Delta E9}$ mice and 20-month-old Tg2576 animals, showing the magnitude of tau pathology in patient vs. transgenic mouse tissue. Non-specific binding (NSB) was assessed in the presence of 50 µM 'cold' flortaucipir. **(C)** Binding was not blocked by co-incubating sections with [^{18}F]Flortaucipir and 1 µM of the amyloid-targeting agent Pittsburgh Compound B (PIB).

Mapt expression

Relative expression of total *Mapt* mRNA was determined by RT-qPCR (Fig. 3). There were no age [$F_{(4,50)}$=0.29, P>0.05], genotype [$F_{(1,50)}$=0.93, P>0.05], or age x genotype interaction effects on the expression levels of *Mapt* [$F_{(4,50)}$=1.21, P>0.05].

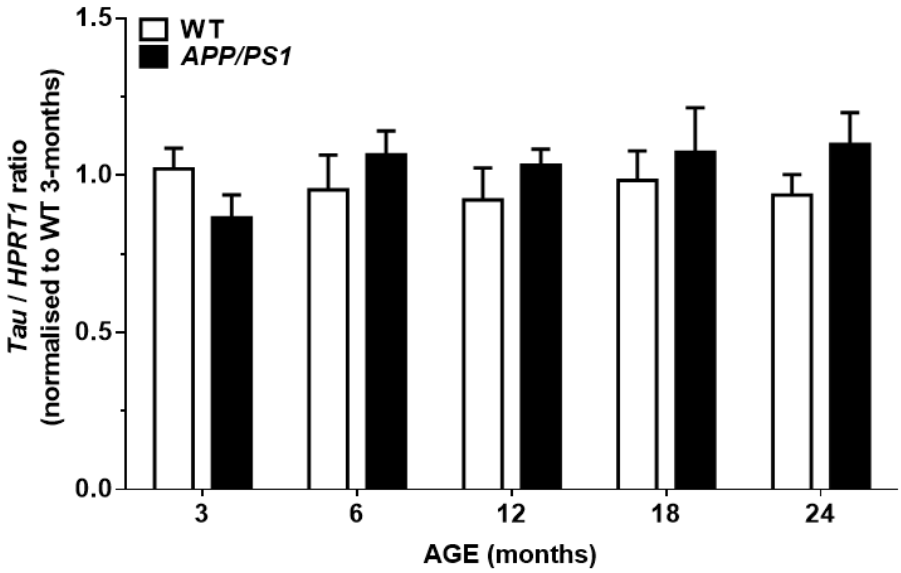

Fig. 3. Regulation of *Mapt* mRNA in aging mice. Levels of endogenous murine *tau* mRNA were not altered by age or genotype. PCR products of x4 diluted *tau* cDNA were determined after 24 cycles. A single peak was obtained by melt-curve analysis, and no signal was detected in the genomic DNA and buffer controls. The efficiency of amplification was 99.2±0.2% for *Hprt1* and 100.3±2.1% for *Mapt*.

Isolation and Transmission Electron Microscopy (TEM) of sarkosyl-insoluble tau

The general methods of Sahara et al. (*20*) and Greenberg and Davies (*21*) were evaluated for the extraction of PHFs from the 24-month-old $APP_{swe}/PS1_{\Delta E9}$ TG brain (Fig. S3). Although longer filaments were isolated by the procedure of Sahara et al., the Greenberg and Davies method was chosen for the isolation of sarkosyl-insoluble tau from 3- and 24-month-old mice, based on immunoblotting experiments, solubility considerations, and to allow for comparisons with literature data (*22*). Soluble and insoluble tau levels were measured in mouse brain homogenates

by using the mouse Total Tau Meso Scale kit (Meso Scale Diagnostics LLC). TEM was used to visualize filaments in the sarkosyl-insoluble extracts from the TG mouse and AD patient brains by negative staining.

Tau protein levels increased with age in the pellet obtained by centrifuging WT and *APP*$_{swe}$/*PS1*$_{\Delta E9}$ homogenates at 27,000 x g [Fig. 4A; age effect: $F_{(1,18)}$=50.0, P<0.001; genotype effect: $F_{(1,18)}$=2.4, P>0.05]. Levels of tau in the supernatant fraction were not different between 3- and 24-month old, WT and *APP*$_{swe}$/*PS1*$_{\Delta E9}$ TG animals [age: $F_{(1,16)}$=0.6, P>0.05; genotype: $F_{(1,16)}$=0.0, P>0.05]. Treatment of the supernatant with 1% sarkosyl for 2 h at 37°C increased the concentration of tau in the detergent-soluble fraction by >3-fold. Sarkosyl-soluble tau levels were lower in the 24- vs. 3-month-old mouse brain [$F_{(1,16)}$=12.5, P<0.01], irrespective of genotype [$F_{(1,16)}$=0.5, P>0.05]. Sarkosyl-insoluble tau was not detected in 3-month-old animals, and its levels were not different between 24-month-old *APP*$_{swe}$/*PS1*$_{\Delta E9}$ and WT mice [$t_{(8)}$=0.7, P>0.05; independent two-tailed Student's t-test].

Fig. 4B shows negatively-stained filaments in the sarkosyl-insoluble extract from the 24-month-old *APP*$_{swe}$/*PS1*$_{\Delta E9}$ mouse and AD patient brain. Fibrils of mean length 104.9±8.3 nm and width 10.1±0.5 nm were isolated from TG mice. Wider fibrils (~20 nm), with or without a pronounced twist, were readily detected (a & e). Longer filaments (271.7±11.3 nm), with axial periodicities of 78.7±9.8 nm, constituted ~8% and ~34% of the fibril population analyzed in the *APP*$_{swe}$/*PS1*$_{\Delta E9}$ and AD brains, respectively (b & f). Clusters of long filaments, which were denser in AD patient material, were present in the insoluble preparation from *APP*$_{swe}$/*PS1*$_{\Delta E9}$ mice (b & f, inserts). Thin, bent fibrils (c & g) and rod-shaped particles (d & h) were observed in

both 24-month-old $APP_{swe}/PS1_{\Delta E9}$ and AD brains. There were no between-species differences in the dimensions of the isolated filaments [short filaments, length: $t_{(82)}=0.1$, $P>0.05$, width: $t_{(82)}=1.2$, $P>0.05$; long filaments, length: $t_{(16)}=0.3$, $P>0.05$, width: $t_{(16)}=0.8$, $P>0.05$; independent two-tailed t-tests].

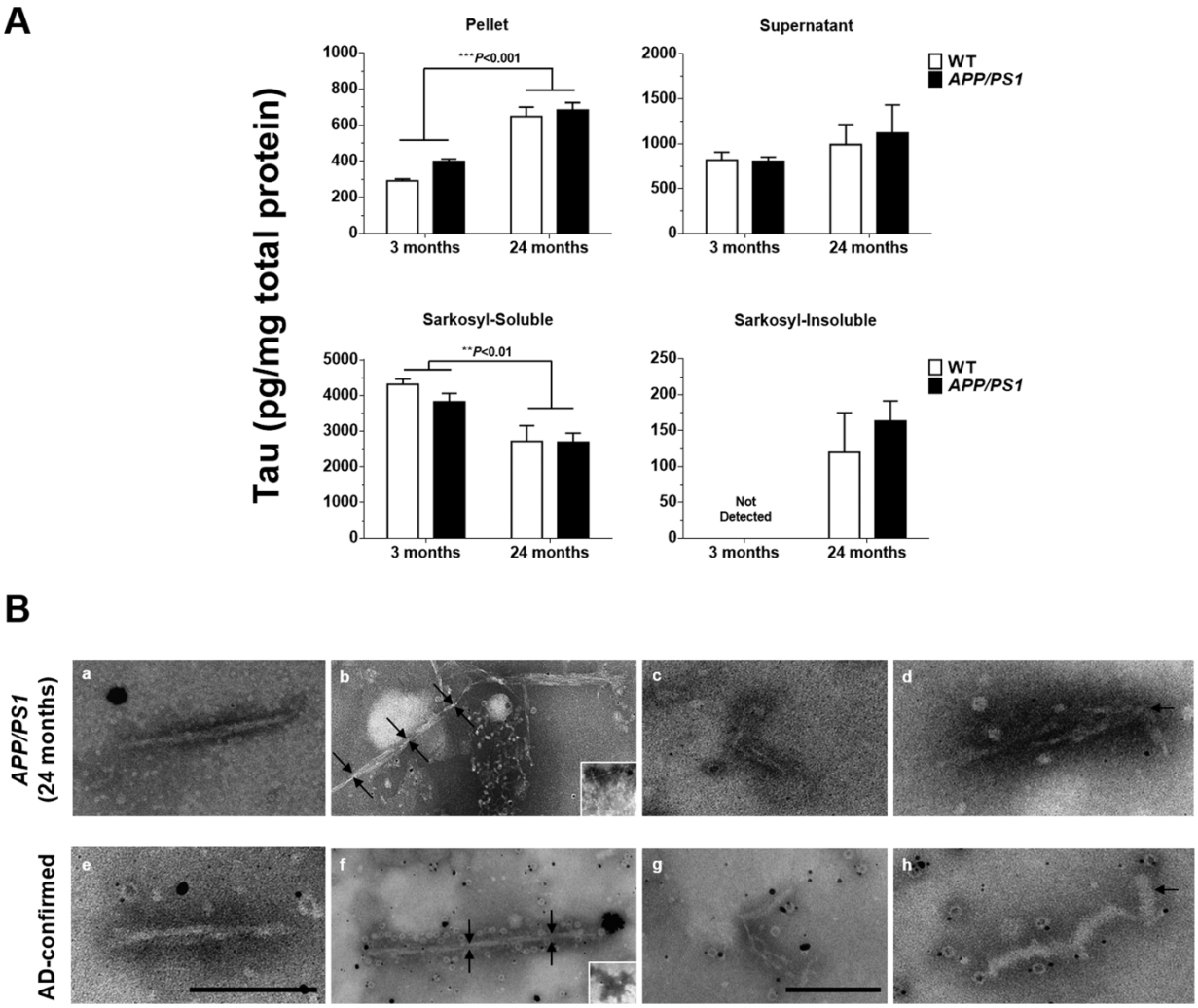

Fig. 4. Isolation and electron microscopy of sarkosyl-insoluble tau. (A) Levels of soluble and insoluble tau were determined with the mouse Total Tau Meso Scale kit. Tau levels increased with age in the pellet obtained by centrifuging brain homogenates at 27,000 x g. The resulting supernatant was treated with 1% sarkosyl and centrifuged at 200,000 x g. The solubility of tau in sarkosyl was decreased with age, irrespective of genotype. **(B)** Overview of negatively-stained filament types in the sarkosyl-insoluble fraction from 24-month-old $APP_{swe}/PS1_{\Delta E9}$ and AD brain tissue. Fibrils of ~20 nm in width, appearing as straight filaments (a) or as two intertwined fibrils (e), each with a diameter of ~10 nm. PHFs with axial periodicities of ~80 nm (b & f; arrows) were present in $APP_{swe}/PS1_{\Delta E9}$ mice, and more frequently observed in AD patient material. The inserts show 'stacked' PHFs, which

were denser in the AD preparation. Structures commonly identified in the detergent-insoluble fractions of the mouse and human brain included bent fibrils of ~7 nm in width (c & g), and rod-shaped particles (d & h; arrows). Scale bars: 200 nm (a, b, e, f), 100 nm (c, d, g, h).

Proteomics of sarkosyl-insoluble tau

The sarkosyl-insoluble fractions extracted from 3- and 24-month-old mouse brain, AD and non-AD individuals, were pooled and digested with trypsin & Lys-C. The peptides were labeled with Tandem Mass Tags (TMT), fractionated, and analyzed by nanoLiquid Chromatography-Electrospray Ionization Mass Spectrometry (LC-ESI MS/MS).

A list of tau-associated proteins quantified in the sarkosyl-insoluble proteome is shown in Table 2. Lists of between-group abundance ratios for all regulated proteins are shown in Data File S1. There were 583 proteins identified in the sarkosyl-insoluble mouse proteome, of which 456 were also present in the human samples. Isoforms of tau with three (3R) and four (4R) microtubule-binding repeats were extracted from both human and the murine brain. In mice, all isoforms collapsed under the term microtubule associated protein (MAP; UniProt accession number: B1AQW2). Mouse MAP was regulated by age, rather than genotype. The protein was enriched 2.1-fold in 24- vs. 3-month-old TG mice, and 1.8-fold in 24- vs. 3-month-old WT mice. Genotype-specific enrichment was observed for mouse tau isoform-B (UniProt accession number: P10637-3), a 3R isoform of tau with an extended C-terminal domain, which was identified by the sequence ^{205}KVQIVYKPVDLSKV^{218}. Tau isoform-B increased 3.2-fold in 24-month-old TG vs. WT mice, and 4.5-fold in 24- vs. 3-month-old TG animals. Human MAP (UniProt accession number: A0A0G2JMX7), containing tau isoforms P10637-2, -4, -6 & -8, was 37-fold enriched in the sarkosyl-insoluble fraction of AD compared to non-AD brain.

UniProt Accesion Number	Protein(s)	Involvement	TG vs. WT 3 months	TG vs. WT 24 months	TG 24 vs. 3 months	WT 24 vs. 3 months	AD vs. non-AD
B1AQW2	Microtubule-associated protein	Tau	0.86	1.00	2.06	1.77	37.15
P10637-3	Microtubule-associated protein tau	Tau Isoform-B	0.61	3.21	4.52	0.86	Fetal form present
Multiple	Small nuclear ribonucleoproteins (snRPN)	Core spliceosomal components	Age- and genotype-specific regulation (Data File S1)				
Multiple	Heterogeneous nuclear ribonucleoproteins	Exon 10 splicing regulation	Multiple proteins regulated (Data File S1)				
Q8BL97	Serine/arginine-rich splicing factor 7	Exon 10 exclusion	0.82	1.05	1.11	0.87	0.69
Q9Z0H4	CUGBP Elav-like family member 2	Exon 10 exclusion	0.40	1.85	1.94	0.42	1.49
P62996	Transformer-2 protein homolog beta	Exon 10 inclusion	0.85	1.13	0.74	0.56	Not identified
Multiple	Tubulin	Tau binding partner	Alpha & beta chains regulated (Data File S1)				
P60710	Actin, cytoplasmic 1	Tau binding partner	0.80	0.53	1.43	2.16	0.71
P08551, P08553, P19246	Neurofilament	Tau binding partner	Light, medium & heavy polypeptides regulated (Data File S1)				
Multiple	Ribosomal proteins 60S, 40S	Tau binding partner	Age- and genotype-specific changes, particularly in the acidic proteins of the 60S subunit (Data File S1)				
O08788	Dynactin	Tau binding partner	1.01	1.34	0.79	0.59	Not identified
P28738	Kinesin	Tau binding partner	0.92	0.75	1.03	1.28	0.90
P11499, Q80Y52, Q3UAD6	Heat shock protein 90	Tau binding partner	Isoforms alpha & beta identified (Data File S1)				
P48722, P17156, Q3U2G2, Q8K0U4	Heat shock protein 70	Tau binding partner	Members 2 & 4 common in mice & humans (Data File S1)				
P0DP26	Calmodulin-1	Tau binding partner	1.68	0.31	0.68	3.63	0.93
Q3UY00	S100β	Tau binding partner	0.99	0.52	1.27	2.44	0.34
O55042	α-Synuclein	Tau binding partner	0.81	0.70	1.29	1.49	0.79
A8IP69, P68510, F6VW30, Q9CQV8, P63101	14-3-3 proteins	Tau binding partner	Isoform-specific changes (Data File S1)				
Q3TXU4	Apolipoprotein E	Tau binding partner/ AD risk factor	0.65	3.58	7.51	1.37	Not identified
O08539	Bin1	Tau binding partner/ AD risk factor	2.11	0.44	0.71	3.41	1.44
Q549A5	Clusterin	Tau interacting partner/ AD risk factor	1.17	1.82	1.87	1.20	Not identified
P11798, Q923T9, A0A0G2JGS4	Ca2+/calmodulin-dependent protein kinase II	Tau kinase	Multiple subunits identified (Data File S1)				
P63318	Protein kinase C, gamma type	Tau kinase	0.71	1.48	1.30	0.62	1.05
P31324	cyclic AMP-dependent protein kinase II	Tau kinase	0.57	0.91	1.61	1.01	0.84
Q63810	Calcineurin subunit B type 1	Tau phosphatase	1.36	0.34	0.96	3.84	Not identified
Q76MZ3	Serine/threonine-protein phosphatase 2A	Tau phosphatase	1.25	0.58	0.87	1.88	0.73

Table 2. Proteomics of sarkosyl-insoluble tau. Tau-associated proteins quantified in the detergent-insoluble fractions of the mouse and human brain. The presented proteins have been selected for their documented roles in the regulation and binding of tau.

The mouse MAP sequence ^{174}KVAVVR**T**PPKSPSA**S**KS^{190}, phosphorylated at Threonine (T) 180 and Serine (S) 188, was more than 20-fold enriched in 24-month-old TG, compared to age-matched WT and 3-month-old *APP*$_{swe}$/*PS1*$_{\Delta E9}$ mice. The peptide sequence was not regulated in aging WT animals. An orthologous sequence of the human MAP was phosphorylated at Threonine (T) 566 and Serine (S) 573 (^{560}KVAVVR**T**PPKSPS**S**AKS^{576}). The reported phosphorylation sites correspond to amino acids (aa) T231 and S238 of the human tau isoform with 441 aa. Indications of additional phosphorylation sites were obtained by searching modified peptides against tau isoform- and species-specific databases. Phosphorylated S396, S400 and S404 on the conserved sequence ^{396}**S**PVV**S**GDT**S**PR^{406} of the human 441 aa isoform were identified in the sarkosyl-insoluble mouse proteome. Phosphorylation at S404 in 24-month-old TG mice was confirmed by immunoblotting (Fig. S4). In addition to phosphorylation, murine MAP was deamidated at Asparagine (N) 44, a site on the N-terminal domain of tau that is not conserved in humans (^{34}AEEAGIGDTP**N**QEDQAAGHVTQAR^{57}). Human MAP was deamidated at position N484, corresponding to N167 of the 441 aa tau isoform (^{473}GAAPPGQKGQA**N**ATRIPAK^{491}).

The database for annotation, visualization and integrated discovery (DAVID, v6.8) was used for gene ontology (GO) enrichment analysis of the sarkosyl-insoluble proteome (*23, 24*). RNA splicing, mRNA processing and translation were among the 10 most enriched biological processes associated with protein upregulation in 24-month-old *APP*$_{swe}$/*PS1*$_{\Delta E9}$ vs. WT mice and AD vs. non-AD subjects. Ribonucleoprotein complexes, ribosomes, and exosomes were among the 10 most enriched cellular components in the insoluble extracts from the mouse and human brain (Fig. 5A). The top 10 molecular functions of the enriched proteins were associated with

poly(A) RNA binding, as well as binding of molecules contributing to the structural integrity of ribosomes and the cytoskeleton (Fig. 5B). Pathway-based enrichment analysis of upregulated proteins in 24-month-old *APP*$_{swe}$/*PS1*$_{\Delta E9}$ vs. WT mice involved GO terms such as Alzheimer's and Huntington's disease, long-term depression, cholinergic, serotonergic and glutamatergic synapse (Fig. 5C). Glycolysis/gluconeogenesis and the Krebs cycle were among the top 10 pathways for downregulated proteins (Fig. 5D).

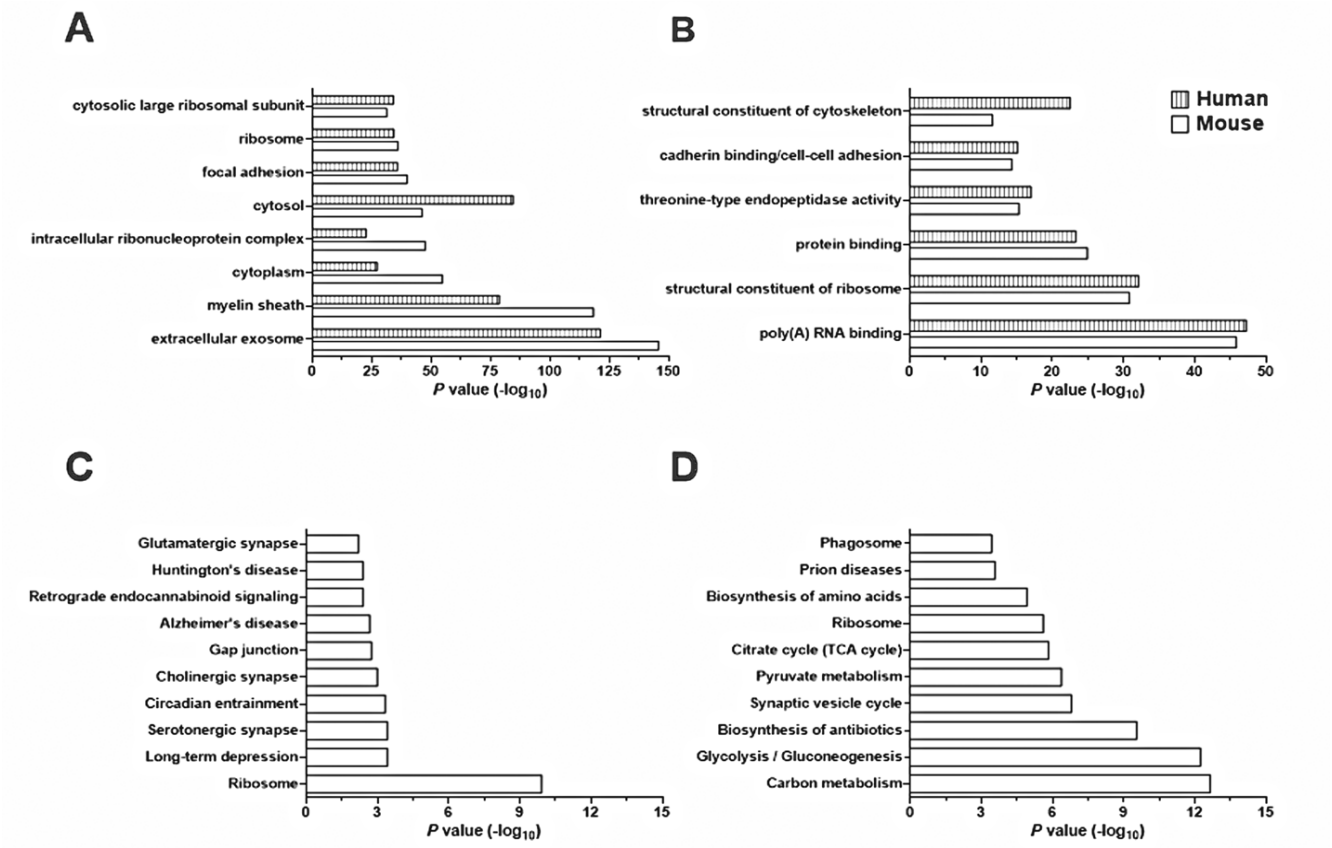

Fig. 5. Gene Ontology (GO) enrichment analysis of the sarkosyl-insoluble proteome. (A) Enriched cellular components; **(B)** Enriched molecular functions; **(C)** Top 10 enriched pathways based on protein upregulation in 24-month-old TG vs. WT mice, according to the Kyoto Encyclopedia of Genes and Genomes (KEGG); **(D)** Top 10 enriched KEGG pathways based on protein downregulation in 24-month-old TG vs. WT mice. Functional annotation clustering was generated by using DAVID software. Maximum enrichment probability (*P* value) was based on an EASE score threshold value of 0.05.

Discussion

The present study describes tauopathy in murine models of familial AD. Neurofibrillary alterations in *APP*$_{swe}$/*PS1*$_{\Delta E9}$ and Tg2576 mice were demonstrated by a set of tools that are currently used for the evaluation of pathological tau clinically, such as the Gallyas silver stain and [^{18}F]Flortaucipir. The presence of PHF tau was confirmed by TEM of sarkosyl-insoluble preparations from the *APP*$_{swe}$/*PS1*$_{\Delta E9}$ mouse brain. As murine tau possesses a remarkably high number of 76 potential serine/threonine and 4 tyrosine phosphorylation sites, an antibody-free proteomics approach was used for the detection of tauopathy-related epitopes. Of the five hyperphosphorylated sites identified, S404 has been associated with the intraneuronal and extracellular deposition of NFTs in AD (*25*). The pathology observed in the present study occurred at physiological levels of endogenous tau, as there was no difference in total tau mRNA and protein between *APP*$_{swe}$/*PS1*$_{\Delta E9}$ and WT mice. Hence, in addition to progressive amyloidosis (*3*), neuroinflammation (*4*) and neurodegeneration (*5*), *APP*$_{swe}$/*PS1*$_{\Delta E9}$ mice develop progressive neurofibrillary pathology of the AD type, mimicking a range of AD pathologies, in a translationally-relevant manner. The observation that endogenous tau accumulates secondarily to Aβ in models of cerebral amyloidosis is entirely consistent with *post-mortem* (*26*) and *in vivo* imaging data (*27*), showing that the development of cortical tau pathology in AD patients is associated with, and may depend on, pre-existing amyloid pathology.

Current approaches to induce tauopathy in mice have been criticized for generating models that poorly recapitulate the situation in the AD brain, as *TAU* in AD is neither overexpressed, nor mutated (*28*). FLTD-linked mutations, in particular, induce tauopathy that is not only morphologically different than that of AD (e.g. Pick bodies), but further characterized by distinct

neurodegenerative processes. For example, cholinergic neurons are extensively lost in AD, but not in FTLD (*29*). Acetylcholinesterase inhibitors, which are prescribed for the symptomatic relief of cognitive impairment in AD, are largely ineffective in FTLD and may even worsen its symptoms (*30*). Thus, the pathophysiology that differentiates AD from primary tauopathies is unlikely to be modeled in mutant *TAU* models. Moreover, neurofibrillary alterations in *TAU* overexpressing mice occur in the absence of Aβ deposition, which is a defining feature of AD histopathology. The present results indicate that amyloidosis models may overcome these limitations, by reproducing both the neurofibrillary pathology of familial AD and the molecular heterogeneity that is associated with it. In addition to the spontaneous aggregation of tau in $APP_{swe}/PS1_{\Delta E9}$ and Tg2576 mice, analysis of the sarkosyl-insoluble $APP_{swe}/PS1_{\Delta E9}$ proteome identified proteins that have been strongly linked to AD pathogenesis, in general, and tau pathology in particular. Among them, APOE and BIN1 are encoded by genes whose variants are known to increase the risk of late-onset AD, through pathways involving interactions with both APP (*31*, *32*) and tau (*33*-*35*). Core components of the spliceosome, on the other hand, particularly Sm-D1 and Sm-D2, are closely related to the deposition of NFTs, but not plaques in familial AD (*36*). This literature implicates multiple mechanisms in AD tauopathy, which occur downstream of Aβ processing in cases of autosomal dominant AD (ADAD) and, as shown here, $APP_{swe}/PS1_{\Delta E9}$ mice.

Although the sporadic and familial forms of AD share common clinical and histopathological features, it is becoming increasingly recognized that they are not precisely equivalent (*37*). Positron emission tomography (PET) with [^{11}C]PIB demonstrates accumulation of Aβ in the cerebellum of familial AD cases, which is not typical of sporadic AD (*38*). Cerebellar deposition

of hyperphosphorylated tau has been observed in ADAD cases harboring the *PSEN1* E280A mutation, but not in sporadic AD (*39*). Thus, the pronounced cerebellar involvement in $APP_{swe}/PS1_{\Delta E9}$ mice, which are known to accumulate Aβ in this region (*40*), suggests that the model mimics familial, rather than the sporadic forms of AD. Reports of cerebellar pathology in ADAD cases and $APP_{swe}/PS1_{\Delta E9}$ mice warrant caution in using the cerebellum as a reference region for the quantification of [^{11}C]PIB and [^{18}F]Flortaucipir PET (*41, 42*), as this is likely to underestimate cortical Aβ and tau pathology, respectively.

Unlike the imbalance in Aβ homeostasis, which is thought to be central in the pathogenesis of AD, gross changes in tau production and clearance were not observed in this study. On the one hand, Gallyas-, [^{18}]Flortaucipir- and thioflavin-S-positive signal was observed in the vasculature of 18-24-month-old $APP_{swe}/PS1_{\Delta E9}$ mice. Moreover, there were age- and genotype-specific changes in multiple components of the phagosome and proteasome in TG vs. WT animals (Data File S1). On the other hand, total tau mRNA and protein levels were not different between 24-month-old WT and TG mice, as evidenced by tau mesoscale, proteomics and PCR. Moreover, age-dependent decreases in the solubility of tau were equally observed in $APP_{swe}/PS1_{\Delta E9}$ and control animals. Notwithstanding that the contribution of individual pathways to tau degradation was not assessed in this study, these findings suggest that the neurofibrillary alterations observed in $APP_{swe}/PS1_{\Delta E9}$ mice are not mediated by an imbalance between the production and clearance of tau. It is important to note that, unlike in TG mice, sarkosyl-insoluble tau was increased in AD vs. non-AD tissue, a finding that is consistent with literature data on the regulation of human tau in AD (*43*). It might be that the increased concentration of brain tau in late-stage AD is associated with heavily impaired clearance pathways or pronounced neuronal damage, processes

that may not be modeled in 24-month-old $APP_{swe}/PS1_{\Delta E9}$ mice. Alternatively, the present data may highlight the involvement of transcriptional and translational mechanisms, rather than production and clearance pathways, in the assembly of PHF tau.

A prevalence of 3R isoforms in the composition of NFTs has been observed in the AD hippocampus by immunohistochemical and biochemical methods (*44*). Moreover, a shift from 4R to 3R isoforms has been associated with the morphological evolution of tau-positive neurons from a pre-tangle to the NFT state (*45*). Although the literature on the regulation of tau isoforms in AD remains scarce, the present results support the notion that an imbalance in tau isoform ratio is involved in the neurofibrillary alterations of AD, with 3R isoforms being preferentially sequestered into the insoluble tau fraction. The identification of tau isoform-B, a 3R isoform that is predominantly expressed in the fetal mouse brain, supports the suggestion that immature tau isoforms participate in AD tauopathy (*46*), and implicates aberrant transcription and translation mechanisms in the disease process. A re-induction of fetal tau may be attributed to the deregulation of core splicing machinery, which was marked in this study and considered to occur early and selectively in AD (*47*). Moreover, as the selection of splice sites is determined by canonical sequences encoded into the genome, the re-expression of fetal isoforms might be a consequence of aberrant DNA replication during cell cycle re-entry (*48*). Cell cycle proteins that were deregulated in an age- and genotype-specific manner in this study include Sub1, cdc42, CEND1, Histone H3 and nucleolin (Data File S1). Clearly, the exact mechanisms underlying tauopathy in AD cannot be resolved by the present set of experiments. The data demonstrate, however, that the formation of PHF tau is associated with loss of regulatory control over *tau* splicing *in vivo*, which may have important implications for the origins and management of

tauopathy in AD. It is tempting to speculate that tau hyperphosphorylation may partly be due to the re-emergence of fetal isoforms, which are known to be over-phosphorylated compared to adult tau (*49*). Moreover, it is plausible that an imbalance in tau isoform ratio mediates protein mislocalization from the axonal to the somatodendritic compartment, as distinct tau isoforms are differentially sorted across the cell (*50*). Of note, cofilin-dependent, 'classical' pathways of tau missorting (*51*) may also be involved in the pathology observed in this study, as cofilin was reduced in the sarkosyl-insoluble proteome of 24-month-old $APP_{swe}/PS1_{\Delta E9}$ mice. Collectively, these data highlight the relevance of amyloidosis models for studying the diverse macroscopic and molecular aspects of AD tauopathy.

The limitations associated with models overexpressing *APP* and *PSEN* mutations have been discussed previously (*2*). To exclude the possibility that tauopathy is an artefact of *APP* or *PSEN* overexpression, it would be important to determine whether it develops in second-generation amyloidosis models, carrying AD-related mutations in endogenous genes. Moreover, as there is evidence of [^{18}F]Flortaucipir binding to monoamine oxidases (MAO; *52*), signal quantification in the presence of MAO inhibitors is warranted to determine the extent of off-target binding, if any (*53*). Practical considerations in using amyloidosis mice to study tauopathy include long waiting times for the accumulation of endogenous murine tau, mouse-on-mouse antibody issues, and the low abundance of pathology as compared to human AD. While ~30% of all Nissl-positive cells in the prefrontal cortex of Braak stage V-VI brains may contain NFTs (*54*), Gallyas-positive signal in this study occupied ~1% of the frontal cortex of 24-month-old $APP_{swe}/PS1_{\Delta E9}$ mice, neuritic structures included. Nevertheless, cognitive impairment in AD is known to correlate with the spread of tau pathology, and the number of brain areas containing at least one NFT has

been shown to be the best explanatory variable of intellectual status in AD (*55*). In this context, it is worth evaluating whether measurements of tauopathy in aging $APP_{swe}/PS1_{\Delta E9}$ mice correlate with the progressive cognitive impairment that these animals exhibit in the Barnes maze assay (*56*).

Materials and Methods

Study design

Mice were grouped according to age and genotype. Sample numbers were based on preliminary studies, showing absence of Gallyas and [^{18}F]Flortaucipir signal in 18-month-old WT vs. TG animals. (Immuno)histochemistry, autoradiography, the isolation of sarkosyl-insoluble tau, and electron microscopy studies were repeated at least three independent times. Tau Meso Scale was performed two independent times. Remaining samples were pooled and subjected to proteomics. To avoid cross-contamination during the isolation of sarkosyl-insoluble tau, glassware was washed in ultrapure de-ionized H_2O (dH_2O, Ultra Clear^{TM}, Siemens), followed by rinses in formic acid (FA, 98-100%; Merck Millipore), dH_2O, ethanol (99%; VWR International) and dH_2O. No samples were excluded from data analysis, which was performed in an unblinded manner. To compare tau pathology in transgenic mouse vs. human brain, tissue from the middle frontal gyrus of an AD-confirmed patient [BB08-002, Female, 80 years old, *post-mortem* interval (PMI): 9 h] and a non-AD subject (BB16-023, Female, 83 years old, PMI unknown) were processed along with the murine samples for the Gallyas silver stain, autoradiography, electron microscopy and proteomics experiments. The AD and non-AD samples were chosen for their abundance and complete lack of tau pathology respectively, as assessed by Gallyas silver

staining and [^{18}F]Flortaucipir autoradiography. To avoid confounding effects of anesthesia on tau phosphorylation, mice were euthanized by cervical dislocation.

Ethical statement

Mouse tissue: All procedures complied with Danish law (Dyreværnsloven-Protection of Animals Act, nr 344/2005) and European Union directive 2010/63/EU, regulating animal research. Ethical permission was granted by the Animal Ethics Inspectorate of Denmark (nr 2011/561-1950).

Human tissue: Fresh-frozen samples from the middle frontal gyrus were obtained from the Maritime Brain Tissue Bank, Department of Medical Neuroscience, Faculty of Medicine, Dalhousie University, Sir Charles Tupper Building, 5850 College Street, Halifax Nova Scotia B3H 4R2. Ethical approval was obtained from the Nova Scotia Health Authority Research Board in Halifax, Canada, and the Danish Biomedical Research Ethical Committee of the region of Southern Denmark (Project ID: S-20070047). Informed, written consent forms were obtained for all subjects.

Animals and tissue sectioning

APP$_{swe}$/*PS1*$_{\Delta E9}$ mice (*57*), originally purchased from the Jackson Laboratories (MMRRC Stock No: 34832-JAX), were bred and maintained on a C57BL/6J background. The animals were group-housed (4-8/cage) in a temperature (21±1°C) and humidity controlled environment (45-65%), under a 12:12 h light:dark cycle (lights on: 7 am). Food and water were available *ad libitum*. Female *APP*$_{swe}$/*PS1*$_{\Delta E9}$ mice were used at 3, 6, 12, and 18 months of age. Sex- and age-matched WT littermates were used as control. Both male and female mice were used in the 24-

month-old groups (n=6/genotype & age-group, total animal number: 60). The animals were euthanized by cervical dislocation, and brains immediately removed and bisected along the midline. Right hemispheres were frozen in isopentane on dry-ice (-30°C). The olfactory bulb, striatum, cortex, hippocampus, diencephalon, brainstem and cerebellum from the left hemisphere were dissected on a petri dish on ice, collected in Eppendorf® tubes, and frozen on dry-ice. The tissue was stored at -80°C until use.

Sectioning was carried out at -17°C using a Leica CM3050S cryostat (Leica Biosystems GmbH). Series of 20 µm-thick sagittal sections were collected at 300 µm intervals. The sections were mounted onto ice-cold Superfrost™ Plus slides (Thermo Fisher Scientific), dried at 4°C in a box containing silica gel for at least 2 h, and stored at -80°C for future experiments. Every 13th and 14th section was collected in Eppendorf® tubes for RNA extraction with Trizol™.

Fresh-frozen coronal brain sections of male and female, 20-month-old Tg2576 and WT mice were provided by the Centre for Biological Sciences, University of Southampton, U.K.

(Immuno)histochemistry, autoradiography and proteomics

The Gallyas silver stain was performed according to Kuninaka et al. (*58*), thioflavin-S according to Sun et al. (*59*), [^{18}F]Flortaucipir autoradiography according to Marquié et al. (*60*), proteomics according to Kempf et al. (*61*). Protocol details are provided in Supplementary Materials and Methods.

Statistical analysis

Parametric testing was employed following inspection of the data for normality with the Kolmogorov-Smirnov test in Prism (v6.01; GraphPad Software). Data sets were analyzed by Statistica^{TM} v10 (TIBCO Software Inc., USA). The effects of age, genotype and brain region on the binding levels of [^{18}F]Flortaucipir were analyzed by three-way ANOVA. Gallyas-positive area fraction and tau gene/protein levels were analyzed by two-way ANOVA for the independent factors age and brain region or genotype, respectively. Where ANOVA yielded significant effects, Bonferroni *post-hoc* comparisons were used to detect between-group regional and age-dependent differences. Levels of sarkosyl-insoluble tau between 24-month-old TG and WT mice, and PHF dimensions extracted from TG vs. AD brain were compared by two-tailed independent Student's t-tests. Significance was set at α=0.05. A 1.3-fold change cut-off value for all TMT ratios was used to rank proteins as up- or down-regulated in the proteomics study (*62*).

Supplementary Materials

Materials and Methods.

Fig. S1. Quantification of Gallyas-positive lesions, photomicrographs of MC-1 immunoreactivity and vascular pathology in *APP*$_{swe}$/*PS1*$_{\Delta E9}$ mice.

Fig. S2. Correlation between Gallyas-positive area fraction and [^{18}F]Flortaucipir binding levels.

Fig. S3. Evaluation of methods for extracting sarkosyl-insoluble tau.

Fig. S4. pS404 immunoblot.

Table S1. Evidence of tau hyperphosphorylation in *APP*$_{swe}$/*PS1*$_{\Delta E9}$ mice.

Data file S1. Regulated proteins in the sarkosyl-insoluble fraction.

References:

1. G. Esquerda-Canals, L. Montoliu-Gaya, J. Guell-Bosch, S. Villegas, Mouse Models of Alzheimer's Disease. *Journal of Alzheimer's disease : JAD* **57**, 1171-1183 (2017).
2. H. Sasaguri, P. Nilsson, S. Hashimoto, K. Nagata, T. Saito, B. De Strooper, J. Hardy, R. Vassar, B. Winblad, T. C. Saido, APP mouse models for Alzheimer's disease preclinical studies. *EMBO J* **36**, 2473-2487 (2017).
3. A. A. Babcock, L. Ilkjaer, B. H. Clausen, B. Villadsen, L. Dissing-Olesen, A. T. Bendixen, L. Lyck, K. L. Lambertsen, B. Finsen, Cytokine-producing microglia have an altered beta-amyloid load in aged APP/PS1 Tg mice. *Brain, behavior, and immunity*, (2015).
4. S. Serriere, C. Tauber, J. Vercouillie, C. Mothes, C. Pruckner, D. Guilloteau, M. Kassiou, A. Domene, L. Garreau, G. Page, S. Chalon, Amyloid load and translocator protein 18 kDa in APPswePS1-dE9 mice: a longitudinal study. *Neurobiology of aging* **36**, 1639-1652 (2015).
5. Y. Liu, M. J. Yoo, A. Savonenko, W. Stirling, D. L. Price, D. R. Borchelt, L. Mamounas, W. E. Lyons, M. E. Blue, M. K. Lee, Amyloid pathology is associated with progressive monoaminergic neurodegeneration in a transgenic mouse model of Alzheimer's disease. *The Journal of neuroscience : the official journal of the Society for Neuroscience* **28**, 13805-13814 (2008).
6. T. A. Kokjohn, A. E. Roher, Amyloid precursor protein transgenic mouse models and Alzheimer's disease: understanding the paradigms, limitations, and contributions. *Alzheimers Dement* **5**, 340-347 (2009).
7. C. Andorfer, Y. Kress, M. Espinoza, R. de Silva, K. L. Tucker, Y. A. Barde, K. Duff, P. Davies, Hyperphosphorylation and aggregation of tau in mice expressing normal human tau isoforms. *Journal of neurochemistry* **86**, 582-590 (2003).
8. J. Gotz, N. Deters, A. Doldissen, L. Bokhari, Y. Ke, A. Wiesner, N. Schonrock, L. M. Ittner, A decade of tau transgenic animal models and beyond. *Brain Pathol* **17**, 91-103 (2007).
9. D. Galimberti, E. Scarpini, Genetics of frontotemporal lobar degeneration. *Front Neurol* **3**, 52 (2012).
10. C. D. Keene, M. Darvas, B. Kraemer, D. Liggitt, C. Sigurdson, W. Ladiges, Neuropathological assessment and validation of mouse models for Alzheimer's disease: applying NIA-AA guidelines. *Pathobiol Aging Age Relat Dis* **6**, 32397 (2016).
11. B. T. Hyman, C. H. Phelps, T. G. Beach, E. H. Bigio, N. J. Cairns, M. C. Carrillo, D. W. Dickson, C. Duyckaerts, M. P. Frosch, E. Masliah, S. S. Mirra, P. T. Nelson, J. A. Schneider, D. R. Thal, B. Thies, J. Q. Trojanowski, H. V. Vinters, T. J. Montine, National Institute on Aging-Alzheimer's Association guidelines for the neuropathologic assessment of Alzheimer's disease. *Alzheimers Dement* **8**, 1-13 (2012).
12. E. Drummond, T. Wisniewski, Alzheimer's disease: experimental models and reality. *Acta Neuropathol* **133**, 155-175 (2017).
13. K. Herrup, The case for rejecting the amyloid cascade hypothesis. *Nat Neurosci* **18**, 794-799 (2015).
14. A. Metaxas, S. J. Kempf, Neurofibrillary tangles in Alzheimer's disease: elucidation of the molecular mechanism by immunohistochemistry and tau protein phospho-proteomics. *Neural Regen Res* **11**, 1579-1581 (2016).
15. J. Gotz, A. Gladbach, L. Pennanen, J. van Eersel, A. Schild, D. David, L. M. Ittner, Animal models reveal role for tau phosphorylation in human disease. *Biochim Biophys Acta* **1802**, 860-871 (2010).
16. T. Kampers, M. Pangalos, H. Geerts, H. Wiech, E. Mandelkow, Assembly of paired helical filaments from mouse tau: implications for the neurofibrillary pathology in transgenic mouse models for Alzheimer's disease. *FEBS Lett* **451**, 39-44 (1999).
17. I. C. Stancu, B. Vasconcelos, D. Terwel, I. Dewachter, Models of beta-amyloid induced Tau-pathology: the long and "folded" road to understand the mechanism. *Molecular neurodegeneration* **9**, 51 (2014).
18. S. Dutta, P. Sengupta, Men and mice: Relating their ages. *Life Sci* **152**, 244-248 (2016).
19. R. M. Cohen, K. Rezai-Zadeh, T. M. Weitz, A. Rentsendorj, D. Gate, I. Spivak, Y. Bholat, V. Vasilevko, C. G. Glabe, J. J. Breunig, P. Rakic, H. Davtyan, M. G. Agadjanyan, V. Kepe, J. R. Barrio, S. Bannykh, C. A. Szekely, R. N. Pechnick, T. Town, A transgenic Alzheimer rat with plaques, tau pathology, behavioral impairment, oligomeric abeta, and frank neuronal loss. *The Journal of neuroscience : the official journal of the Society for Neuroscience* **33**, 6245-6256 (2013).
20. N. Sahara, J. Lewis, M. DeTure, E. McGowan, D. W. Dickson, M. Hutton, S. H. Yen, Assembly of tau in transgenic animals expressing P301L tau: alteration of phosphorylation and solubility. *Journal of neurochemistry* **83**, 1498-1508 (2002).

21. S. G. Greenberg, P. Davies, A preparation of Alzheimer paired helical filaments that displays distinct tau proteins by polyacrylamide gel electrophoresis. *Proceedings of the National Academy of Sciences of the United States of America* **87**, 5827-5831 (1990).
22. C. Julien, A. Bretteville, E. Planel, Biochemical isolation of insoluble tau in transgenic mouse models of tauopathies. *Methods Mol Biol* **849**, 473-491 (2012).
23. W. Huang da, B. T. Sherman, R. A. Lempicki, Systematic and integrative analysis of large gene lists using DAVID bioinformatics resources. *Nat Protoc* **4**, 44-57 (2009).
24. W. Huang da, B. T. Sherman, R. A. Lempicki, Bioinformatics enrichment tools: paths toward the comprehensive functional analysis of large gene lists. *Nucleic Acids Res* **37**, 1-13 (2009).
25. J. C. Augustinack, A. Schneider, E. M. Mandelkow, B. T. Hyman, Specific tau phosphorylation sites correlate with severity of neuronal cytopathology in Alzheimer's disease. *Acta Neuropathol* **103**, 26-35 (2002).
26. P. T. Nelson, H. Braak, W. R. Markesbery, Neuropathology and cognitive impairment in Alzheimer disease: a complex but coherent relationship. *Journal of neuropathology and experimental neurology* **68**, 1-14 (2009).
27. M. J. Pontecorvo, M. D. Devous, Sr., M. Navitsky, M. Lu, S. Salloway, F. W. Schaerf, D. Jennings, A. K. Arora, A. McGeehan, N. C. Lim, H. Xiong, A. D. Joshi, A. Siderowf, M. A. Mintun, F. A.-A. investigators, Relationships between flortaucipir PET tau binding and amyloid burden, clinical diagnosis, age and cognition. *Brain* **140**, 748-763 (2017).
28. C. Czech, F. Grueninger, Recent advances in the treatment of Alzheimers. *Drug Discovery Today: Therapeutic Strategies* **10**, e73-e78 (2013).
29. E. D. Huey, K. T. Putnam, J. Grafman, A systematic review of neurotransmitter deficits and treatments in frontotemporal dementia. *Neurology* **66**, 17-22 (2006).
30. R. M. Tsai, A. L. Boxer, Treatment of frontotemporal dementia. *Curr Treat Options Neurol* **16**, 319 (2014).
31. F. Ubelmann, T. Burrinha, L. Salavessa, R. Gomes, C. Ferreira, N. Moreno, C. Guimas Almeida, Bin1 and CD2AP polarise the endocytic generation of beta-amyloid. *EMBO Rep* **18**, 102-122 (2017).
32. Y. A. Huang, B. Zhou, M. Wernig, T. C. Sudhof, ApoE2, ApoE3, and ApoE4 Differentially Stimulate APP Transcription and Abeta Secretion. *Cell* **168**, 427-441 e421 (2017).
33. J. Chapuis, F. Hansmannel, M. Gistelinck, A. Mounier, C. Van Cauwenberghe, K. V. Kolen, F. Geller, Y. Sottejeau, D. Harold, P. Dourlen, B. Grenier-Boley, Y. Kamatani, B. Delepine, F. Demiautte, D. Zelenika, N. Zommer, M. Hamdane, C. Bellenguez, J. F. Dartigues, J. J. Hauw, F. Letronne, A. M. Ayral, K. Sleegers, A. Schellens, L. V. Broeck, S. Engelborghs, P. P. De Deyn, R. Vandenberghe, M. O'Donovan, M. Owen, J. Epelbaum, M. Mercken, E. Karran, M. Bantscheff, G. Drewes, G. Joberty, D. Campion, J. N. Octave, C. Berr, M. Lathrop, P. Callaerts, D. Mann, J. Williams, L. Buee, I. Dewachter, C. Van Broeckhoven, P. Amouyel, D. Moechars, B. Dermaut, J. C. Lambert, G. consortium, Increased expression of BIN1 mediates Alzheimer genetic risk by modulating tau pathology. *Molecular psychiatry* **18**, 1225-1234 (2013).
34. Y. Shi, K. Yamada, S. A. Liddelow, S. T. Smith, L. Zhao, W. Luo, R. M. Tsai, S. Spina, L. T. Grinberg, J. C. Rojas, G. Gallardo, K. Wang, J. Roh, G. Robinson, M. B. Finn, H. Jiang, P. M. Sullivan, C. Baufeld, M. W. Wood, C. Sutphen, L. McCue, C. Xiong, J. L. Del-Aguila, J. C. Morris, C. Cruchaga, I. Alzheimer's Disease Neuroimaging, A. M. Fagan, B. L. Miller, A. L. Boxer, W. W. Seeley, O. Butovsky, B. A. Barres, S. M. Paul, D. M. Holtzman, ApoE4 markedly exacerbates tau-mediated neurodegeneration in a mouse model of tauopathy. *Nature* **549**, 523-527 (2017).
35. S. Calafate, W. Flavin, P. Verstreken, D. Moechars, Loss of Bin1 Promotes the Propagation of Tau Pathology. *Cell Rep* **17**, 931-940 (2016).
36. C. M. Hales, N. T. Seyfried, E. B. Dammer, D. Duong, H. Yi, M. Gearing, J. C. Troncoso, E. J. Mufson, M. Thambisetty, A. I. Levey, J. J. Lah, U1 small nuclear ribonucleoproteins (snRNPs) aggregate in Alzheimer's disease due to autosomal dominant genetic mutations and trisomy 21. *Molecular neurodegeneration* **9**, 15 (2014).
37. A. E. Roher, C. L. Maarouf, T. A. Kokjohn, Familial Presenilin Mutations and Sporadic Alzheimer's Disease Pathology: Is the Assumption of Biochemical Equivalence Justified? *Journal of Alzheimer's disease : JAD* **50**, 645-658 (2016).
38. W. D. Knight, A. A. Okello, N. S. Ryan, F. E. Turkheimer, S. Rodriguez Martinez de Llano, P. Edison, J. Douglas, N. C. Fox, D. J. Brooks, M. N. Rossor, Carbon-11-Pittsburgh compound B positron emission tomography imaging of amyloid deposition in presenilin 1 mutation carriers. *Brain* **134**, 293-300 (2011).

39. D. Sepulveda-Falla, J. Matschke, C. Bernreuther, C. Hagel, B. Puig, A. Villegas, G. Garcia, J. Zea, B. Gomez-Mancilla, I. Ferrer, F. Lopera, M. Glatzel, Deposition of hyperphosphorylated tau in cerebellum of PS1 E280A Alzheimer's disease. *Brain Pathol* **21**, 452-463 (2011).
40. M. Brendel, A. Jaworska, E. Griessinger, C. Rotzer, S. Burgold, F. J. Gildehaus, J. Carlsen, P. Cumming, K. Baumann, C. Haass, H. Steiner, P. Bartenstein, J. Herms, A. Rominger, Cross-sectional comparison of small animal [18F]-florbetaben amyloid-PET between transgenic AD mouse models. *PloS one* **10**, e0116678 (2015).
41. Y. T. Quiroz, R. A. Sperling, D. J. Norton, A. Baena, J. F. Arboleda-Velasquez, D. Cosio, A. Schultz, M. Lapoint, E. Guzman-Velez, J. B. Miller, L. A. Kim, K. Chen, P. N. Tariot, F. Lopera, E. M. Reiman, K. A. Johnson, Association Between Amyloid and Tau Accumulation in Young Adults With Autosomal Dominant Alzheimer Disease. *JAMA Neurol*, (2018).
42. B. A. Gordon, T. M. Blazey, Y. Su, A. Hari-Raj, A. Dincer, S. Flores, J. Christensen, E. McDade, G. Wang, C. Xiong, N. J. Cairns, J. Hassenstab, D. S. Marcus, A. M. Fagan, C. R. Jack, Jr., R. C. Hornbeck, K. L. Paumier, B. M. Ances, S. B. Berman, A. M. Brickman, D. M. Cash, J. P. Chhatwal, S. Correia, S. Forster, N. C. Fox, N. R. Graff-Radford, C. la Fougere, J. Levin, C. L. Masters, M. N. Rossor, S. Salloway, A. J. Saykin, P. R. Schofield, P. M. Thompson, M. M. Weiner, D. M. Holtzman, M. E. Raichle, J. C. Morris, R. J. Bateman, T. L. S. Benzinger, Spatial patterns of neuroimaging biomarker change in individuals from families with autosomal dominant Alzheimer's disease: a longitudinal study. *Lancet Neurol* **17**, 241-250 (2018).
43. K. Iqbal, F. Liu, C. X. Gong, I. Grundke-Iqbal, Tau in Alzheimer disease and related tauopathies. *Current Alzheimer research* **7**, 656-664 (2010).
44. M. Espinoza, R. de Silva, D. W. Dickson, P. Davies, Differential incorporation of tau isoforms in Alzheimer's disease. *Journal of Alzheimer's disease : JAD* **14**, 1-16 (2008).
45. M. Hara, K. Hirokawa, S. Kamei, T. Uchihara, Isoform transition from four-repeat to three-repeat tau underlies dendrosomatic and regional progression of neurofibrillary pathology. *Acta Neuropathol* **125**, 565-579 (2013).
46. K. S. Kosik, L. D. Orecchio, S. Bakalis, R. L. Neve, Developmentally regulated expression of specific tau sequences. *Neuron* **2**, 1389-1397 (1989).
47. B. Bai, C. M. Hales, P. C. Chen, Y. Gozal, E. B. Dammer, J. J. Fritz, X. Wang, Q. Xia, D. M. Duong, C. Street, G. Cantero, D. Cheng, D. R. Jones, Z. Wu, Y. Li, I. Diner, C. J. Heilman, H. D. Rees, H. Wu, L. Lin, K. E. Szulwach, M. Gearing, E. J. Mufson, D. A. Bennett, T. J. Montine, N. T. Seyfried, T. S. Wingo, Y. E. Sun, P. Jin, J. Hanfelt, D. M. Willcock, A. Levey, J. J. Lah, J. Peng, U1 small nuclear ribonucleoprotein complex and RNA splicing alterations in Alzheimer's disease. *Proceedings of the National Academy of Sciences of the United States of America* **110**, 16562-16567 (2013).
48. D. Kim, L. H. Tsai, Linking cell cycle reentry and DNA damage in neurodegeneration. *Annals of the New York Academy of Sciences* **1170**, 674-679 (2009).
49. G. T. Bramblett, M. Goedert, R. Jakes, S. E. Merrick, J. Q. Trojanowski, V. M. Lee, Abnormal tau phosphorylation at Ser396 in Alzheimer's disease recapitulates development and contributes to reduced microtubule binding. *Neuron* **10**, 1089-1099 (1993).
50. C. Liu, J. Gotz, Profiling murine tau with 0N, 1N and 2N isoform-specific antibodies in brain and peripheral organs reveals distinct subcellular localization, with the 1N isoform being enriched in the nucleus. *PloS one* **8**, e84849 (2013).
51. H. Zempel, F. J. A. Dennissen, Y. Kumar, J. Luedtke, J. Biernat, E. M. Mandelkow, E. Mandelkow, Axodendritic sorting and pathological missorting of Tau are isoform-specific and determined by axon initial segment architecture. *J Biol Chem* **292**, 12192-12207 (2017).
52. C. Vermeiren, P. Motte, D. Viot, G. Mairet-Coello, J. P. Courade, M. Citron, J. Mercier, J. Hannestad, M. Gillard, The tau positron-emission tomography tracer AV-1451 binds with similar affinities to tau fibrils and monoamine oxidases. *Mov Disord* **33**, 273-281 (2018).
53. A. K. Hansen, D. J. Brooks, P. Borghammer, MAO-B Inhibitors Do Not Block In Vivo Flortaucipir([(18)F]-AV-1451) Binding. *Mol Imaging Biol* **20**, 356-360 (2018).
54. T. Bussiere, G. Gold, E. Kovari, P. Giannakopoulos, C. Bouras, D. P. Perl, J. H. Morrison, P. R. Hof, Stereologic analysis of neurofibrillary tangle formation in prefrontal cortex area 9 in aging and Alzheimer's disease. *Neuroscience* **117**, 577-592 (2003).
55. C. Duyckaerts, M. Bennecib, Y. Grignon, T. Uchihara, Y. He, F. Piette, J. J. Hauw, Modeling the relation between neurofibrillary tangles and intellectual status. *Neurobiology of aging* **18**, 267-273 (1997).

56. A. Metaxas, R. Vaitheeswaran, S. Li, K. L. Lambertsen, B. Finsen, Modeling progressive cognitive impairment in the APPswe/PS1dE9 mouse model of amyloidosis by using the Barnes maze test. Program No. 012.02. 2017 Neuroscience Meeting Planner. Washington, DC: *Society for Neuroscience*, 2017. Online.
57. J. L. Jankowsky, D. J. Fadale, J. Anderson, G. M. Xu, V. Gonzales, N. A. Jenkins, N. G. Copeland, M. K. Lee, L. H. Younkin, S. L. Wagner, S. G. Younkin, D. R. Borchelt, Mutant presenilins specifically elevate the levels of the 42 residue beta-amyloid peptide in vivo: evidence for augmentation of a 42-specific gamma secretase. *Hum Mol Genet* **13**, 159-170 (2004).
58. N. Kuninaka, M. Kawaguchi, M. Ogawa, A. Sato, K. Arima, S. Murayama, Y. Saito, Simplification of the modified Gallyas method. *Neuropathology* **35**, 10-15 (2015).
59. A. Sun, X. V. Nguyen, G. Bing, Comparative analysis of an improved thioflavin-s stain, Gallyas silver stain, and immunohistochemistry for neurofibrillary tangle demonstration on the same sections. *J Histochem Cytochem* **50**, 463-472 (2002).
60. M. Marquie, M. D. Normandin, C. R. Vanderburg, I. M. Costantino, E. A. Bien, L. G. Rycyna, W. E. Klunk, C. A. Mathis, M. D. Ikonomovic, M. L. Debnath, N. Vasdev, B. C. Dickerson, S. N. Gomperts, J. H. Growdon, K. A. Johnson, M. P. Frosch, B. T. Hyman, T. Gomez-Isla, Validating novel tau positron emission tomography tracer [F-18]-AV-1451 (T807) on postmortem brain tissue. *Annals of neurology* **78**, 787-800 (2015).
61. S. J. Kempf, A. Metaxas, M. Ibanez-Vea, S. Darvesh, B. Finsen, M. R. Larsen, An integrated proteomics approach shows synaptic plasticity changes in an APP/PS1 Alzheimer's mouse model. *Oncotarget* **7**, 33627-33648 (2016).
62. S. J. Kempf, A. Casciati, S. Buratovic, D. Janik, C. von Toerne, M. Ueffing, F. Neff, S. Moertl, B. Stenerlow, A. Saran, M. J. Atkinson, P. Eriksson, S. Pazzaglia, S. Tapio, The cognitive defects of neonatally irradiated mice are accompanied by changed synaptic plasticity, adult neurogenesis and neuroinflammation. *Molecular neurodegeneration* **9**, 57 (2014).
63. E. W. Deutsch, A. Csordas, Z. Sun, A. Jarnuczak, Y. Perez-Riverol, T. Ternent, D. S. Campbell, M. Bernal-Llinares, S. Okuda, S. Kawano, R. L. Moritz, J. J. Carver, M. Wang, Y. Ishihama, N. Bandeira, H. Hermjakob, J. A. Vizcaino, The ProteomeXchange consortium in 2017: supporting the cultural change in proteomics public data deposition. *Nucleic Acids Res* **45**, D1100-D1106 (2017).
64. J. A. Vizcaino, A. Csordas, N. del-Toro, J. A. Dianes, J. Griss, I. Lavidas, G. Mayer, Y. Perez-Riverol, F. Reisinger, T. Ternent, Q. W. Xu, R. Wang, H. Hermjakob, 2016 update of the PRIDE database and its related tools. *Nucleic Acids Res* **44**, D447-456 (2016).
65. F. Gallyas, Silver staining of Alzheimer's neurofibrillary changes by means of physical development. *Acta Morphol Acad Sci Hung* **19**, 1-8 (1971).
66. T. M. Shoup, D. L. Yokell, P. A. Rice, R. N. Jackson, E. Livni, K. A. Johnson, T. J. Brady, N. Vasdev, A concise radiosynthesis of the tau radiopharmaceutical, [(18) F]T807. *J Labelled Comp Radiopharm* **56**, 736-740 (2013).
67. K. Engholm-Keller, P. Birck, J. Storling, F. Pociot, T. Mandrup-Poulsen, M. R. Larsen, TiSH--a robust and sensitive global phosphoproteomics strategy employing a combination of TiO2, SIMAC, and HILIC. *J Proteomics* **75**, 5749-5761 (2012).
68. M. R. Larsen, S. S. Jensen, L. A. Jakobsen, N. H. Heegaard, Exploring the sialiome using titanium dioxide chromatography and mass spectrometry. *Mol Cell Proteomics* **6**, 1778-1787 (2007).
69. D. E. McNulty, R. S. Annan, Hydrophilic interaction chromatography reduces the complexity of the phosphoproteome and improves global phosphopeptide isolation and detection. *Mol Cell Proteomics* **7**, 971-980 (2008).
70. M. N. Melo-Braga, M. Ibanez-Vea, M. R. Larsen, K. Kulej, Comprehensive protocol to simultaneously study protein phosphorylation, acetylation, and N-linked sialylated glycosylation. *Methods Mol Biol* **1295**, 275-292 (2015).
71. M. Morris, G. M. Knudsen, S. Maeda, J. C. Trinidad, A. Ioanoviciu, A. L. Burlingame, L. Mucke, Tau post-translational modifications in wild-type and human amyloid precursor protein transgenic mice. *Nat Neurosci* **18**, 1183-1189 (2015).
72. M. Grebing, H. H. Nielsen, C. D. Fenger, T. J. K, C. U. von Linstow, B. H. Clausen, M. Soderman, K. L. Lambertsen, M. Thomassen, T. A. Kruse, B. Finsen, Myelin-specific T cells induce interleukin-1beta expression in lesion-reactive microglial-like cells in zones of axonal degeneration. *Glia* **64**, 407-424 (2016).

73. P. McMillan, E. Korvatska, P. Poorkaj, Z. Evstafjeva, L. Robinson, L. Greenup, J. Leverenz, G. D. Schellenberg, I. D'Souza, Tau isoform regulation is region- and cell-specific in mouse brain. *J Comp Neurol* **511**, 788-803 (2008).
74. G. Paxinos, K. B. J. Franklin, *The mouse brain in stereotaxic coordinates*. (Academic Press, San Diego, ed. 2nd, 2001).
75. A. Metaxas, R. Vaitheeswaran, K. T. Jensen, C. Thygesen, L. Ilkjaer, S. Darvesh, B. Finsen, Reduced Serotonin Transporter Levels and Inflammation in the Midbrain Raphe of 12 Month Old APPswe/PSEN1dE9 Mice. *Current Alzheimer research* **15**, 420-428 (2018).
76. C. Li, X. D. Guo, M. Lei, J. Y. Wu, J. Z. Jin, X. F. Shi, Z. Y. Zhu, V. Rukachaisirikul, L. H. Hu, T. Q. Wen, X. Shen, Thamnolia vermicularis extract improves learning ability in APP/PS1 transgenic mice by ameliorating both Abeta and Tau pathologies. *Acta Pharmacol Sin* **38**, 9-28 (2017).
77. C. Tapia-Rojas, F. Aranguiz, L. Varela-Nallar, N. C. Inestrosa, Voluntary Running Attenuates Memory Loss, Decreases Neuropathological Changes and Induces Neurogenesis in a Mouse Model of Alzheimer's Disease. *Brain Pathol* **26**, 62-74 (2016).
78. T. Li, K. E. Braunstein, J. Zhang, A. Lau, L. Sibener, C. Deeble, P. C. Wong, The neuritic plaque facilitates pathological conversion of tau in an Alzheimer's disease mouse model. *Nature communications* **7**, 12082 (2016).
79. X. T. Huang, Z. M. Qian, X. He, Q. Gong, K. C. Wu, L. R. Jiang, L. N. Lu, Z. J. Zhu, H. Y. Zhang, W. H. Yung, Y. Ke, Reducing iron in the brain: a novel pharmacologic mechanism of huperzine A in the treatment of Alzheimer's disease. *Neurobiology of aging* **35**, 1045-1054 (2014).
80. E. Barbero-Camps, A. Fernandez, L. Martinez, J. C. Fernandez-Checa, A. Colell, APP/PS1 mice overexpressing SREBP-2 exhibit combined Abeta accumulation and tau pathology underlying Alzheimer's disease. *Hum Mol Genet* **22**, 3460-3476 (2013).
81. I. Carrera, I. Etcheverria, L. Fernandez-Novoa, V. Lombardi, R. Cacabelos, C. Vigo, Vaccine Development to Treat Alzheimer's Disease Neuropathology in APP/PS1 Transgenic Mice. *Int J Alzheimers Dis* **2012**, 376138 (2012).
82. G. I. Cancino, K. Perez de Arce, P. U. Castro, E. M. Toledo, R. von Bernhardi, A. R. Alvarez, c-Abl tyrosine kinase modulates tau pathology and Cdk5 phosphorylation in AD transgenic mice. *Neurobiology of aging* **32**, 1249-1261 (2011).
83. N. C. Inestrosa, C. Tapia-Rojas, T. N. Griffith, F. J. Carvajal, M. J. Benito, A. Rivera-Dictter, A. R. Alvarez, F. G. Serrano, J. L. Hancke, P. V. Burgos, J. Parodi, L. Varela-Nallar, Tetrahydrohyperforin prevents cognitive deficit, Abeta deposition, tau phosphorylation and synaptotoxicity in the APPswe/PSEN1DeltaE9 model of Alzheimer's disease: a possible effect on APP processing. *Transl Psychiatry* **1**, e20 (2011).
84. Y. Ding, A. Qiao, Z. Wang, J. S. Goodwin, E. S. Lee, M. L. Block, M. Allsbrook, M. P. McDonald, G. H. Fan, Retinoic acid attenuates beta-amyloid deposition and rescues memory deficits in an Alzheimer's disease transgenic mouse model. *The Journal of neuroscience : the official journal of the Society for Neuroscience* **28**, 11622-11634 (2008).
85. M. Ettcheto, E. Sanchez-Lopez, L. Pons, O. Busquets, J. Olloquequi, C. Beas-Zarate, M. Pallas, M. L. Garcia, C. Auladell, J. Folch, A. Camins, Dexibuprofen prevents neurodegeneration and cognitive decline in APPswe/PS1dE9 through multiple signaling pathways. *Redox Biol* **13**, 345-352 (2017).
86. X. L. Bu, Y. Xiang, W. S. Jin, J. Wang, L. L. Shen, Z. L. Huang, K. Zhang, Y. H. Liu, F. Zeng, J. H. Liu, H. L. Sun, Z. Q. Zhuang, S. H. Chen, X. Q. Yao, B. Giunta, Y. C. Shan, J. Tan, X. W. Chen, Z. F. Dong, H. D. Zhou, X. F. Zhou, W. Song, Y. J. Wang, Blood-derived amyloid-beta protein induces Alzheimer's disease pathologies. *Molecular psychiatry*, (2017).
87. S. H. Yang, D. K. Lee, J. Shin, S. Lee, S. Baek, J. Kim, H. Jung, J. M. Hah, Y. Kim, Nec-1 alleviates cognitive impairment with reduction of Abeta and tau abnormalities in APP/PS1 mice. *EMBO Mol Med* **9**, 61-77 (2017).
88. J. Zhang, S. Wang, W. Huang, D. A. Bennett, D. W. Dickson, D. Wang, R. Wang, Tissue Transglutaminase and Its Product Isopeptide Are Increased in Alzheimer's Disease and APPswe/PS1dE9 Double Transgenic Mice Brains. *Mol Neurobiol* **53**, 5066-5078 (2016).
89. Y. Du, J. Qu, W. Zhang, M. Bai, Q. Zhou, Z. Zhang, Z. Li, J. Miao, Morin reverses neuropathological and cognitive impairments in APPswe/PS1dE9 mice by targeting multiple pathogenic mechanisms. *Neuropharmacology* **108**, 1-13 (2016).
90. S. Jeon, J. E. Park, J. Lee, Q. F. Liu, H. J. Jeong, S. C. Pak, S. Yi, M. H. Kim, C. W. Kim, J. K. Park, G. W. Kim, B. S. Koo, Illite improves memory impairment and reduces Abeta level in the Tg-APPswe/PS1dE9

mouse model of Alzheimers disease through Akt/CREB and GSK-3beta phosphorylation in the brain. *J Ethnopharmacol* **160**, 69-77 (2015).

91. J. Y. Vargas, J. Ahumada, M. S. Arrazola, M. Fuenzalida, N. C. Inestrosa, WASP-1, a canonical Wnt signaling potentiator, rescues hippocampal synaptic impairments induced by Abeta oligomers. *Experimental neurology* **264**, 14-25 (2015).
92. Q. Zhou, M. Wang, Y. Du, W. Zhang, M. Bai, Z. Zhang, Z. Li, J. Miao, Inhibition of c-Jun N-terminal kinase activation reverses Alzheimer disease phenotypes in APPswe/PS1dE9 mice. *Annals of neurology* **77**, 637-654 (2015).
93. I. Pedros, D. Petrov, M. Allgaier, F. Sureda, E. Barroso, C. Beas-Zarate, C. Auladell, M. Pallas, M. Vazquez-Carrera, G. Casadesus, J. Folch, A. Camins, Early alterations in energy metabolism in the hippocampus of APPswe/PS1dE9 mouse model of Alzheimer's disease. *Biochim Biophys Acta* **1842**, 1556-1566 (2014).
94. E. Aso, S. Juves, R. Maldonado, I. Ferrer, CB2 cannabinoid receptor agonist ameliorates Alzheimer-like phenotype in AbetaPP/PS1 mice. *Journal of Alzheimer's disease : JAD* **35**, 847-858 (2013).
95. E. Aso, S. Lomoio, I. Lopez-Gonzalez, L. Joda, M. Carmona, N. Fernandez-Yague, J. Moreno, S. Juves, A. Pujol, R. Pamplona, M. Portero-Otin, V. Martin, M. Diaz, I. Ferrer, Amyloid generation and dysfunctional immunoproteasome activation with disease progression in animal model of familial Alzheimer's disease. *Brain Pathol* **22**, 636-653 (2012).
96. L. Li, T. Cheung, J. Chen, K. Herrup, A comparative study of five mouse models of Alzheimer's disease: cell cycle events reveal new insights into neurons at risk for death. *Int J Alzheimers Dis* **2011**, 171464 (2011).
97. C. Wei, W. Zhang, Q. Zhou, C. Zhao, Y. Du, Q. Yan, Z. Li, J. Miao, Mithramycin A Alleviates Cognitive Deficits and Reduces Neuropathology in a Transgenic Mouse Model of Alzheimer's Disease. *Neurochem Res* **41**, 1924-1938 (2016).
98. D. Porquet, P. Andres-Benito, C. Grinan-Ferre, A. Camins, I. Ferrer, A. M. Canudas, J. Del Valle, M. Pallas, Amyloid and tau pathology of familial Alzheimer's disease APP/PS1 mouse model in a senescence phenotype background (SAMP8). *Age (Dordr)* **37**, 9747 (2015).
99. J. J. Ramos-Rodriguez, O. Ortiz-Barajas, C. Gamero-Carrasco, P. R. de la Rosa, C. Infante-Garcia, N. Zopeque-Garcia, A. M. Lechuga-Sancho, M. Garcia-Alloza, Prediabetes-induced vascular alterations exacerbate central pathology in APPswe/PS1dE9 mice. *Psychoneuroendocrinology* **48**, 123-135 (2014).
100. J. Q. Shi, B. R. Wang, Y. Y. Tian, J. Xu, L. Gao, S. L. Zhao, T. Jiang, H. G. Xie, Y. D. Zhang, Antiepileptics topiramate and levetiracetam alleviate behavioral deficits and reduce neuropathology in APPswe/PS1dE9 transgenic mice. *CNS Neurosci Ther* **19**, 871-881 (2013).
101. J. J. Ramos-Rodriguez, S. Molina-Gil, R. Rey-Brea, E. Berrocoso, M. Garcia-Alloza, Specific serotonergic denervation affects tau pathology and cognition without altering senile plaques deposition in APP/PS1 mice. *PloS one* **8**, e79947 (2013).
102. S. Lomoio, I. Lopez-Gonzalez, E. Aso, M. Carmona, B. Torrejon-Escribano, E. Scherini, I. Ferrer, Cerebellar amyloid-beta plaques: disturbed cortical circuitry in AbetaPP/PS1 transgenic mice as a model of familial Alzheimer's disease. *Journal of Alzheimer's disease : JAD* **31**, 285-300 (2012).
103. Y. S. Hu, P. Xu, G. Pigino, S. T. Brady, J. Larson, O. Lazarov, Complex environment experience rescues impaired neurogenesis, enhances synaptic plasticity, and attenuates neuropathology in familial Alzheimer's disease-linked APPswe/PS1DeltaE9 mice. *FASEB J* **24**, 1667-1681 (2010).
104. M. Demars, Y. S. Hu, A. Gadadhar, O. Lazarov, Impaired neurogenesis is an early event in the etiology of familial Alzheimer's disease in transgenic mice. *J Neurosci Res* **88**, 2103-2117 (2010).

Acknowledgments: We thank Andrew Reid, senior technician and manager of the Maritime Brain Tissue Bank, for organizing the transportation of human tissue. We acknowledge the Core Facility for Integrated Microscopy, Faculty of Health and Medical Sciences, University of Copenhagen, for assisting with TEM. The Villum Center for Bioanalytical Sciences at SDU is acknowledged for supporting the proteomics part of the study. Precursor material for the synthesis of [^{18}F]Flortaucipir was generously supplied by AVID Radiopharmaceuticals, Philadelphia, PA, USA.

Funding: This work was supported by SDU2020 (CoPING AD: Collaborative Project on the Interaction between Neurons and Glia in AD) and the A.P. Møller og Hustru Chastine Mc-Kinney Møllers Fond.

Author contributions: AM designed the project and wrote the manuscript, performed (immuno)histochemistry, autoradiography, tau isolation studies, and assisted with TEM. CT and SJK performed proteomics and immunoblotting. MA and RV performed tissue sectioning, (immuno)histochemistry, autoradiography and tau filament analysis. SP performed PCR and tau Meso Scale. AML organized and performed autoradiography. HA synthesized [^{18}F]Flortaucipir. JLT performed (immuno)histochemistry and provided Tg2576 tissue, SD provided human tissues and critically reviewed the manuscript. DJB, MRL and BF supervised the project and contributed to its design. All authors assisted with data interpretation, participated in drafting the manuscript and approved its final version.

Competing interests: None related to the design and completion of this study.

Data and materials availability: The proteomics data have been deposited to the ProteomeXchange Consortium (*63*) via the PRIDE partner repository with the dataset identifier

PXD009306 [username: reviewer39090@ebi.ac.uk; password: HdJxxVxU (*64*)]. The MC-1 antibody, and material for the synthesis of [^{18}F]Flortaucipir were obtained through an MTA.

Supplementary Materials:

Materials and Methods

Gallyas silver staining

The Kuninaka et al. simplification of the modified Gallyas method was used to examine neurofibrillary pathology (*58, 65*). Fresh-frozen sections were directly immersed in 4% neutral buffered formalin (NBF) at 4°C for 24 h. The sections were thoroughly washed in ultrapure deionized H_2O (dH_2O; Ultra Clear^{TM}, Siemens), dried at room temperature (RT) for 10 min and defatted for 1 h in a solution of chloroform/99% ethanol (1:1) in the dark. Following hydration through a series of graded ethanols into dH_2O (2 x 1 min: 99%, 96%, 70%), slides were immersed into an aqueous solution of 0.25% potassium permanganate (20 min), washed in dH_2O (1 min), and incubated in 1% oxalic acid (2 min). After washing in dH_2O (2 x 5 min), sections were transferred into the alkaline silver iodide solution (1 min), washed with 0.5% acetic acid (2 x 5 min), and developed in a water bath at 15°C, until the appearance of a brownish shade (12-14 min). The developed sections were washed in 0.5% acetic acid (3 min), toned with 0.1% gold chloride (10 min), fixed with 1% sodium thiosulfate (5 min), and counterstained with 0.1% nuclear fast red (3 min). Ethanol and chloroform were from VWR International. The remaining chemicals were from Sigma-Aldrich Co.

Aβ immunohistochemistry on silver-stained sections

The biotinylated 6E10 antibody (SIG-39340, Nordic BioSite) was used to investigate the association between neurofibrillary pathology and Aβ load in *APP*$_{swe}$/*PS1*$_{\Delta E9}$ mice. Clone 6E10 is raised against amino acids 1-16 of human Aβ, recognizing multiple amyloid peptides and precursor forms (manufacturer information). Silver-stained sections were immersed in 70%

formic acid for 30 min, rinsed for 10 min in 50 mM Tris-buffered saline (TBS, pH 7.4), and further washed/permeabilised in TBS containing 1% Triton X-100 (3 x 15 min). Sections were subsequently blocked for 30 min in TBS, containing 10% fetal bovine serum (FBS). Incubation with the 6E10 anti-β-amyloid antibody was carried out overnight at 4°C, in TBS containing 10% FBS (1:500 dilution of stock). Adjacent, negative control sections were incubated with biotin-labeled mouse IgG1 (MG115, Thermo Fisher Scientific), diluted to the same protein concentration as the primary antibody. Following incubation with 6E10, the sections were adjusted to RT for 30 min and washed in TBS+1% Triton X-100 (3 x 15 min). Endogenous peroxidase activity was quenched for 20 min in a solution of TBS/methanol/H_2O_2 (8:1:1). After washing in TBS+1% Triton X-100 (3 x 15 min), sections were incubated for 3 h with HRP-streptavidin in TBS/10% FBS (1:200; GE Healthcare Life Sciences). After a final wash in TBS (3 x 10 min), peroxidase activity was visualised with 0.05% 3,3′diaminobenzidine (DAB) in TBS buffer, containing 0.01% H_2O_2 (Sigma Aldrich Co.).

MC-1 immunohistochemistry

Fresh-frozen sections were directly immersed in 4% NBF at 4°C for 24 h. The sections were thoroughly washed in dH_2O, dried at RT for 10 min, and defatted for 1 h in a solution of chloroform/99% ethanol (1:1) in the dark. Following hydration through a series of graded ethanols into dH_2O (2 x 1 min: 99%, 96%, 70%), endogenous peroxidase activity was quenched for 30 min with 1.5% H_2O_2 in TBS. The sections were washed and blocked for 1 h at RT using 10% FBS in 0.05% Triton X-100 (TBS-Tx; blocking buffer). The mouse anti-human MC-1 antibody, a generous gift from Dr. Peter Davies, was diluted in blocking buffer (1:10 dilution of stock). Negative control sections were incubated in blocking buffer with mouse IgG1 (1:100;

MG100, Thermo Fisher Scientific). Following overnight incubation at 4°C, the sections were washed in TBS-Tx (4 x 5 min) and incubated at RT for 3 h with biotin-labeled goat anti-mouse IgG1 (abcam, ab97238), diluted 1:300 in TBS-Tx, containing 50% Superblock (Thermo Fisher Scientific; #37580). After washing in TBS-Tx (4 x 5 min), sections were incubated for 1 h with HRP-streptavidin, diluted 1:200 in TBS-Tx containing 50% Superblock. The sections were washed in TBS (4 x 5 min) and developed with 50 mg DAB and 0.01% H_2O_2, in TBS containing 10 mM imidazole and 0.5% nickel ammonium hexahydrate (pH 7.4).

For all light microscopy studies, the developed sections were thoroughly washed in dH_2O, dehydrated in graded alcohols, cleared in xylene, and cover-slipped with PERTEX® (Histolab Products AB).

Thioflavin-S staining

Thioflavin-S staining was performed according to Sun et al. (*59*). Fresh-frozen sections were directly immersed in 4% NBF at 4°C for 24 h. The sections were thoroughly washed in ultrapure dH_2O, dried at RT for 10 min, and defatted for 1 h in a solution of chloroform/99% ethanol (1:1) in the dark. Following hydration through a series of graded ethanols into dH_2O (2 x 1 min: 99%, 96%, 70%), slides were immersed into an aqueous solution of 0.25% potassium permanganate (5 min), washed in dH_2O (1 min), and incubated in 1% oxalic acid (2 min). After washing in dH_2O (2 x 2.5 min), the sections were incubated with freshly-prepared 0.25% $NaBH_4$ (2 x 5 min), washed in dH_2O (5 x 2 min), and transferred into a 0.1% thioflavin-S solution (8 min; dark incubation). The sections were differentiated in 80% ethanol (2 x 10 s), washed in dH_2O (3 x 5 dips), and incubated for 30 min at 4ºC in the dark with high-concentration phosphate buffer, to

prevent photobleaching (411 mM NaCl, 8.1 mM KCl, 30 mM Na_2HPO_4; 5.2 mM KH_2PO_4). Following a dip in dH_2O, the sections were counterstained with DAPI (30 µM) for 10 min and mounted with Aquatex® mounting medium (Sigma Aldrich Co.).

Immuno(histochemistry) images were acquired with an Olympus DP71 digital camera, mounted on an Olympus BX51 microscope equipped for Epi-Fluorescence illumination, or an Olympus DP80 Dual Monochrome CCD camera, mounted on a motorized BX63 Olympus microscope.

[^{18}F]Flortaucipir autoradiography

Autoradiography experiments were conducted at the Department of Nuclear Medicine and PET-centre, Aarhus University, Denmark. [^{18}F]Flortaucipir was synthesised in Aarhus using previously detailed methods (*66*).

[^{18}F]Flortaucipir autoradiography was performed as described previously (*60*), with minor modifications. Sections were thawed to RT for 20 min and fixed/permeabilised in 100% methanol for 20 min. The sections were incubated for a period of 60 min in a 160 mL bath of 10 mM phosphate buffered saline (PBS, pH 7.4), containing 38.4±9.6 MBq [^{18}F]Flortaucipir (specific activity: 145±68 GBq/µmol). A series of adjacent brain sections was incubated with identical amounts of radioligand in the presence of 50 µM 'cold' flortaucipir, to assess non-specific binding (NSB). Following incubation, sections were serially washed in PBS (1 min), 70% ethanol in PBS (2 x 1min), 30% ethanol in PBS (1 min) and PBS (1 min). After rapid drying under a stream of cold air, the sections were placed in light-tight cassettes and exposed against FUJI multi-sensitive phosphor screens for 30 min (BAS-IP SR2025, GE Healthcare Life

Sciences). To allow quantification, standards of known radioactive concentration were prepared by serial dilution of the [^{18}F]Flortaucipir incubation solution, and exposed along with the sections. Images were developed in a BAS-5000 phosphor-imager at 25 µm resolution.

For image analysis, the intensity values produced by the ^{18}F standards were entered with their corresponding radioactivity values (kBq/mL) into a calibration table, and the relationship between radioactivity and intensity determined by using ImageJ software (v. 1.51c; National Institutes of Health, USA). Adjustments were undertaken to allow for the radioactive decay of [^{18}F]Flortaucipir. Values of specific binding were derived after subtraction of NSB from total binding images.

Isolation of sarkosyl-insoluble Tau

The general procedure by Greenberg and Davies (*21*) was used to isolate PHFs. Left brain hemispheres from two mice per group were pooled and weighed (467.1±3.1 mg). The tissue was thoroughly homogenised with a motor driven Potter-Elvehjem tissue grinder (WHEATON), in a 5-fold excess (v/w) of 10 mM Tris-HCl buffer (pH 7.4), containing 800 mM NaCl, 1 mM EGTA, 10% sucrose, protease inhibitors (cOmplete^{TM} Protease Inhibitor; Roche Diagnostics) and phosphatase inhibitors (PhosSTOP^{TM}; Roche Diagnostics; H buffer). The homogenate was centrifuged at 4°C for 20 min in a refrigerated ultracentrifuge (27,000 x g; Sorvall RC M150 GX). The supernatant was decanted and kept on ice, the pellet (P1) suspended in 5 vol of H-buffer and re-centrifuged at 27,000 x g for 20 min (4°C). The combined supernatants (S1) were brought to 1% sarkosyl in H buffer and incubated for 2 h at 37°C in a C24 incubator shaker (100 rpm; New Brunswick Scientific). Following centrifugation at 200,000 x g for 40 min (4°C), the

sarkosyl-soluble fraction was decanted and kept on ice, and the sarkosyl-insoluble pellet suspended in H buffer, containing 1% CHAPS hydrate (Sigma Aldrich Co.). After filtering through acetate cellulose filters (0.45 µm; VWR International), the filtrates were centrifuged at 200,000 g for 70 min, and the final pellet suspended in 250 µL dH_2O. Aliquots of 150 µL from the P1, S1, sarkosyl soluble and insoluble fractions were kept for determining Tau protein levels. Samples were stored at -80°C until further processed.

Tau Meso Scale

Tau protein concentration in soluble and insoluble fractions was measured with the mouse Total Tau kit (K151DSD-1; Mesoscale Diagnostics LLC). The anti-mouse monoclonal antibody used for detection binds between amino acids 150-200 of Tau, but the clone number and exact epitope recognition site(s) are proprietary. Plates were processed in a SECTOR® Imager 6000 plate reader (Meso Scale Diagnostics LLC), and data acquired with Discovery Workbench software (v.4.0; Meso Scale Diagnostics LLC). Results are presented as pg of Tau/mg of total protein, the latter measured at A562 nm with a Pierce™ BCA protein kit and bovine serum albumin as standard (Thermo Fisher Scientific).

Transmission electron microscopy (TEM)

Electron microscopy was performed in the Core Facility for Integrated Microscopy, Faculty of Health and Medical Sciences, University of Copenhagen, Denmark. Carbon-coated copper grids (200 mesh; Ted Pella Inc.) were glow-discharged with a Leica EM ACE 200 (Leica Biosystems Nussloch GmbH), and loaded with 6 µL of sarkosyl-insoluble sample. The sample was adsorbed for 1 min, blotted and stained with 2% phosphotungstic acid in dH_20 for 2 min. After blotting

and a quick wash with dH_20, the samples were examined with a Philips CM 100 TEM (Koninklijke Philips N.V.), operated at an accelerating voltage of 80 kV. Digital images were acquired at a nominal magnification of x180,000, by using an OSIS Veleta digital slow scan 2k x 2k CCD camera and the iTEM software package (Olympus Corporation). Filaments shorter and longer than 200 µm were analyzed in at least two fields of view with ImageJ software. Reported values are mean ± SEM of 70 and 32 PHFs for *APP*$_{swe}$/*PS1*$_{\Delta E9}$ and AD tissue, respectively.

Mass spectrometry-based proteomics

Reduction, alkylation and enzymatic digestion

Sarkosyl-insoluble samples were dried down and denatured at RT with 6 M Urea, 2 M Thiourea and 10 mM dithiothreithol (DTT; Sigma-Aldrich Co.) in dH_2O (pH 7.5), supplemented with cOmplete™ protease inhibitors and PhosSTOP™ phosphatase inhibitors (Roche Diagnostics). After vortexing and sonication, 100 µg total protein/condition was alkylated in 20 mM iodoacetamide (IAA) for 20 min in the dark. A total of 2 µL of endoproteinase Lys-C was added to the protein sample (6 µg/µL; Wako Chemicals GmbH), and the solution incubated for 2 h at RT. The sample was then diluted 10 times with 20 mM TEAB, pH 7.5, and digested with trypsin overnight (1:50 w/w trypsin:protein). The enzymatic digestion was stopped with 5% formic acid (FA) and the peptide sample cleared by centrifugation (14,000 x g, 15 min). Protein and peptide quantification was performed by Qubit™ fluorometric quantitation (Invitrogen™).

Tandem Mass Tag (TMT) labeling

A total of 100 µg tryptic peptides were dried and desalted with R2/R3 columns, before TMT-10plex labeling (AB Sciex Pte. Ltd.). The desalting procedure is detailed below. Labeling was

performed according to manufacturer instructions: TMT-126 for WT-3 months(1), TMT-127N WT-3 months(2), TMT-127C Tg-3 months(1), TMT-128N Tg-3 months(2), TMT-128C for WT-24 months(1), TMT-129N for WT-24 months(2), TMT-129C for Tg-24 months(1), 130N for Tg-24 months(2), TMT-130C for human non-AD and TMT-131 for human AD. The labeled peptides from all groups were mixed 1:1, dried down and stored for further enrichment and analysis. Human AD and non-AD samples were included for validation, as well as for taking advantage of the stacking effect of the TMT10-plex, in order to increase identification rates.

Enrichment of phosphopeptides and formerly sialylated N-linked glycopeptides (deglycosylated)

Multi- and mono-phosphorylated peptides, as well as sialylated N-linked glycopeptides, were separated from unmodified peptides by using a TiO_2 workflow (*67*). Modified peptides bind to TiO_2 beads because the phospho and sialic groups are acidic and retained on the column, whereas unmodified peptides flow-through. The eluted modified peptides were deglycosylated to remove N-linked glycans (*68*). Hydrophilic interaction chromatography (HILIC) was used for sample fractionation prior to nano liquid chromatography-tandem mass spectrometry [LC-MS/MS; (*67*)].

Briefly, the combined labelled peptides (~1000 µg) were dissolved in TiO_2 loading buffer [80% acetonitrile (ACN), 5% trifluoroacetic acid (TFA), 1 M glycolic acid] and incubated for 30 min at RT with 6 mg of TiO_2 beads (5020 Titansphere^{TM} TiO_2, 5 µm; gift from GL Sciences). The beads were sequentially washed with TiO_2 loading buffer, 80% ACN/1% TFA and 10% ACN/0.1% TFA. Modified peptides were eluted with 1.5% ammonium hydroxide solution, pH 11.3, and dried-down in a vacuum centrifuge. The unbound TiO_2 fraction and the combined

washing fractions contain unmodified peptides. The dried modified peptides were deglycosylated at 37°C overnight in 20 mM TEAB buffer, pH 8.0, containing N-glycosidase F (P0705L, New England Biolabs Inc.) and Sialidase A™ (GK80046, ProZyme). Unmodified and modified peptides were dried and desalted on micro-columns before capillary HILIC fractionation.

Sample desalting with R2/R3 micro-column

Samples were desalted by using home-made P200 tip-based columns, packed with equal ratios of reversed-phase resin material Poros R2 (Oligo R2 Reversed Phase Resin 1-1112-46, Thermo Fisher Scientific) and Poros R3 (OligoR3 Reversed Phase Resin 1-1339-03, Thermo Fisher Scientific). The end of the tip was blocked with C8 material (Model 2314, 3m Empore™ C8). The column was prepared by short centrifugation (1000 x g) of the R3 reversed-phase resin (100% ACN), equilibrated with 0.1% TFA, and centrifuged again. The acidified samples were loaded onto the columns and washed three times with 0.1% TFA. Peptides were eluted with 50% ACN, 0.1% TFA and dried by vacuum centrifugation.

HILIC fractionation

The fractions containing unmodified peptides were fractionated prior to nanoLC-MS/MS analysis using HILIC, as described previously (*69*, *70*). Peptides were dissolved in 90% ACN, 0.1% TFA (solvent B), and loaded onto a 450 µm OD x 320 µm ID x 17 cm micro-capillary column packed with TSK Amide-80 (3 µm; Tosoh Bioscience LLC). The peptides were separated on a 1200 Series HPLC (Agilent Technologies) over 30 min, by using a gradient from 100–60% solvent B (A = 0.1% TFA), at a flow-rate of 6 µL/min. Fractions were collected every

1 min based on the UV chromatogram. Subsequently, the peptide fractions were dried by vacuum centrifugation.

Reversed-phase nanoLC-ESI-MS/MS

The peptides were resuspended in 0.1% FA, and automatically injected on a ReproSil-Pur C18 AQ, in-house packed-trap column (Dr. Maisch GmbH; 2 cm x 100 µm inner diameter; 5 µm). The peptides were separated by reversed phase chromatography at 250 nL/min on an analytical ReproSil-Pur C18 AQ column (Dr. Maisch GmbH), packed in-house (17 cm x 75 µm; 3 µm), which was operated on an EASY-nanoLC system (Thermo Fisher Scientific). Mobile phase was 95% ACN/ 0.1% FA (B) and water/0.1% FA (A). The gradient was from 1% to 30% B over 80 min for mono-phosphorylated, deglycosylated and unmodified peptides, and 1% to 30% solvent B over 110 min for multi-phosphorylated peptides, followed by 30 - 50% B over 10 min, 50 - 100% B over 5 min, and 8 min at 100% B. The nano-LC was connected online to a Q Exactive HF Hybrid Quadrupole-Orbitrap mass spectrometer (Thermo Fisher Scientific), operating in positive ion mode and using data-dependent acquisition. The eluent was directed toward the ion transfer tube of the Orbitrap instrument by dynamic electrospray ionization. The Orbitrap acquired the full MS scan with an automatic gain control target value of $3x10^6$ ions and a maximum fill time of 100 ms. Each MS scan was acquired in the Orbitrap at high-resolution [120,000 full-width half maximum (FWHM)] at m/z 200 with a mass range of 400-1400 Da. The 12 most abundant peptide ions were selected from the MS for higher energy collision-induced dissociation fragmentation (collision energy: 34 V) if they were at least doubly-charged. Fragmentation was performed at high resolution (60,000 FWHM) for a target of $1x10^5$ and a

maximum injection time of 60 ms using an isolation window of 1.2 m/z and a dynamic exclusion of 20 s.

Data search & analysis

Raw data were searched against the mus musculus or homo sapiens reference databases from swissprot and uniprot via Mascot (v2.3.02, Matrix Science) and Sequest HT search engines, respectively, using Proteome Discoverer (v2.1, Thermo Fisher Scientific). A precursor mass tolerance of 20 ppm and a product ion mass tolerance of 0.05 Da was applied, allowing two missed cleavages for trypsin. Fixed modifications included carbamidomethylation of Cys/Arg and TMT-10plex labeling for Lys and N-termini. Variable modifications contained phosphorylation on Ser/Thr/Tyr, acetylation on the N-termini, oxidation of Met and deamidation of Asn. The TMT datasets were quantified using the centroid peak intensity with the 'reporter ions quantifier' node. To ensure high-confident identification, the Mascot percolator algorithm (q value filter set to 0.01), Mascot and Sequest HT peptide rank 1, a cut-off Mascot score value of ≥18, and a Sequest HTΔCn of 0.1 were used. Only high confident peptides were used for further analysis. The peptides were filtered against a Decoy database resulting into a false discovery rate (FDR) of <0.01. Two murine biological replicates per group without missing values were considered for the analysis, and normalization was performed on the protein median. Based on the mean technical variation from repetitive measurements of murine brain samples (*61, 62*), the threshold for determining regulated proteins was set to 1.3-fold, i.e. proteins with TMT ratios >1.30 were considered upregulated and <0.77 downregulated. Tau isoform-specific searches were performed by creating a Uniprot database of isoform sequences for mouse Tau (Uniprot ID: P10637-1, -2, -3. -4, -5, -6) and human Tau (Uniprot ID: P10636-1, -2, -3, -4, -5, -6, -7, -8, -9),

as performed by Morris et al. (*71*). Moderate confidence peptides (FDR<0.05) were included in the isoform-specific search.

RT-qPCR

For reverse transcription, quantitative polymerase chain reaction (RT-qPCR), Trizol™-isolated RNA (2 µg) from brain sections of WT and TG mice was reverse-transcribed to cDNA, by using the Applied Biosystems™ high-capacity cDNA transcription kit (Thermo Fisher Scientific). Samples were analyzed in triplicate on a StepOnePlus™ Real-Time PCR system (Applied Biosystems™, Thermo Fisher Scientific). Each 20 µL sample contained nuclease-free H_2O (Thermo Fisher Scientific), 1x Maxima SYBR® green/probe master mix (Thermo Fisher Scientific), 500 nM forward and reverse primers (TAG Copenhagen A/S), 4x diluted cDNA for *Mapt* and 10x diluted cDNA for hypoxanthine phosphoribosyltransferase (*Hprt1*), which was used as a reference gene. *Hprt1* sequences *(72)* and mouse-specific *Mapt* primers spanning exon 10 have been described previously (*73*). Conventional PCR cycling conditions were used [95°C (10 min), followed by 40 cycles of 95°C (15s)/60°C (1 min)], followed by a melt curve. After normalization to *Hprt1*, data were expressed as fold change from the mean value of the 3-month-old WT samples. Nuclease-free H_2O and genomic DNA were used as controls.

Immunoblotting of sarkosyl-insoluble Tau

Ten µg of lysed, denatured protein were separated on 4-12% Bolt Bis-Tris gradient gels (NW04125Box, Novex®), and transferred to polyvinylidene fluoride (PVDF) membranes using the Trans-Blot SD Semi-Dry Transfer Cell system (Bio-Rad Laboratories Inc.). Protein content on the PVDF membranes was visualized with PonceauS. Following washing (10 min) and blocking for 1 h in Roti®-Block (Carl Roth GmbH), the membranes were incubated overnight at

4°C in blocking solution, containing rabbit anti-tau (1:1000; A0024, Dako Agilent) or rabbit anti-phopshoSer404 primary antibodies (1:200; OAAF07796, Aviva Systems Biology). The blots were washed in TBS+1% Triton X-100 (3 x 15 min; TBS-Tx) and incubated for 2 h with horseradish peroxidase-conjugated secondary antibody (anti-rabbit IgG, HRP-linked antibody, #7074; Cell Signaling Technology®). After a final wash in TBS-Tx (3 x 15 min), the blots were developed with enhanced *chemiluminescent* substrate (ECL), according to manufacturer instructions (Luminata™ Forte Western HRP Substrate, WBLUF0100, Merck Millipore).

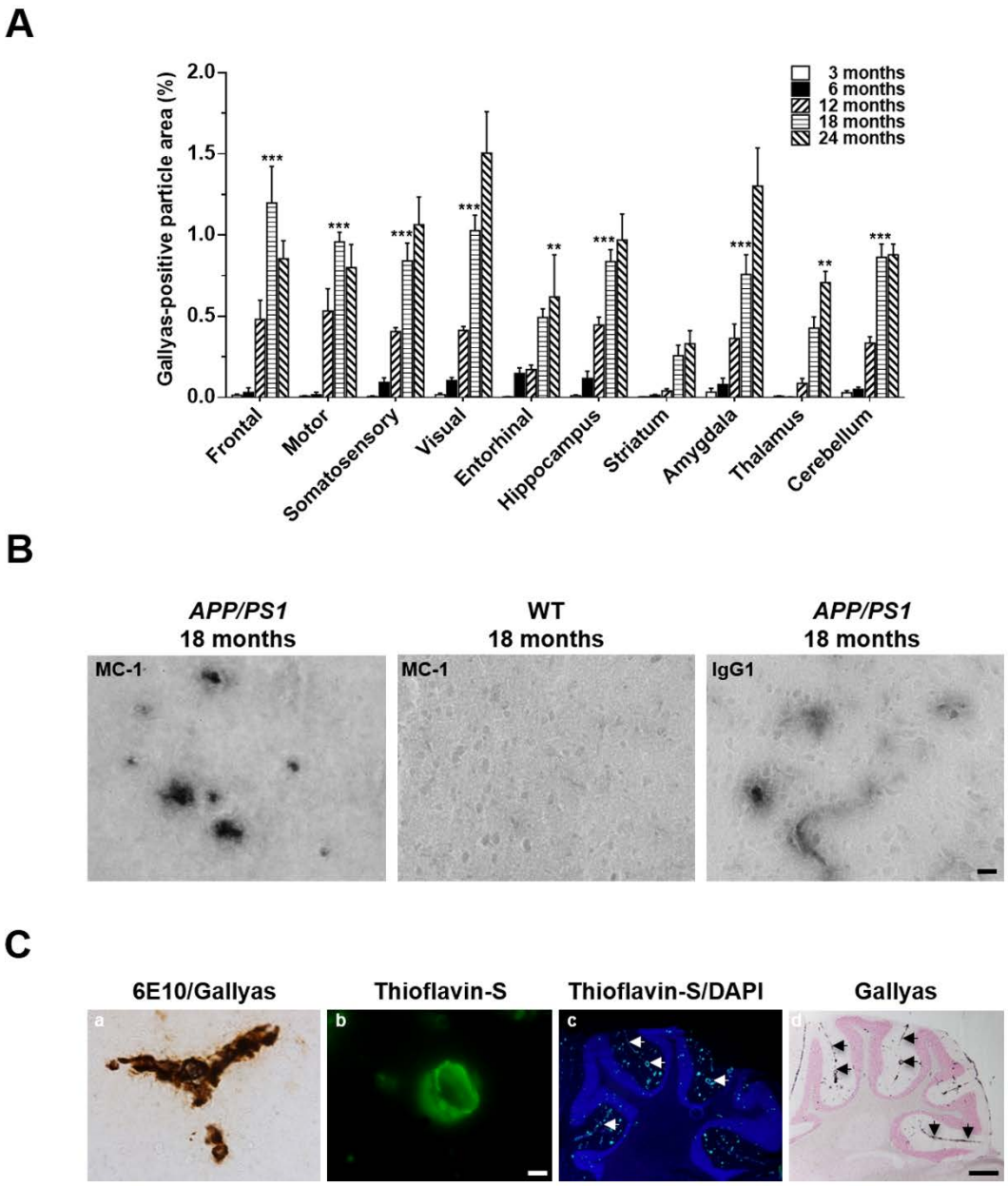

Fig. S1. (A) Quantification of Gallyas-positive signal in aging $APP_{swe}/PS1_{\Delta E9}$ mice. Regions of interest were manually drawn by reference to the mouse brain atlas of Paxinos and Franklin (*74*). Gallyas-positive particles were measured with the particle analysis plugin in ImageJ, after thresholding ROIs on a black and white image display mode, by using default software settings. Data are presented as the mean area fraction occupied by Gallyas-positive particles ± standard error of the mean (SEM), in brain regions of 5-6 animals/group. Asterisks denote the age when

Gallyas signal was first increased compared to 3-month old *APP*$_{swe}$/*PS1*$_{\Delta E9}$ mice (***P*<0.01, ****P*<0.001, Bonferroni *post-hoc* tests). Increased silver deposition across all brain areas analyzed was detected in 12- vs. 3- and 6-month-old *APP*$_{swe}$/*PS1*$_{\Delta E9}$ mice (*P*<0.001), with additional accumulation occurring in 18- vs. 12- (*P*<0.001), and 24- vs. 18-month-old TG animals (*P*<0.05, Bonferroni *post hoc* tests). Two-way ANOVA confirmed significant main effects of age [$F_{(4,245)}$=169.9, *P*<0.001] and brain region [$F_{(9,245)}$=11.4, *P*<0.001], as well as significant age x region interaction effects on the fraction of brain tissue bearing Gallyas-positive signal [$F_{(36,245)}$=3.2, *P*<0.001]. **(B)** MC-1 immunoreactivity in the neocortex of 24-month-old TG and WT mice. Indications of conformationally modified tau were obtained by using the conformation-dependent MC-1 antibody. In mice, part of the MC-1 signal may be derived from non-specific binding to mouse immunoglobulin 1 (IgG1). Scale bar: 20 µm. **(C)** Vascular and meningeal lesions in 18-month-old *APP*$_{swe}$/*PS1*$_{\Delta E9}$ mice. Gallyas/6E10- (a) and thioflavin-S-positive vascular pathology (b). The arrows in (c) & (d) respectively point to thioflavin-S and Gallyas signal in the meninges of the cerebellum. Scale bars: 10 µm (a & b), 200 µm (c & d).

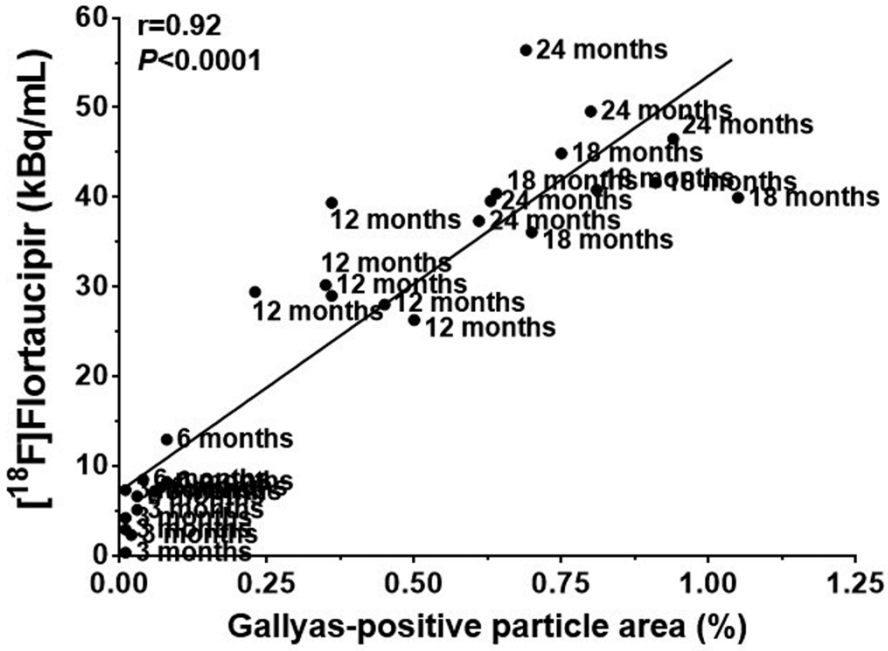

Fig. S2. Correlation between Gallyas-positive area fraction and [^{18}F]Flortaucipir binding levels. Signals from the Gallyas silver stain and [^{18}F]Flortaucipir autoradiography monitor the propagation of identical pathology, most likely tau-associated lesions. Each dot represents values from a single TG animal.

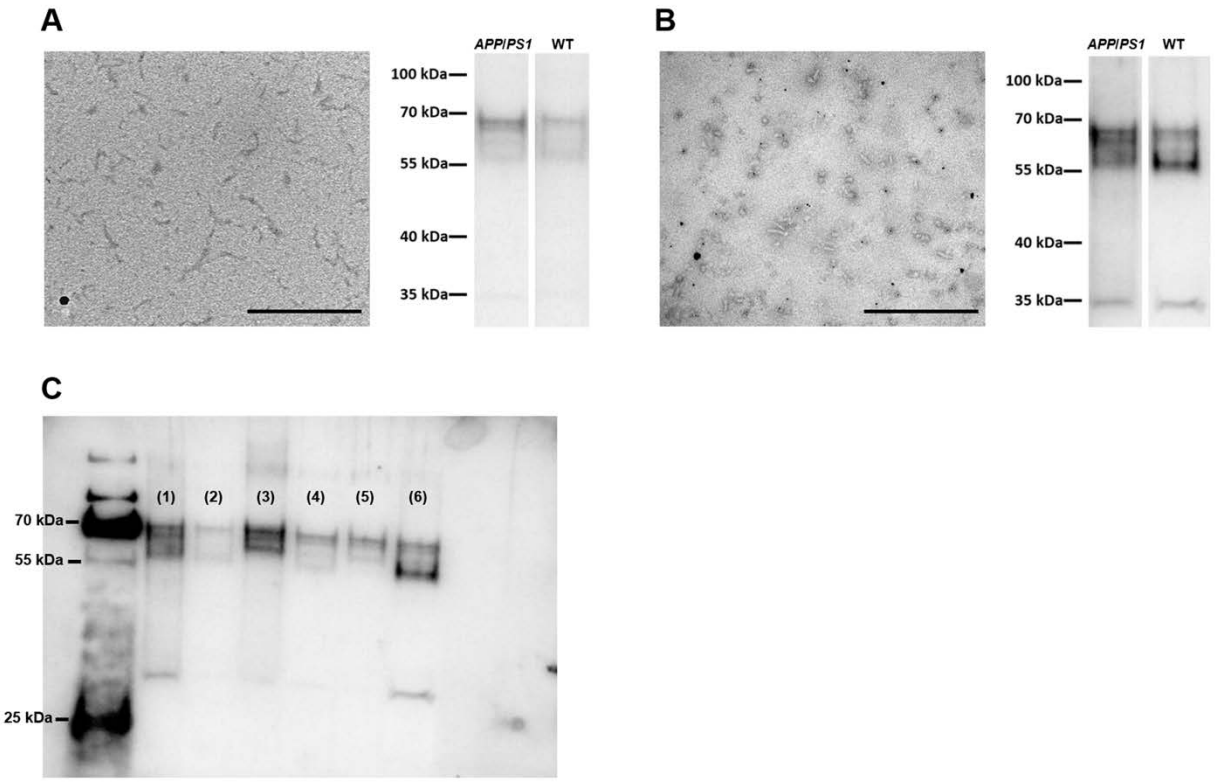

Fig. S3. Evaluation of methods for extracting sarkosyl-insoluble tau. TEM and immunoblotting of sarkosyl-insoluble tau, extracted according to **(A)** Sahara et al. (*20*) and **(B)** Greenberg and Davies (*21*). A triplet of immunoreactive bands in the 55-70 kDa range was detected by both methods, by using a rabbit antibody directed to the C-terminal domain of unmodified tau (aa 243-441; A0024, Dako Agilent). **(C)** Bands in A & B were spliced from gel in C, showing total tau immunoreactivity in the following groups: (1) TG 24 months, (6) WT 24 months (Greenberg and Davies method). (2) WT 24 months, (3) Human AD, (4) TG 18 months, (5) TG 24 months (Sarhara et al. method).

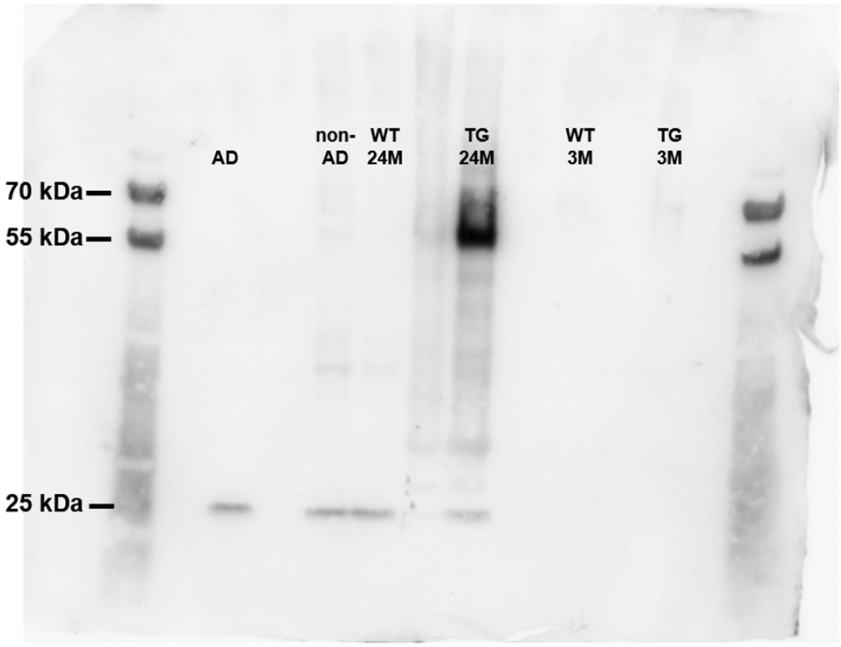

Fig. S4. pS404 immunoblot. The accumulation of sarkosyl-insoluble tau hyperphosphorylated at pS404 in 24-month-old transgenic (TG) mice was confirmed with a rabbit anti-phopshoSer404 antibody (1:200; OAAF07796, Aviva Systems Biology).

Background strain	Age (Months)	Gender	Method of Euthanasia	Method of Tau Evaluation	Antibody/Epitope	Brain Region	Reference
B6.C3	12	Female	Anesthesia	IHC	pS262	NCx	(*75*)
B6.C3	~9	Male	Not reported	IF & WB	pS396	NCx & Hip	(*76*)
B6.C3	~7.5	Not reported	Anesthesia	IF	AT8 (pS202/pT205)	NCx & Hip	(*77*)
B6.C3	6 to >24	Male & Female	Anesthesia	IHC	PHF1, CP13, pT231, p262, pS396, pS422	Entire Brain	(*78*)
B6.C3	8	Not reported	Anesthesia	IHC	AT8 (pS202/pT205)	NCx & Hip	(*79*)
B6.C3	10	Male	Not reported	WB & Gallyas	AT8 (pS202/pT205)	Entire Brain	(*80*)
B6.C3	11 & 18	Not reported	Anesthesia	IHC	AB1518 (not reported)	Hip	(*81*)
B6.C3	11	Not reported	Anesthesia	IHC	PHF1 (pS396/pS404)	NCx & Hip	(*82*)
B6.C3	~7.5	Not reported	Anesthesia (?)	WB & IHC	AT8 (pS202/pT205) PHF1 (pS369/pS404)	NCx & Hip	(*83*)
B6.C3	~7	Male	Anesthesia	WB	pS519, pS202, pS235, pS396, pS404	FrCx & Hip	(*84*)
C57BL/6	6	Female	Cervical dislocation	WB	pT205, pS396, pS404	Hip	(*85*)
C57BL/6J	22	Female	Anesthesia	WB & IHC	pS199, pS396	NCx & Entire Brain	(*86*)
C57BL/6J	7	Male	Not reported	IF	pS199	NCx & Hip	(*87*)
C57BL/6J	3-12	Not reported	Not reported	WB	PHF1 (pS396/pS404)	FrCx	(*88*)
C57BL/6J	12	Male	Cervical dislocation	Proteomics & Gallyas	N/A	NCx & Hip, Olf. Bulb, Brainstem	(*61*)
C57BL/6	~9	Female	Anesthesia	WB	pS235, pT205	Entire Brain	(*89*)
C57BL/6J	~7.5	Male	Not reported	WB	pS262	NCx & Hip	(*90*)
C57BL/6	7	Male	Decapitation	WB	PHF1 (pS396/pS404)	Hip	(*91*)
C57BL/6	~12	Female	Anesthesia	WB	pS235, pT205	NCx & Hip	(*92*)
C57BL/6	3 & 6	Male	Not reported	WB	pS199, pT205, pS396, pS404	Hip	(*93*)
C57BL/6J	~7.5	Male	Not reported	IF	pT181	NCx & Hip	(*94*)
C57BL/6J	6 & 9	Male	Anesthesia	IF	pS199, pS202, pS262, pT181	NCx	(*95*)
C57BL/6	6-7	Not reported	Anesthesia	IHC	AT8 (pS202/pT205)	Amygdala	(*96*)
C57BL/6J	12	Not reported	Anesthesia	IHC/IF	AT8 (pS202/pT205) PHF1 (pS369/pS404)	NCx	(*5*)
Not reported	~12	Male	Anesthesia	WB	pS235, pT205	Entire Brain	(*97*)
Not reported	3-12	Not reported	Anesthesia	WB	pS199, pT205, pS396, pS404	Entire Brain	(*98*)
Not reported	6	Not reported	Anesthesia	WB	AT8 (pS202/pT205)	NCx	(*99*)
Not reported	7	Not reported	Anesthesia	WB	pS396	Brain hemisphere	(*100*)
Not reported	~7	Not reported	Anesthesia	WB	AT8 (pS202/pT205)	NCx	(*101*)
Not reported	>18	Not reported	Anesthesia	IHC	pS199, pT231	Cerebellum	(*102*)
Not reported	~2-3	Male	Anesthesia	WB	PHF1 (pS396/pS404)	NCx & Hip	(*103*)
Not reported	2	Male	Anesthesia	WB	AT8 (pS202/pT205) PHF1 (pS396/pS404)	Subventricular zone, NCx & Hip	(*104*)

Table S1. Evidence of tau hyperphosphorylation in *APP*$_{swe}$/*PS1*$_{\Delta E9}$ mice. Abbreviations: IHC: Immunohistochemistry; WB: Western Blot; IF: Immunofluorescence; NCx: Neocortex; Fr Cx: Frotnal Cortex; Hip: Hippocampus.

DATA FILE S1

REGULATED PROTEINS 3 MONTHS: TG vs. WT

Accession	Description	Abundance Ratio: (TG3) / (WT3)
Q3V117	ATP-citrate synthase OS=Mus musculus GN=Acly PE=1 SV=1	5,526
Q3TTY5	Keratin, type II cytoskeletal 2 epidermal OS=Mus musculus GN=Krt2 PE=1 SV=1	2,979
Q8BL66	Early endosome antigen 1 OS=Mus musculus GN=Eea1 PE=1 SV=2	2,834
B1AQ77	Keratin 15, isoform CRA_a OS=Mus musculus GN=Krt15 PE=1 SV=1	2,777
Q32P04	Keratin 5 OS=Mus musculus GN=Krt5 PE=2 SV=2	2,716
Q4VWZ5	Acyl-CoA-binding protein OS=Mus musculus GN=Dbi PE=1 SV=1	2,416
Q61782	Type I epidermal keratin mRNA, 3'end (Fragment) OS=Mus musculus PE=2 SV=1	2,363
Q91VB8	Alpha globin 1 OS=Mus musculus GN=haemaglobin alpha 2 PE=1 SV=1	2,309
Q3UBP6	Putative uncharacterized protein OS=Mus musculus GN=Actb PE=2 SV=1	2,147
D3YXH0	Immunoglobulin superfamily member 5 OS=Mus musculus GN=Igsf5 PE=4 SV=1	2,139
O08539	Myc box-dependent-interacting protein 1 OS=Mus musculus GN=Bin1 PE=1 SV=1	2,109
Q3UV17	Keratin, type II cytoskeletal 2 oral OS=Mus musculus GN=Krt76 PE=2 SV=1	2,096
P63005	Platelet-activating factor acetylhydrolase IB subunit alpha OS=Mus musculus GN=Pafah1b1 PE=1 SV=2	2,078
Q548F2	Guanine deaminase OS=Mus musculus GN=Gda PE=2 SV=1	1,997
G5E902	MCG10343, isoform CRA_b OS=Mus musculus GN=Slc25a3 PE=1 SV=1	1,993
Q9DCW4	Electron transfer flavoprotein subunit beta OS=Mus musculus GN=Etfb PE=1 SV=3	1,984
Q149Z9	Histone cluster 1, H1d OS=Mus musculus GN=Hist1h1d PE=2 SV=1	1,883
Q6ZWX2	Thymosin, beta 4, X chromosome OS=Mus musculus GN=Tmsb4x PE=2 SV=1	1,832
B1AWD9	Clathrin light chain A OS=Mus musculus GN=Clta PE=1 SV=1	1,816
Q08331	Calretinin OS=Mus musculus GN=Calb2 PE=1 SV=3	1,814
P14115	60S ribosomal protein L27a OS=Mus musculus GN=Rpl27a PE=2 SV=5	1,809
P84086	Complexin-2 OS=Mus musculus GN=Cplx2 PE=1 SV=1	1,806
P02802	Metallothionein-1 OS=Mus musculus GN=Mt1 PE=1 SV=1	1,796
Q8CI43	Myosin light chain 6B OS=Mus musculus GN=Myl6b PE=2 SV=1	1,771
P47962	60S ribosomal protein L5 OS=Mus musculus GN=Rpl5 PE=1 SV=3	1,757
A8DUK4	Beta-globin OS=Mus musculus GN=Hbbt1 PE=1 SV=1	1,749
P99024	Tubulin beta-5 chain OS=Mus musculus GN=Tubb5 PE=1 SV=1	1,713
Q546G4	Albumin 1 OS=Mus musculus GN=Alb PE=2 SV=1	1,688
P20065	Thymosin beta-4 OS=Mus musculus GN=Tmsb4x PE=1 SV=1	1,682
P62717	60S ribosomal protein L18a OS=Mus musculus GN=Rpl18a PE=1 SV=1	1,68
P62204	Calmodulin OS=Mus musculus GN=Calm1 PE=1 SV=2	1,677
P19157	Glutathione S-transferase P 1 OS=Mus musculus GN=Gstp1 PE=1 SV=2	1,651
Q9R0P9	Ubiquitin carboxyl-terminal hydrolase isozyme L1 OS=Mus musculus GN=Uchl1 PE=1 SV=1	1,647
Q8VDD5	Myosin-9 OS=Mus musculus GN=Myh9 PE=1 SV=4	1,624
Q9EQU5-2	Isoform 2 of Protein SET OS=Mus musculus GN=Set	1,604
P17742	Peptidyl-prolyl cis-trans isomerase A OS=Mus musculus GN=Ppia PE=1 SV=2	1,595
Q810U4	Neuronal cell adhesion molecule OS=Mus musculus GN=Nrcam PE=1 SV=2	1,586
Q6IFX2	Keratin, type I cytoskeletal 42 OS=Mus musculus GN=Krt42 PE=1 SV=1	1,586
P14869	60S acidic ribosomal protein P0 OS=Mus musculus GN=Rplp0 PE=1 SV=3	1,576
Q9WV69	Dematin OS=Mus musculus GN=Dmtn PE=1 SV=1	1,561

P17751	Triosephosphate isomerase OS=Mus musculus GN=Tpi1 PE=1 SV=4	1,556
P63101	14-3-3 protein zeta/delta OS=Mus musculus GN=Ywhaz PE=1 SV=1	1,541
Q5BLK1	40S ribosomal protein S6 OS=Mus musculus GN=Rps6 PE=2 SV=1	1,531
P99027	60S acidic ribosomal protein P2 OS=Mus musculus GN=Rplp2 PE=1 SV=3	1,519
O55091	Protein IMPACT OS=Mus musculus GN=Impact PE=1 SV=2	1,514
P98086	Complement C1q subcomponent subunit A OS=Mus musculus GN=C1qa PE=1 SV=2	1,493
E9Q557	Desmoplakin OS=Mus musculus GN=Dsp PE=1 SV=1	1,474
F8WGL3	Cofilin-1 OS=Mus musculus GN=Cfl1 PE=1 SV=1	1,429
Q9CZC8	Secernin-1 OS=Mus musculus GN=Scrn1 PE=1 SV=1	1,415
Q9DBJ1	Phosphoglycerate mutase 1 OS=Mus musculus GN=Pgam1 PE=1 SV=3	1,411
Q8C2Q7	Heterogeneous nuclear ribonucleoprotein H OS=Mus musculus GN=Hnrnph1 PE=1 SV=1	1,401
Q545V3	Enolase 2, gamma neuronal, isoform CRA_a OS=Mus musculus GN=Eno2 PE=2 SV=1	1,401
Q505A8	MCG17585 OS=Mus musculus GN=Rpl39 PE=2 SV=1	1,399
P68510	14-3-3 protein eta OS=Mus musculus GN=Ywhah PE=1 SV=2	1,394
Q8K183	Pyridoxal kinase OS=Mus musculus GN=Pdxk PE=1 SV=1	1,391
Q3TT94	Serine/threonine-protein phosphatase 2A 55 kDa regulatory subunit B OS=Mus musculus GN=Ppp2r2a PE=2 SV=1	1,381
D3Z4B2	Gamma-soluble NSF attachment protein (Fragment) OS=Mus musculus GN=Napg PE=1 SV=1	1,369
P99028	Cytochrome b-c1 complex subunit 6, mitochondrial OS=Mus musculus GN=Uqcrh PE=1 SV=2	1,367
Q3UR55	ATPase, Na+/K+ transporting, beta 2 polypeptide, isoform CRA_b OS=Mus musculus GN=Atp1b2 PE=2 SV=1	1,366
Q63810	Calcineurin subunit B type 1 OS=Mus musculus GN=Ppp3r1 PE=1 SV=3	1,355
G5E866	Splicing factor 3B subunit 1 OS=Mus musculus GN=Sf3b1 PE=1 SV=1	1,353
P05132	cAMP-dependent protein kinase catalytic subunit alpha OS=Mus musculus GN=Prkaca PE=1 SV=3	1,349
P01831	Thy-1 membrane glycoprotein OS=Mus musculus GN=Thy1 PE=1 SV=1	1,323
Q3UH59	Myosin-10 OS=Mus musculus GN=Myh10 PE=1 SV=1	1,32
P47963	60S ribosomal protein L13 OS=Mus musculus GN=Rpl13 PE=1 SV=3	1,319
Q80YN3	Breast carcinoma-amplified sequence 1 homolog OS=Mus musculus GN=Bcas1 PE=1 SV=3	1,312
Q5XJF6	Ribosomal protein OS=Mus musculus GN=Rpl10a PE=1 SV=1	1,302
Q8VDN2	Sodium/potassium-transporting ATPase subunit alpha-1 OS=Mus musculus GN=Atp1a1 PE=1 SV=1	0,775
Q99KI0	Aconitate hydratase, mitochondrial OS=Mus musculus GN=Aco2 PE=1 SV=1	0,773
Q52KC1	Eukaryotic translation initiation factor 4A2 OS=Mus musculus GN=Eif4a2 PE=2 SV=1	0,772
Q91XV3	Brain acid soluble protein 1 OS=Mus musculus GN=Basp1 PE=1 SV=3	0,771
Q548L4	Glutamate decarboxylase OS=Mus musculus GN=Gad2 PE=2 SV=1	0,771
A0A075B5P2	Protein Igkc (Fragment) OS=Mus musculus GN=Igkc PE=1 SV=1	0,769
Q80YX1	Tenascin OS=Mus musculus GN=Tnc PE=1 SV=1	0,768
V9GX76	Unconventional myosin-VI OS=Mus musculus GN=Myo6 PE=1 SV=1	0,768
P63163	Small nuclear ribonucleoprotein-associated protein N OS=Mus musculus GN=Snrpn PE=2 SV=1	0,766
S4R1P5	Dystonin OS=Mus musculus GN=Dst PE=1 SV=1	0,765
P60766	Cell division control protein 42 homolog OS=Mus musculus GN=Cdc42 PE=1 SV=2	0,765
Q9CZ13	Cytochrome b-c1 complex subunit 1, mitochondrial OS=Mus musculus GN=Uqcrc1 PE=1 SV=2	0,764
P61264	Syntaxin-1B OS=Mus musculus GN=Stx1b PE=1 SV=1	0,764
P40336	Vacuolar protein sorting-associated protein 26A OS=Mus musculus GN=Vps26a PE=1 SV=1	0,76
B2RTL5	Aldehyde dehydrogenase family 1, subfamily A7 OS=Mus musculus GN=Aldh1a7 PE=2 SV=1	0,76
E9Q455	Tropomyosin alpha-1 chain OS=Mus musculus GN=Tpm1 PE=1 SV=1	0,759
Q9Z2T6	Keratin, type II cuticular Hb5 OS=Mus musculus GN=Krt85 PE=2 SV=2	0,758

Q9CZU6	Citrate synthase, mitochondrial OS=Mus musculus GN=Cs PE=1 SV=1	0,757
P62858	40S ribosomal protein S28 OS=Mus musculus GN=Rps28 PE=1 SV=1	0,757
P26883	Peptidyl-prolyl cis-trans isomerase FKBP1A OS=Mus musculus GN=Fkbp1a PE=1 SV=2	0,755
P53395	Lipoamide acyltransferase component of branched-chain alpha-keto acid dehydrogenase complex, mitochondrial OS=Mus musculus GN=Dbt PE=1 SV=2	0,755
Q61838	Alpha-2-macroglobulin OS=Mus musculus GN=A2m PE=1 SV=3	0,754
Q3TLP8	RAS-related C3 botulinum substrate 1, isoform CRA_a OS=Mus musculus GN=Rac1 PE=1 SV=1	0,753
Q9JHU4	Cytoplasmic dynein 1 heavy chain 1 OS=Mus musculus GN=Dync1h1 PE=1 SV=2	0,753
S4R249	Ankyrin-2 OS=Mus musculus GN=Ank2 PE=1 SV=1	0,753
Q9EQF6	Dihydropyrimidinase-related protein 5 OS=Mus musculus GN=Dpysl5 PE=1 SV=1	0,746
F6TYB7	Myelin basic protein (Fragment) OS=Mus musculus GN=Mbp PE=1 SV=1	0,745
Q9WUM4	Coronin-1C OS=Mus musculus GN=Coro1c PE=1 SV=2	0,744
Q9WUB3	Glycogen phosphorylase, muscle form OS=Mus musculus GN=Pygm PE=1 SV=3	0,744
Q8VCE0	Sodium/potassium-transporting ATPase subunit alpha OS=Mus musculus GN=Atp1a3 PE=1 SV=1	0,74
P17427	AP-2 complex subunit alpha-2 OS=Mus musculus GN=Ap2a2 PE=1 SV=2	0,739
Q8CI94	Glycogen phosphorylase, brain form OS=Mus musculus GN=Pygb PE=1 SV=3	0,737
Q3U2G2	Heat shock 70 kDa protein 4 OS=Mus musculus GN=Hspa4 PE=1 SV=1	0,736
P35486	Pyruvate dehydrogenase E1 component subunit alpha, somatic form, mitochondrial OS=Mus musculus GN=Pdha1 PE=1 SV=1	0,735
Q9JLM8	Serine/threonine-protein kinase DCLK1 OS=Mus musculus GN=Dclk1 PE=1 SV=1	0,731
Q5SXR6	Clathrin heavy chain OS=Mus musculus GN=Cltc PE=1 SV=1	0,73
Q8C522	Endonuclease domain-containing 1 protein OS=Mus musculus GN=Endod1 PE=1 SV=2	0,729
Q9JKC6	Cell cycle exit and neuronal differentiation protein 1 OS=Mus musculus GN=Cend1 PE=1 SV=1	0,725
B2RTM0	Histone H4 OS=Mus musculus GN=Hist2h4 PE=2 SV=1	0,725
P63276	40S ribosomal protein S17 OS=Mus musculus GN=Rps17 PE=1 SV=2	0,724
Q62261	Spectrin beta chain, non-erythrocytic 1 OS=Mus musculus GN=Sptbn1 PE=1 SV=2	0,724
A2AUK5	Band 4.1-like protein 1 OS=Mus musculus GN=Epb41l1 PE=1 SV=1	0,722
Q8BVI4	Dihydropteridine reductase OS=Mus musculus GN=Qdpr PE=1 SV=2	0,72
P47857	ATP-dependent 6-phosphofructokinase, muscle type OS=Mus musculus GN=Pfkm PE=1 SV=3	0,72
P60202	Myelin proteolipid protein OS=Mus musculus GN=Plp1 PE=1 SV=2	0,719
E9Q7Q3	Tropomyosin alpha-3 chain OS=Mus musculus GN=Tpm3 PE=1 SV=1	0,718
Q5SYD0	Unconventional myosin-Id OS=Mus musculus GN=Myo1d PE=1 SV=1	0,718
Q9QWL7	Keratin, type I cytoskeletal 17 OS=Mus musculus GN=Krt17 PE=1 SV=3	0,71
P84078	ADP-ribosylation factor 1 OS=Mus musculus GN=Arf1 PE=1 SV=2	0,71
P43274	Histone H1.4 OS=Mus musculus GN=Hist1h1e PE=1 SV=2	0,71
Q9WV92	Band 4.1-like protein 3 OS=Mus musculus GN=Epb41l3 PE=1 SV=1	0,709
G5E924	Heterogeneous nuclear ribonucleoprotein L (Fragment) OS=Mus musculus GN=Hnrnpl PE=1 SV=1	0,708
P63318	Protein kinase C gamma type OS=Mus musculus GN=Prkcg PE=1 SV=1	0,707
Q9CZY3	Ubiquitin-conjugating enzyme E2 variant 1 OS=Mus musculus GN=Ube2v1 PE=1 SV=1	0,707
P48771	Cytochrome c oxidase subunit 7A2, mitochondrial OS=Mus musculus GN=Cox7a2 PE=1 SV=2	0,706
Q3TI05	Chaperonin containing Tcp1, subunit 6a (Zeta) OS=Mus musculus GN=Cct6a PE=2 SV=1	0,706
B2RRX2	Serine/threonine-protein phosphatase OS=Mus musculus GN=Ppp3ca PE=2 SV=1	0,704
Q9D0M3	Cytochrome c1, heme protein, mitochondrial OS=Mus musculus GN=Cyc1 PE=1 SV=1	0,701
P56399	Ubiquitin carboxyl-terminal hydrolase 5 OS=Mus musculus GN=Usp5 PE=1 SV=1	0,701
Q543Y7	Putative uncharacterized protein OS=Mus musculus GN=Pacsin1 PE=2 SV=1	0,7
Q9DCD0	6-phosphogluconate dehydrogenase, decarboxylating OS=Mus musculus GN=Pgd PE=1 SV=3	0,693

A0A0A0MQA5	Tubulin alpha chain (Fragment) OS=Mus musculus GN=Tuba4a PE=1 SV=1	0,693
P46097	Synaptotagmin-2 OS=Mus musculus GN=Syt2 PE=1 SV=1	0,689
P39053	Dynamin-1 OS=Mus musculus GN=Dnm1 PE=1 SV=2	0,689
Q9Z1G4	V-type proton ATPase 116 kDa subunit a isoform 1 OS=Mus musculus GN=Atp6v0a1 PE=1 SV=3	0,688
Q9CX86	Heterogeneous nuclear ribonucleoprotein A0 OS=Mus musculus GN=Hnrnpa0 PE=1 SV=1	0,688
P26645	Myristoylated alanine-rich C-kinase substrate OS=Mus musculus GN=Marcks PE=1 SV=2	0,682
Q78ZJ8	MCG22989, isoform CRA_b OS=Mus musculus GN=Rab11b PE=2 SV=1	0,681
Q8R001	Microtubule-associated protein RP/EB family member 2 OS=Mus musculus GN=Mapre2 PE=1 SV=1	0,68
P11798	Calcium/calmodulin-dependent protein kinase type II subunit alpha OS=Mus musculus GN=Camk2a PE=1 SV=2	0,677
Q3UNV7	Putative uncharacterized protein OS=Mus musculus GN=Mlf2 PE=2 SV=1	0,675
E9Q401	Ryanodine receptor 2 OS=Mus musculus GN=Ryr2 PE=1 SV=1	0,675
Q9D051	Pyruvate dehydrogenase E1 component subunit beta, mitochondrial OS=Mus musculus GN=Pdhb PE=1 SV=1	0,674
Q3UMU9	Hepatoma-derived growth factor-related protein 2 OS=Mus musculus GN=Hdgfrp2 PE=1 SV=1	0,674
Q9Z2I9	Succinate--CoA ligase [ADP-forming] subunit beta, mitochondrial OS=Mus musculus GN=Sucla2 PE=1 SV=2	0,674
P14148	60S ribosomal protein L7 OS=Mus musculus GN=Rpl7 PE=1 SV=2	0,673
P19001	Keratin, type I cytoskeletal 19 OS=Mus musculus GN=Krt19 PE=1 SV=1	0,672
Q922J6	Tetraspanin-2 OS=Mus musculus GN=Tspan2 PE=1 SV=1	0,672
P62317	Small nuclear ribonucleoprotein Sm D2 OS=Mus musculus GN=Snrpd2 PE=3 SV=1	0,67
O70318	Band 4.1-like protein 2 OS=Mus musculus GN=Epb41l2 PE=1 SV=2	0,667
Q923T9	Calcium/calmodulin-dependent protein kinase type II subunit gamma OS=Mus musculus GN=Camk2g PE=1 SV=1	0,666
A0A0G2JFT8	Protein RUFY3 OS=Mus musculus GN=Rufy3 PE=1 SV=1	0,666
Q3UHL1	CaM kinase-like vesicle-associated protein OS=Mus musculus GN=Camkv PE=1 SV=2	0,662
P62305	Small nuclear ribonucleoprotein E OS=Mus musculus GN=Snrpe PE=1 SV=1	0,661
Q5DQJ3	Capping protein (Actin filament) muscle Z-line, alpha 2, isoform CRA_c OS=Mus musculus GN=Capza2 PE=2 SV=1	0,659
Q7TSJ2	Microtubule-associated protein 6 OS=Mus musculus GN=Map6 PE=1 SV=2	0,657
Q9Z1B3	1-phosphatidylinositol 4,5-bisphosphate phosphodiesterase beta-1 OS=Mus musculus GN=Plcb1 PE=1 SV=2	0,655
Q3UYK6	Amino acid transporter OS=Mus musculus GN=Slc1a2 PE=2 SV=1	0,655
B2RXY7	Carbonyl reductase 1 OS=Mus musculus GN=Cbr1 PE=2 SV=1	0,654
P52480-2	Isoform M1 of Pyruvate kinase PKM OS=Mus musculus GN=Pkm	0,652
Q3TXU4	Apolipoprotein E, isoform CRA_h OS=Mus musculus GN=Apoe PE=2 SV=1	0,652
P62715	Serine/threonine-protein phosphatase 2A catalytic subunit beta isoform OS=Mus musculus GN=Ppp2cb PE=1 SV=1	0,652
P80313	T-complex protein 1 subunit eta OS=Mus musculus GN=Cct7 PE=1 SV=1	0,651
P61255	60S ribosomal protein L26 OS=Mus musculus GN=Rpl26 PE=1 SV=1	0,648
Q4FJX4	Csrp1 protein OS=Mus musculus GN=Csrp1 PE=2 SV=1	0,648
Q8VEK3	Heterogeneous nuclear ribonucleoprotein U OS=Mus musculus GN=Hnrnpu PE=1 SV=1	0,647
Q3UAD6	Heat shock protein 90kDa beta (Grp94), member 1 OS=Mus musculus GN=Hsp90b1 PE=2 SV=1	0,645
Q9QUM9	Proteasome subunit alpha type-6 OS=Mus musculus GN=Psma6 PE=1 SV=1	0,643
P47757	F-actin-capping protein subunit beta OS=Mus musculus GN=Capzb PE=1 SV=3	0,642
Q9R1P1	Proteasome subunit beta type-3 OS=Mus musculus GN=Psmb3 PE=1 SV=1	0,642
P12382	ATP-dependent 6-phosphofructokinase, liver type OS=Mus musculus GN=Pfkl PE=1 SV=4	0,639
Q8BMS1	Trifunctional enzyme subunit alpha, mitochondrial OS=Mus musculus GN=Hadha PE=1 SV=1	0,638
E9PYH0	Versican core protein OS=Mus musculus GN=Vcan PE=1 SV=1	0,632
P27773	Protein disulfide-isomerase A3 OS=Mus musculus GN=Pdia3 PE=1 SV=2	0,632
Q8BG05	Heterogeneous nuclear ribonucleoprotein A3 OS=Mus musculus GN=Hnrnpa3 PE=1 SV=1	0,628

P00920	Carbonic anhydrase 2 OS=Mus musculus GN=Ca2 PE=1 SV=4	0,626
E9QAX2	Unconventional myosin-XVIIIa OS=Mus musculus GN=Myo18a PE=1 SV=1	0,625
P19246	Neurofilament heavy polypeptide OS=Mus musculus GN=Nefh PE=1 SV=3	0,623
P17426	AP-2 complex subunit alpha-1 OS=Mus musculus GN=Ap2a1 PE=1 SV=1	0,623
Q68FL4	Putative adenosylhomocysteinase 3 OS=Mus musculus GN=Ahcyl2 PE=1 SV=1	0,619
Q2PFD7	PH and SEC7 domain-containing protein 3 OS=Mus musculus GN=Psd3 PE=1 SV=2	0,615
Q3UY21	Myelin-oligodendrocyte glycoprotein OS=Mus musculus GN=Mog PE=1 SV=1	0,614
P10637-3	Isoform Tau-B of Microtubule-associated protein tau OS=Mus musculus GN=Mapt	0,611
Q8BFZ9	Erlin-2 OS=Mus musculus GN=Erlin2 PE=1 SV=1	0,61
E9PVP0	PCTP-like protein OS=Mus musculus GN=Stard10 PE=1 SV=1	0,609
Q8R0Y6	Cytosolic 10-formyltetrahydrofolate dehydrogenase OS=Mus musculus GN=Aldh1l1 PE=1 SV=1	0,608
Q61282	Aggrecan core protein OS=Mus musculus GN=Acan PE=1 SV=2	0,607
O09061	Proteasome subunit beta type-1 OS=Mus musculus GN=Psmb1 PE=1 SV=1	0,599
Q542X7	Chaperonin subunit 2 (Beta), isoform CRA_a OS=Mus musculus GN=Cct2 PE=2 SV=1	0,597
O55143	Sarcoplasmic/endoplasmic reticulum calcium ATPase 2 OS=Mus musculus GN=Atp2a2 PE=1 SV=2	0,591
Q5FWI9	Adaptor protein complex AP-2, mu1 OS=Mus musculus GN=Ap2m1 PE=2 SV=1	0,587
Q7M6W1	Reticulon OS=Mus musculus GN=Rtn1 PE=1 SV=1	0,587
P55066	Neurocan core protein OS=Mus musculus GN=Ncan PE=2 SV=1	0,585
Q8BYI9	Tenascin-R OS=Mus musculus GN=Tnr PE=1 SV=2	0,584
Q9JLZ3	Methylglutaconyl-CoA hydratase, mitochondrial OS=Mus musculus GN=Auh PE=1 SV=1	0,58
P62307	Small nuclear ribonucleoprotein F OS=Mus musculus GN=Snrpf PE=1 SV=1	0,58
Q544E3	Phosphatidylinositol-4-phosphate 5-kinase, type II, alpha OS=Mus musculus GN=Pip4k2a PE=2 SV=1	0,579
P48036	Annexin A5 OS=Mus musculus GN=Anxa5 PE=1 SV=1	0,573
P31324	cAMP-dependent protein kinase type II-beta regulatory subunit OS=Mus musculus GN=Prkar2b PE=1 SV=3	0,572
Q99M71	Mammalian ependymin-related protein 1 OS=Mus musculus GN=Epdr1 PE=2 SV=1	0,571
P70202	Latexin OS=Mus musculus GN=Lxn PE=1 SV=2	0,57
P12023	Amyloid beta A4 protein OS=Mus musculus GN=App PE=1 SV=3	0,57
Q9QUP5	Hyaluronan and proteoglycan link protein 1 OS=Mus musculus GN=Hapln1 PE=1 SV=1	0,568
Q04690	Neurofibromin OS=Mus musculus GN=Nf1 PE=1 SV=1	0,566
Q9CU62	Structural maintenance of chromosomes protein 1A OS=Mus musculus GN=Smc1a PE=1 SV=4	0,566
Q9QYC0	Alpha-adducin OS=Mus musculus GN=Add1 PE=1 SV=2	0,564
Q9ESM3	Hyaluronan and proteoglycan link protein 2 OS=Mus musculus GN=Hapln2 PE=1 SV=1	0,563
Q5BLK0	MCG18564, isoform CRA_a OS=Mus musculus GN=Rpl12 PE=2 SV=1	0,56
P31650	Sodium- and chloride-dependent GABA transporter 3 OS=Mus musculus GN=Slc6a11 PE=1 SV=2	0,56
Q9R1P0	Proteasome subunit alpha type-4 OS=Mus musculus GN=Psma4 PE=1 SV=1	0,56
Q9QXS1	Plectin OS=Mus musculus GN=Plec PE=1 SV=3	0,559
Q9Z331	Keratin, type II cytoskeletal 6B OS=Mus musculus GN=Krt6b PE=1 SV=3	0,558
P09528	Ferritin heavy chain OS=Mus musculus GN=Fth1 PE=1 SV=2	0,558
P11881	Inositol 1,4,5-trisphosphate receptor type 1 OS=Mus musculus GN=Itpr1 PE=1 SV=2	0,557
F8WHB1	Calcium-transporting ATPase OS=Mus musculus GN=Atp2b2 PE=1 SV=1	0,556
P97300	Neuroplastin OS=Mus musculus GN=Nptn PE=1 SV=3	0,555
Q5SS83	Flotillin 2, isoform CRA_a OS=Mus musculus GN=Flot2 PE=1 SV=1	0,555
Q91ZX7	Prolow-density lipoprotein receptor-related protein 1 OS=Mus musculus GN=Lrp1 PE=1 SV=1	0,554
Q3TQ70	Beta1 subnuit of GTP-binding protein OS=Mus musculus GN=Gnb1 PE=2 SV=1	0,549

Q60692	Proteasome subunit beta type-6 OS=Mus musculus GN=Psmb6 PE=1 SV=3	0,547
A6H611	Mitochondrial intermediate peptidase OS=Mus musculus GN=Mipep PE=1 SV=1	0,544
Q9CXS4	Centromere protein V OS=Mus musculus GN=Cenpv PE=1 SV=2	0,543
Q9Z2U0	Proteasome subunit alpha type-7 OS=Mus musculus GN=Psma7 PE=1 SV=1	0,541
Q8C605	ATP-dependent 6-phosphofructokinase OS=Mus musculus GN=Pfkp PE=1 SV=1	0,54
P48722	Heat shock 70 kDa protein 4L OS=Mus musculus GN=Hspa4l PE=1 SV=2	0,54
P63011	Ras-related protein Rab-3A OS=Mus musculus GN=Rab3a PE=1 SV=1	0,539
A0A0G2JGS4	Calcium/calmodulin-dependent protein kinase type II subunit delta OS=Mus musculus GN=Camk2d PE=4 SV=1	0,539
P17156	Heat shock-related 70 kDa protein 2 OS=Mus musculus GN=Hspa2 PE=1 SV=2	0,539
P99026	Proteasome subunit beta type-4 OS=Mus musculus GN=Psmb4 PE=1 SV=1	0,538
Q9R1P4	Proteasome subunit alpha type-1 OS=Mus musculus GN=Psma1 PE=1 SV=1	0,53
P01592	Immunoglobulin J chain OS=Mus musculus GN=Igj PE=2 SV=4	0,53
P35235	Tyrosine-protein phosphatase non-receptor type 11 OS=Mus musculus GN=Ptpn11 PE=1 SV=2	0,527
Q99PU5	Long-chain-fatty-acid--CoA ligase ACSBG1 OS=Mus musculus GN=Acsbg1 PE=1 SV=1	0,523
P60879	Synaptosomal-associated protein 25 OS=Mus musculus GN=Snap25 PE=1 SV=1	0,522
Q80TL4	PHD finger protein 24 OS=Mus musculus GN=Phf24 PE=1 SV=2	0,521
Q545X8	40S ribosomal protein S4 OS=Mus musculus GN=Rps4x PE=2 SV=1	0,52
Q9QYX7	Protein piccolo OS=Mus musculus GN=Pclo PE=1 SV=4	0,518
D0VYV6	Erythrocyte protein band 4.1-like 3 isoform B OS=Mus musculus GN=Epb4.1l3 PE=2 SV=1	0,518
Q8BVE3	V-type proton ATPase subunit H OS=Mus musculus GN=Atp6v1h PE=1 SV=1	0,517
O08917	Flotillin-1 OS=Mus musculus GN=Flot1 PE=1 SV=1	0,513
Q9WTL4	Insulin receptor-related protein OS=Mus musculus GN=Insrr PE=1 SV=2	0,512
P21460	Cystatin-C OS=Mus musculus GN=Cst3 PE=1 SV=2	0,501
P62814	V-type proton ATPase subunit B, brain isoform OS=Mus musculus GN=Atp6v1b2 PE=1 SV=1	0,5
A0A076FRG6	KCC2a variant 1 OS=Mus musculus GN=Slc12a5 PE=2 SV=1	0,497
O55234	Proteasome subunit beta type-5 OS=Mus musculus GN=Psmb5 PE=1 SV=3	0,487
P49722	Proteasome subunit alpha type-2 OS=Mus musculus GN=Psma2 PE=1 SV=3	0,484
Q9D2G2	Dihydrolipoyllysine-residue succinyltransferase component of 2-oxoglutarate dehydrogenase complex, mitochondrial OS=Mus musculus GN=Dlst PE=1 SV=1	0,481
Q9CPX4	Ferritin OS=Mus musculus GN=Ftl1 PE=1 SV=1	0,477
Q8BGT8	Phytanoyl-CoA hydroxylase-interacting protein-like OS=Mus musculus GN=Phyhipl PE=2 SV=1	0,476
P70441	Na(+)/H(+) exchange regulatory cofactor NHE-RF1 OS=Mus musculus GN=Slc9a3r1 PE=1 SV=3	0,475
Q0VF55	Calcium-transporting ATPase OS=Mus musculus GN=Atp2b3 PE=1 SV=1	0,472
P63085	Mitogen-activated protein kinase 1 OS=Mus musculus GN=Mapk1 PE=1 SV=3	0,47
Q3UGC8	Propionyl-Coenzyme A carboxylase, alpha polypeptide, isoform CRA_b OS=Mus musculus GN=Pcca PE=2 SV=1	0,468
Q9Z2U1	Proteasome subunit alpha type-5 OS=Mus musculus GN=Psma5 PE=1 SV=1	0,463
P62827	GTP-binding nuclear protein Ran OS=Mus musculus GN=Ran PE=1 SV=3	0,462
Q9JIS5	Synaptic vesicle glycoprotein 2A OS=Mus musculus GN=Sv2a PE=1 SV=1	0,46
Q9R1P3	Proteasome subunit beta type-2 OS=Mus musculus GN=Psmb2 PE=1 SV=1	0,459
Q9QZQ8	Core histone macro-H2A.1 OS=Mus musculus GN=H2afy PE=1 SV=3	0,454
Q91VE0	Long-chain fatty acid transport protein 4 OS=Mus musculus GN=Slc27a4 PE=1 SV=1	0,454
O35955	Proteasome subunit beta type-10 OS=Mus musculus GN=Psmb10 PE=1 SV=1	0,45
O54962	Barrier-to-autointegration factor OS=Mus musculus GN=Banf1 PE=1 SV=1	0,448
A2AWN8	YTH domain family 1, isoform CRA_a OS=Mus musculus GN=Ythdf1 PE=1 SV=1	0,448
P70195	Proteasome subunit beta type-7 OS=Mus musculus GN=Psmb7 PE=1 SV=1	0,447

P14106	Complement C1q subcomponent subunit B OS=Mus musculus GN=C1qb PE=1 SV=2	0,441
Q8BKZ9	Pyruvate dehydrogenase protein X component, mitochondrial OS=Mus musculus GN=Pdhx PE=1 SV=1	0,438
Q91ZU6	Dystonin OS=Mus musculus GN=Dst PE=1 SV=2	0,438
Q8R016	Bleomycin hydrolase OS=Mus musculus GN=Blmh PE=1 SV=1	0,437
Q3U7E0	Putative uncharacterized protein OS=Mus musculus GN=Atp6v1g1 PE=2 SV=1	0,436
A2CEK3	Phosphoglucomutase-2 OS=Mus musculus GN=Pgm2 PE=1 SV=1	0,431
B9EIC7	MCG3853 OS=Mus musculus GN=Phyhip PE=2 SV=1	0,43
E9PUA3	IQ motif and SEC7 domain-containing protein 1 OS=Mus musculus GN=Iqsec1 PE=1 SV=1	0,421
Q8BMF4	Dihydrolipoyllysine-residue acetyltransferase component of pyruvate dehydrogenase complex, mitochondrial OS=Mus musculus GN=Dlat PE=1 SV=2	0,407
P42669	Transcriptional activator protein Pur-alpha OS=Mus musculus GN=Pura PE=1 SV=1	0,398
Q9Z0H4	CUGBP Elav-like family member 2 OS=Mus musculus GN=Celf2 PE=1 SV=1	0,395
Q58EV4	Proteasome subunit alpha type OS=Mus musculus GN=Psma3 PE=2 SV=1	0,393
Q9Z0E0	Neurochondrin OS=Mus musculus GN=Ncdn PE=1 SV=1	0,39
Q58EA6	MCG10725, isoform CRA_a OS=Mus musculus GN=Rps25 PE=2 SV=1	0,366
P11983	T-complex protein 1 subunit alpha OS=Mus musculus GN=Tcp1 PE=1 SV=3	0,365
Q9JM93	ADP-ribosylation factor-like protein 6-interacting protein 4 OS=Mus musculus GN=Arl6ip4 PE=1 SV=1	0,34
Q5SQX6	Cytoplasmic FMR1-interacting protein 2 OS=Mus musculus GN=Cyfip2 PE=1 SV=2	0,327
F6YVP7	Protein Gm10260 OS=Mus musculus GN=Gm10260 PE=3 SV=2	0,286
F6VPT0	Protein Ccdc163 (Fragment) OS=Mus musculus GN=Ccdc163 PE=4 SV=1	0,284
Q02105	Complement C1q subcomponent subunit C OS=Mus musculus GN=C1qc PE=2 SV=2	0,274
Q99MN9	Propionyl-CoA carboxylase beta chain, mitochondrial OS=Mus musculus GN=Pccb PE=1 SV=2	0,229
Q3V0Q1	Dynein heavy chain 12, axonemal OS=Mus musculus GN=Dnah12 PE=1 SV=2	0,227
Q3TVK3	Aspartyl aminopeptidase OS=Mus musculus GN=Dnpep PE=1 SV=1	0,224
Q9D8B3	Charged multivesicular body protein 4b OS=Mus musculus GN=Chmp4b PE=1 SV=2	0,201
Q8R1B4	Eukaryotic translation initiation factor 3 subunit C OS=Mus musculus GN=Eif3c PE=1 SV=1	0,189

DATA FILE S1

REGULATED PROTEINS 24 MONTHS: TG vs. WT

Accession	Description	Abundance Ratio: (TG24) / (WT24)
P12023	Amyloid beta A4 protein OS=Mus musculus GN=App PE=1 SV=3	14,021
Q3SYP5	Keratin 16 OS=Mus musculus GN=Krt16 PE=2 SV=1	8,4
Q9Z331	Keratin, type II cytoskeletal 6B OS=Mus musculus GN=Krt6b PE=1 SV=3	5,956
Q6IFX2	Keratin, type I cytoskeletal 42 OS=Mus musculus GN=Krt42 PE=1 SV=1	5,635
Q9JM93	ADP-ribosylation factor-like protein 6-interacting protein 4 OS=Mus musculus GN=Arl6ip4 PE=1 SV=1	5,486
Q61782	Type I epidermal keratin mRNA, 3'end (Fragment) OS=Mus musculus PE=2 SV=1	4,628
Q9QWL7	Keratin, type I cytoskeletal 17 OS=Mus musculus GN=Krt17 PE=1 SV=3	4,351
Q99MN9	Propionyl-CoA carboxylase beta chain, mitochondrial OS=Mus musculus GN=Pccb PE=1 SV=2	3,96
Q9CZY3	Ubiquitin-conjugating enzyme E2 variant 1 OS=Mus musculus GN=Ube2v1 PE=1 SV=1	3,89
Q9WTL4	Insulin receptor-related protein OS=Mus musculus GN=Insrr PE=1 SV=2	3,852
P62715	Serine/threonine-protein phosphatase 2A catalytic subunit beta isoform OS=Mus musculus GN=Ppp2cb PE=1 SV=1	3,674
Q61781	Keratin, type I cytoskeletal 14 OS=Mus musculus GN=Krt14 PE=1 SV=2	3,606
P19001	Keratin, type I cytoskeletal 19 OS=Mus musculus GN=Krt19 PE=1 SV=1	3,598
Q3TXU4	Apolipoprotein E, isoform CRA_h OS=Mus musculus GN=Apoe PE=2 SV=1	3,577
P43276	Histone H1.5 OS=Mus musculus GN=Hist1h1b PE=1 SV=2	3,402
P10637-3	Isoform Tau-B of Microtubule-associated protein tau OS=Mus musculus GN=Mapt	3,212
P14685	26S proteasome non-ATPase regulatory subunit 3 OS=Mus musculus GN=Psmd3 PE=1 SV=3	3,164
Q9D0M3	Cytochrome c1, heme protein, mitochondrial OS=Mus musculus GN=Cyc1 PE=1 SV=1	2,935
Q80YX1	Tenascin OS=Mus musculus GN=Tnc PE=1 SV=1	2,749
Q9JLM8	Serine/threonine-protein kinase DCLK1 OS=Mus musculus GN=Dclk1 PE=1 SV=1	2,736
A0A140T8K6	60S ribosomal protein L36 OS=Mus musculus GN=Rpl36-ps3 PE=3 SV=1	2,694
P12787	Cytochrome c oxidase subunit 5A, mitochondrial OS=Mus musculus GN=Cox5a PE=1 SV=2	2,555
Q3V0Q1	Dynein heavy chain 12, axonemal OS=Mus musculus GN=Dnah12 PE=1 SV=2	2,526
Q91VE0	Long-chain fatty acid transport protein 4 OS=Mus musculus GN=Slc27a4 PE=1 SV=1	2,47
Q564G0	Guanylate kinase OS=Mus musculus GN=Guk1 PE=1 SV=1	2,384
Q8R366	Immunoglobulin superfamily member 8 OS=Mus musculus GN=Igsf8 PE=1 SV=2	2,374
E9Q557	Desmoplakin OS=Mus musculus GN=Dsp PE=1 SV=1	2,319
Q9D823	60S ribosomal protein L37 OS=Mus musculus GN=Rpl37 PE=3 SV=3	2,302
P62855	40S ribosomal protein S26 OS=Mus musculus GN=Rps26 PE=1 SV=3	2,296
Q32P04	Keratin 5 OS=Mus musculus GN=Krt5 PE=2 SV=2	2,268
Q8R1B4	Eukaryotic translation initiation factor 3 subunit C OS=Mus musculus GN=Eif3c PE=1 SV=1	2,204
Q8C1Y8	Vacuolar fusion protein CCZ1 homolog OS=Mus musculus GN=Ccz1 PE=1 SV=1	2,201
V9GX76	Unconventional myosin-VI OS=Mus musculus GN=Myo6 PE=1 SV=1	2,143
Q9CXS4	Centromere protein V OS=Mus musculus GN=Cenpv PE=1 SV=2	2,142
Q9QXS1	Plectin OS=Mus musculus GN=Plec PE=1 SV=3	2,138
P62717	60S ribosomal protein L18a OS=Mus musculus GN=Rpl18a PE=1 SV=1	2,133
P62307	Small nuclear ribonucleoprotein F OS=Mus musculus GN=Snrpf PE=1 SV=1	2,066
Q9CYR0	Single-stranded DNA-binding protein, mitochondrial OS=Mus musculus GN=Ssbp1 PE=1 SV=1	2,033

Q8C522	Endonuclease domain-containing 1 protein OS=Mus musculus GN=Endod1 PE=1 SV=2	2,031
P97499	Telomerase protein component 1 OS=Mus musculus GN=Tep1 PE=1 SV=1	2,01
Q9R062	Glycogenin-1 OS=Mus musculus GN=Gyg1 PE=1 SV=3	1,985
Q9QWI6	SRC kinase signaling inhibitor 1 OS=Mus musculus GN=Srcin1 PE=1 SV=2	1,98
P63163	Small nuclear ribonucleoprotein-associated protein N OS=Mus musculus GN=Snrpn PE=2 SV=1	1,948
P17427	AP-2 complex subunit alpha-2 OS=Mus musculus GN=Ap2a2 PE=1 SV=2	1,948
Q5BLK0	MCG18564, isoform CRA_a OS=Mus musculus GN=Rpl12 PE=2 SV=1	1,948
J3QMG3	Voltage-dependent anion-selective channel protein 3 OS=Mus musculus GN=Vdac3 PE=1 SV=1	1,911
Q9DCW4	Electron transfer flavoprotein subunit beta OS=Mus musculus GN=Etfb PE=1 SV=3	1,906
Q58EW0	60S ribosomal protein L18 OS=Mus musculus GN=Rpl18 PE=2 SV=1	1,886
Q8BMF4	Dihydrolipoyllysine-residue acetyltransferase component of pyruvate dehydrogenase complex, mitochondrial OS=Mus musculus GN=Dlat PE=1 SV=2	1,856
Q9Z0H4	CUGBP Elav-like family member 2 OS=Mus musculus GN=Celf2 PE=1 SV=1	1,845
P46660	Alpha-internexin OS=Mus musculus GN=Ina PE=1 SV=3	1,828
P08752	Guanine nucleotide-binding protein G(i) subunit alpha-2 OS=Mus musculus GN=Gnai2 PE=1 SV=5	1,823
Q549A5	Clusterin OS=Mus musculus GN=Clu PE=2 SV=1	1,822
Q8BTI8	Serine/arginine repetitive matrix protein 2 OS=Mus musculus GN=Srrm2 PE=1 SV=3	1,819
Q3TI05	Chaperonin containing Tcp1, subunit 6a (Zeta) OS=Mus musculus GN=Cct6a PE=2 SV=1	1,814
O55091	Protein IMPACT OS=Mus musculus GN=Impact PE=1 SV=2	1,778
F6TYB7	Myelin basic protein (Fragment) OS=Mus musculus GN=Mbp PE=1 SV=1	1,776
Q04690	Neurofibromin OS=Mus musculus GN=Nf1 PE=1 SV=1	1,722
P03995	Glial fibrillary acidic protein OS=Mus musculus GN=Gfap PE=1 SV=4	1,694
E9Q401	Ryanodine receptor 2 OS=Mus musculus GN=Ryr2 PE=1 SV=1	1,689
Q5BLJ9	60S ribosomal protein L27 OS=Mus musculus GN=Rpl27 PE=2 SV=1	1,688
A2CEK3	Phosphoglucomutase-2 OS=Mus musculus GN=Pgm2 PE=1 SV=1	1,675
P61514	60S ribosomal protein L37a OS=Mus musculus GN=Rpl37a PE=3 SV=2	1,667
Q505A8	MCG17585 OS=Mus musculus GN=Rpl39 PE=2 SV=1	1,64
P11983	T-complex protein 1 subunit alpha OS=Mus musculus GN=Tcp1 PE=1 SV=3	1,637
Q9D0M5	Dynein light chain 2, cytoplasmic OS=Mus musculus GN=Dynll2 PE=1 SV=1	1,626
Q5M9J8	MCG13936 OS=Mus musculus GN=Rpl28 PE=2 SV=1	1,621
P31938	Dual specificity mitogen-activated protein kinase kinase 1 OS=Mus musculus GN=Map2k1 PE=1 SV=2	1,596
Q8BGT8	Phytanoyl-CoA hydroxylase-interacting protein-like OS=Mus musculus GN=Phyhipl PE=2 SV=1	1,584
E9PYK3	Poly [ADP-ribose] polymerase OS=Mus musculus GN=Parp4 PE=1 SV=1	1,583
Q4VAG4	MCG12304 OS=Mus musculus GN=Rpl22 PE=2 SV=1	1,575
Q8BL66	Early endosome antigen 1 OS=Mus musculus GN=Eea1 PE=1 SV=2	1,564
P11881	Inositol 1,4,5-trisphosphate receptor type 1 OS=Mus musculus GN=Itpr1 PE=1 SV=2	1,562
P12382	ATP-dependent 6-phosphofructokinase, liver type OS=Mus musculus GN=Pfkl PE=1 SV=4	1,544
P62320	Small nuclear ribonucleoprotein Sm D3 OS=Mus musculus GN=Snrpd3 PE=1 SV=1	1,523
A0A0A0MQA5	Tubulin alpha chain (Fragment) OS=Mus musculus GN=Tuba4a PE=1 SV=1	1,516
Q2PFD7	PH and SEC7 domain-containing protein 3 OS=Mus musculus GN=Psd3 PE=1 SV=2	1,487
Q9JHU4	Cytoplasmic dynein 1 heavy chain 1 OS=Mus musculus GN=Dync1h1 PE=1 SV=2	1,48
P63318	Protein kinase C gamma type OS=Mus musculus GN=Prkcg PE=1 SV=1	1,476
P14106	Complement C1q subcomponent subunit B OS=Mus musculus GN=C1qb PE=1 SV=2	1,473

P01592	Immunoglobulin J chain OS=Mus musculus GN=Igj PE=2 SV=4	1,472
Q8VDD5	Myosin-9 OS=Mus musculus GN=Myh9 PE=1 SV=4	1,471
Q3TQ70	Beta1 subnuit of GTP-binding protein OS=Mus musculus GN=Gnb1 PE=2 SV=1	1,468
P62918	60S ribosomal protein L8 OS=Mus musculus GN=Rpl8 PE=1 SV=2	1,461
P86048	60S ribosomal protein L10-like OS=Mus musculus GN=Rpl10l PE=2 SV=1	1,461
Q8BMS1	Trifunctional enzyme subunit alpha, mitochondrial OS=Mus musculus GN=Hadha PE=1 SV=1	1,458
P14148	60S ribosomal protein L7 OS=Mus musculus GN=Rpl7 PE=1 SV=2	1,449
Q9CR57	60S ribosomal protein L14 OS=Mus musculus GN=Rpl14 PE=1 SV=3	1,443
Q9EQK5	Major vault protein OS=Mus musculus GN=Mvp PE=1 SV=4	1,426
A0A097PUG4	Anti-lox-1 15C4 light chain OS=Mus musculus PE=2 SV=1	1,416
A2AQR0	Glycerol-3-phosphate dehydrogenase OS=Mus musculus GN=Gpd2 PE=1 SV=1	1,412
E9Q8N8	Anion exchange protein OS=Mus musculus GN=Slc4a4 PE=1 SV=1	1,409
P27773	Protein disulfide-isomerase A3 OS=Mus musculus GN=Pdia3 PE=1 SV=2	1,396
Q9R1P3	Proteasome subunit beta type-2 OS=Mus musculus GN=Psmb2 PE=1 SV=1	1,395
Q0VF55	Calcium-transporting ATPase OS=Mus musculus GN=Atp2b3 PE=1 SV=1	1,393
Q9WV34	MAGUK p55 subfamily member 2 OS=Mus musculus GN=Mpp2 PE=1 SV=1	1,391
P27659	60S ribosomal protein L3 OS=Mus musculus GN=Rpl3 PE=1 SV=3	1,384
Q8BH58	TIP41-like protein OS=Mus musculus GN=Tiprl PE=1 SV=1	1,384
P62267	40S ribosomal protein S23 OS=Mus musculus GN=Rps23 PE=1 SV=3	1,379
Q9CQV8	14-3-3 protein beta/alpha OS=Mus musculus GN=Ywhab PE=1 SV=3	1,378
Q99104	Unconventional myosin-Va OS=Mus musculus GN=Myo5a PE=1 SV=2	1,378
Q4FJX4	Csrp1 protein OS=Mus musculus GN=Csrp1 PE=2 SV=1	1,375
Q9WUB3	Glycogen phosphorylase, muscle form OS=Mus musculus GN=Pygm PE=1 SV=3	1,374
Q3UNV7	Putative uncharacterized protein OS=Mus musculus GN=Mlf2 PE=2 SV=1	1,373
P20152	Vimentin OS=Mus musculus GN=Vim PE=1 SV=3	1,368
P62880	Guanine nucleotide-binding protein G(I)/G(S)/G(T) subunit beta-2 OS=Mus musculus GN=Gnb2 PE=1 SV=3	1,368
Q3U7E0	Putative uncharacterized protein OS=Mus musculus GN=Atp6v1g1 PE=2 SV=1	1,364
P49722	Proteasome subunit alpha type-2 OS=Mus musculus GN=Psma2 PE=1 SV=3	1,356
P19096	Fatty acid synthase OS=Mus musculus GN=Fasn PE=1 SV=2	1,355
Q9DAK9	14 kDa phosphohistidine phosphatase OS=Mus musculus GN=Phpt1 PE=1 SV=1	1,355
P62827	GTP-binding nuclear protein Ran OS=Mus musculus GN=Ran PE=1 SV=3	1,343
O08788	Dynactin subunit 1 OS=Mus musculus GN=Dctn1 PE=1 SV=3	1,341
P29341	Polyadenylate-binding protein 1 OS=Mus musculus GN=Pabpc1 PE=1 SV=2	1,34
P56480	ATP synthase subunit beta, mitochondrial OS=Mus musculus GN=Atp5b PE=1 SV=2	1,335
Q3UH59	Myosin-10 OS=Mus musculus GN=Myh10 PE=1 SV=1	1,334
Q497E9	40S ribosomal protein S8 OS=Mus musculus GN=Rps8 PE=2 SV=1	1,325
P62305	Small nuclear ribonucleoprotein E OS=Mus musculus GN=Snrpe PE=1 SV=1	1,322
Q61838	Alpha-2-macroglobulin OS=Mus musculus GN=A2m PE=1 SV=3	1,32
P63085	Mitogen-activated protein kinase 1 OS=Mus musculus GN=Mapk1 PE=1 SV=3	1,32
Q5SQX6	Cytoplasmic FMR1-interacting protein 2 OS=Mus musculus GN=Cyfip2 PE=1 SV=2	1,319
P68040	Receptor of activated protein C kinase 1 OS=Mus musculus GN=Rack1 PE=1 SV=3	1,313
O70318	Band 4.1-like protein 2 OS=Mus musculus GN=Epb41l2 PE=1 SV=2	1,31

Q9QZQ8	Core histone macro-H2A.1 OS=Mus musculus GN=H2afy PE=1 SV=3	1,308
Q8VEK3	Heterogeneous nuclear ribonucleoprotein U OS=Mus musculus GN=Hnrnpu PE=1 SV=1	1,305
Q9JIS5	Synaptic vesicle glycoprotein 2A OS=Mus musculus GN=Sv2a PE=1 SV=1	1,302
Q548L4	Glutamate decarboxylase OS=Mus musculus GN=Gad2 PE=2 SV=1	0,774
P19253	60S ribosomal protein L13a OS=Mus musculus GN=Rpl13a PE=1 SV=4	0,772
Q91V12-2	Isoform A of Cytosolic acyl coenzyme A thioester hydrolase OS=Mus musculus GN=Acot7	0,771
A0A075B6A0	Ig mu chain C region (Fragment) OS=Mus musculus GN=Ighm PE=1 SV=2	0,77
P60202	Myelin proteolipid protein OS=Mus musculus GN=Plp1 PE=1 SV=2	0,77
P47963	60S ribosomal protein L13 OS=Mus musculus GN=Rpl13 PE=1 SV=3	0,763
P06745	Glucose-6-phosphate isomerase OS=Mus musculus GN=Gpi PE=1 SV=4	0,762
Q5YLW3	Ribosomal protein S3 OS=Mus musculus GN=Rps3 PE=2 SV=1	0,762
P47962	60S ribosomal protein L5 OS=Mus musculus GN=Rpl5 PE=1 SV=3	0,756
B2RTM0	Histone H4 OS=Mus musculus GN=Hist2h4 PE=2 SV=1	0,753
Q9D051	Pyruvate dehydrogenase E1 component subunit beta, mitochondrial OS=Mus musculus GN=Pdhb PE=1 SV=1	0,753
P17710	Hexokinase-1 OS=Mus musculus GN=Hk1 PE=1 SV=3	0,749
P28738	Kinesin heavy chain isoform 5C OS=Mus musculus GN=Kif5c PE=1 SV=3	0,746
P62281	40S ribosomal protein S11 OS=Mus musculus GN=Rps11 PE=1 SV=3	0,743
P21460	Cystatin-C OS=Mus musculus GN=Cst3 PE=1 SV=2	0,742
O08553	Dihydropyrimidinase-related protein 2 OS=Mus musculus GN=Dpysl2 PE=1 SV=2	0,735
P97351	40S ribosomal protein S3a OS=Mus musculus GN=Rps3a PE=1 SV=3	0,735
P35486	Pyruvate dehydrogenase E1 component subunit alpha, somatic form, mitochondrial OS=Mus musculus GN=Pdha1 PE=1 SV=1	0,734
Q9CPU0	Lactoylglutathione lyase OS=Mus musculus GN=Glo1 PE=1 SV=3	0,732
Q7TSJ2	Microtubule-associated protein 6 OS=Mus musculus GN=Map6 PE=1 SV=2	0,732
Q80YN3	Breast carcinoma-amplified sequence 1 homolog OS=Mus musculus GN=Bcas1 PE=1 SV=3	0,731
P62137	Serine/threonine-protein phosphatase PP1-alpha catalytic subunit OS=Mus musculus GN=Ppp1ca PE=1 SV=1	0,731
Q8K183	Pyridoxal kinase OS=Mus musculus GN=Pdxk PE=1 SV=1	0,729
Q02105	Complement C1q subcomponent subunit C OS=Mus musculus GN=C1qc PE=2 SV=2	0,728
Q9D8B3	Charged multivesicular body protein 4b OS=Mus musculus GN=Chmp4b PE=1 SV=2	0,728
Q3TVK3	Aspartyl aminopeptidase OS=Mus musculus GN=Dnpep PE=1 SV=1	0,727
Q7TMM9	Tubulin beta-2A chain OS=Mus musculus GN=Tubb2a PE=1 SV=1	0,724
B9EHN0	Ubiquitin-activating enzyme E1, Chr X OS=Mus musculus GN=Uba1 PE=2 SV=1	0,721
P70349	Histidine triad nucleotide-binding protein 1 OS=Mus musculus GN=Hint1 PE=1 SV=3	0,716
Q80Y52	Heat shock protein 90, alpha (Cytosolic), class A member 1 OS=Mus musculus GN=Hsp90aa1 PE=2 SV=2	0,716
G5E902	MCG10343, isoform CRA_b OS=Mus musculus GN=Slc25a3 PE=1 SV=1	0,71
H3BKH6	S-formylglutathione hydrolase OS=Mus musculus GN=Esd PE=1 SV=1	0,709
P63017	Heat shock cognate 71 kDa protein OS=Mus musculus GN=Hspa8 PE=1 SV=1	0,708
F6RSK3	Protein Gm17430 OS=Mus musculus GN=Gm17430 PE=4 SV=1	0,705
Q7M6W1	Reticulon OS=Mus musculus GN=Rtn1 PE=1 SV=1	0,705
O55042	Alpha-synuclein OS=Mus musculus GN=Snca PE=1 SV=2	0,704
F6YVP7	Protein Gm10260 OS=Mus musculus GN=Gm10260 PE=3 SV=2	0,704
Q546G4	Albumin 1 OS=Mus musculus GN=Alb PE=2 SV=1	0,703
P70202	Latexin OS=Mus musculus GN=Lxn PE=1 SV=2	0,703

P50396	Rab GDP dissociation inhibitor alpha OS=Mus musculus GN=Gdi1 PE=1 SV=3	0,701
Q810U4	Neuronal cell adhesion molecule OS=Mus musculus GN=Nrcam PE=1 SV=2	0,699
P11499	Heat shock protein HSP 90-beta OS=Mus musculus GN=Hsp90ab1 PE=1 SV=3	0,699
Q542X7	Chaperonin subunit 2 (Beta), isoform CRA_a OS=Mus musculus GN=Cct2 PE=2 SV=1	0,699
Q642L7	MCG13441 OS=Mus musculus GN=Rps27a PE=2 SV=1	0,692
A2ARP8	Microtubule-associated protein 1A OS=Mus musculus GN=Map1a PE=1 SV=1	0,692
P99028	Cytochrome b-c1 complex subunit 6, mitochondrial OS=Mus musculus GN=Uqcrh PE=1 SV=2	0,691
Q3UMU9	Hepatoma-derived growth factor-related protein 2 OS=Mus musculus GN=Hdgfrp2 PE=1 SV=1	0,69
D0VYV6	Erythrocyte protein band 4.1-like 3 isoform B OS=Mus musculus GN=Epb4.1l3 PE=2 SV=1	0,689
P57780	Alpha-actinin-4 OS=Mus musculus GN=Actn4 PE=1 SV=1	0,686
A2ALV3	Endophilin-A1 OS=Mus musculus GN=Sh3gl2 PE=1 SV=1	0,68
Q9Z204	Heterogeneous nuclear ribonucleoproteins C1/C2 OS=Mus musculus GN=Hnrnpc PE=1 SV=1	0,679
Q91VB8	Alpha globin 1 OS=Mus musculus GN=haemaglobin alpha 2 PE=1 SV=1	0,67
P17742	Peptidyl-prolyl cis-trans isomerase A OS=Mus musculus GN=Ppia PE=1 SV=2	0,669
Q9Z1G4	V-type proton ATPase 116 kDa subunit a isoform 1 OS=Mus musculus GN=Atp6v0a1 PE=1 SV=3	0,669
Q01853	Transitional endoplasmic reticulum ATPase OS=Mus musculus GN=Vcp PE=1 SV=4	0,668
Q3V117	ATP-citrate synthase OS=Mus musculus GN=Acly PE=1 SV=1	0,665
Q9ERD7	Tubulin beta-3 chain OS=Mus musculus GN=Tubb3 PE=1 SV=1	0,665
P28651	Carbonic anhydrase-related protein OS=Mus musculus GN=Ca8 PE=1 SV=5	0,664
Q9Z2T6	Keratin, type II cuticular Hb5 OS=Mus musculus GN=Krt85 PE=2 SV=2	0,66
P52480	Pyruvate kinase PKM OS=Mus musculus GN=Pkm PE=1 SV=4	0,659
Q58E64	Elongation factor 1-alpha OS=Mus musculus GN=Eef1a1 PE=2 SV=1	0,658
Q9D6R2	Isocitrate dehydrogenase [NAD] subunit alpha, mitochondrial OS=Mus musculus GN=Idh3a PE=1 SV=1	0,657
Q60829	Protein phosphatase 1 regulatory subunit 1B OS=Mus musculus GN=Ppp1r1b PE=2 SV=2	0,656
Q7TQD2	Tubulin polymerization-promoting protein OS=Mus musculus GN=Tppp PE=1 SV=1	0,656
A0A087WQN2	Prothymosin alpha (Fragment) OS=Mus musculus GN=Ptma PE=1 SV=1	0,654
P62082	40S ribosomal protein S7 OS=Mus musculus GN=Rps7 PE=2 SV=1	0,654
B0QZN5	Vesicle-associated membrane protein 2 OS=Mus musculus GN=Vamp2 PE=1 SV=1	0,648
P68369	Tubulin alpha-1A chain OS=Mus musculus GN=Tuba1a PE=1 SV=1	0,648
Q08331	Calretinin OS=Mus musculus GN=Calb2 PE=1 SV=3	0,647
P26443	Glutamate dehydrogenase 1, mitochondrial OS=Mus musculus GN=Glud1 PE=1 SV=1	0,646
P01787	Ig heavy chain V regions TEPC 15/S107/HPCM1/HPCM2/HPCM3 OS=Mus musculus PE=1 SV=1	0,644
P61255	60S ribosomal protein L26 OS=Mus musculus GN=Rpl26 PE=1 SV=1	0,644
D3Z722	40S ribosomal protein S19 OS=Mus musculus GN=Rps19 PE=1 SV=1	0,637
B9EKR1	Receptor-type tyrosine-protein phosphatase zeta OS=Mus musculus GN=Ptprz1 PE=1 SV=1	0,635
P63005	Platelet-activating factor acetylhydrolase IB subunit alpha OS=Mus musculus GN=Pafah1b1 PE=1 SV=2	0,629
Q5SXR6	Clathrin heavy chain OS=Mus musculus GN=Cltc PE=1 SV=1	0,621
P18872	Guanine nucleotide-binding protein G(o) subunit alpha OS=Mus musculus GN=Gnao1 PE=1 SV=3	0,619
Q60864	Stress-induced-phosphoprotein 1 OS=Mus musculus GN=Stip1 PE=1 SV=1	0,612
P62889	60S ribosomal protein L30 OS=Mus musculus GN=Rpl30 PE=1 SV=2	0,611
F6RT34	Myelin basic protein (Fragment) OS=Mus musculus GN=Mbp PE=1 SV=1	0,61
O54962	Barrier-to-autointegration factor OS=Mus musculus GN=Banf1 PE=1 SV=1	0,608

A8DUK4	Beta-globin OS=Mus musculus GN=Hbbt1 PE=1 SV=1	0,603
P62259	14-3-3 protein epsilon OS=Mus musculus GN=Ywhae PE=1 SV=1	0,603
Q9D6F9	Tubulin beta-4A chain OS=Mus musculus GN=Tubb4a PE=1 SV=3	0,6
Q99PT1	Rho GDP-dissociation inhibitor 1 OS=Mus musculus GN=Arhgdia PE=1 SV=3	0,596
Q9JLZ3	Methylglutaconyl-CoA hydratase, mitochondrial OS=Mus musculus GN=Auh PE=1 SV=1	0,596
Q9QYX7	Protein piccolo OS=Mus musculus GN=Pclo PE=1 SV=4	0,596
Q04447	Creatine kinase B-type OS=Mus musculus GN=Ckb PE=1 SV=1	0,595
Q8K0U4	Heat shock 70 kDa protein 12A OS=Mus musculus GN=Hspa12a PE=1 SV=1	0,595
F6VW30	14-3-3 protein theta (Fragment) OS=Mus musculus GN=Ywhaq PE=1 SV=1	0,594
P14873	Microtubule-associated protein 1B OS=Mus musculus GN=Map1b PE=1 SV=2	0,591
Q548F2	Guanine deaminase OS=Mus musculus GN=Gda PE=2 SV=1	0,59
A0A075B5P2	Protein Igkc (Fragment) OS=Mus musculus GN=Igkc PE=1 SV=1	0,59
A0A0A6YXW6	Protein Igha (Fragment) OS=Mus musculus GN=Igha PE=1 SV=1	0,589
F8WGL3	Cofilin-1 OS=Mus musculus GN=Cfl1 PE=1 SV=1	0,584
Q76MZ3	Serine/threonine-protein phosphatase 2A 65 kDa regulatory subunit A alpha isoform OS=Mus musculus GN=Ppp2r1a PE=1 SV=3	0,584
P09411	Phosphoglycerate kinase 1 OS=Mus musculus GN=Pgk1 PE=1 SV=4	0,584
P05063	Fructose-bisphosphate aldolase C OS=Mus musculus GN=Aldoc PE=1 SV=4	0,583
P58252	Elongation factor 2 OS=Mus musculus GN=Eef2 PE=1 SV=2	0,583
Q6W8Q3	Purkinje cell protein 4-like protein 1 OS=Mus musculus GN=Pcp4l1 PE=1 SV=1	0,582
Q9DBJ1	Phosphoglycerate mutase 1 OS=Mus musculus GN=Pgam1 PE=1 SV=3	0,579
Q99KI0	Aconitate hydratase, mitochondrial OS=Mus musculus GN=Aco2 PE=1 SV=1	0,579
P27661	Histone H2AX OS=Mus musculus GN=H2afx PE=1 SV=2	0,577
P60766	Cell division control protein 42 homolog OS=Mus musculus GN=Cdc42 PE=1 SV=2	0,577
P52760	Ribonuclease UK114 OS=Mus musculus GN=Hrsp12 PE=1 SV=3	0,576
Q5EBQ2	MCG7941, isoform CRA_f OS=Mus musculus GN=Pebp1 PE=2 SV=1	0,576
Q545B6	Stathmin OS=Mus musculus GN=Stmn1 PE=2 SV=1	0,574
P20357	Microtubule-associated protein 2 OS=Mus musculus GN=Map2 PE=1 SV=2	0,574
P62858	40S ribosomal protein S28 OS=Mus musculus GN=Rps28 PE=1 SV=1	0,574
Q545P0	ATPase, Na+/K+ transporting, beta 1 polypeptide OS=Mus musculus GN=Atp1b1 PE=2 SV=1	0,565
A0A087WP80	Limbic system-associated membrane protein OS=Mus musculus GN=Lsamp PE=1 SV=1	0,559
Q9R0Y5	Adenylate kinase isoenzyme 1 OS=Mus musculus GN=Ak1 PE=1 SV=1	0,559
Q3UL22	Chaperonin subunit 8 (Theta), isoform CRA_a OS=Mus musculus GN=Cct8 PE=2 SV=1	0,557
P35700	Peroxiredoxin-1 OS=Mus musculus GN=Prdx1 PE=1 SV=1	0,556
P16125	L-lactate dehydrogenase B chain OS=Mus musculus GN=Ldhb PE=1 SV=2	0,552
P10649	Glutathione S-transferase Mu 1 OS=Mus musculus GN=Gstm1 PE=1 SV=2	0,55
D3Z4B2	Gamma-soluble NSF attachment protein (Fragment) OS=Mus musculus GN=Napg PE=1 SV=1	0,545
P98086	Complement C1q subcomponent subunit A OS=Mus musculus GN=C1qa PE=1 SV=2	0,542
P08249	Malate dehydrogenase, mitochondrial OS=Mus musculus GN=Mdh2 PE=1 SV=3	0,542
Q61361	Brevican core protein OS=Mus musculus GN=Bcan PE=1 SV=2	0,54
P63101	14-3-3 protein zeta/delta OS=Mus musculus GN=Ywhaz PE=1 SV=1	0,537
E9PVP0	PCTP-like protein OS=Mus musculus GN=Stard10 PE=1 SV=1	0,537
Q91ZZ3	Beta-synuclein OS=Mus musculus GN=Sncb PE=1 SV=1	0,535

P62631	Elongation factor 1-alpha 2 OS=Mus musculus GN=Eef1a2 PE=1 SV=1	0,533
Q9DBG3	AP-2 complex subunit beta OS=Mus musculus GN=Ap2b1 PE=1 SV=1	0,532
P51863	V-type proton ATPase subunit d 1 OS=Mus musculus GN=Atp6v0d1 PE=1 SV=2	0,531
P60710	Actin, cytoplasmic 1 OS=Mus musculus GN=Actb PE=1 SV=1	0,531
P68433	Histone H3.1 OS=Mus musculus GN=Hist1h3a PE=1 SV=2	0,525
Q3UY00	Protein S100 OS=Mus musculus GN=S100b PE=2 SV=1	0,517
Q3U1N0	Coronin OS=Mus musculus GN=Coro1a PE=2 SV=1	0,512
Q5FW97	Enolase 1, alpha non-neuron OS=Mus musculus GN=EG433182 PE=2 SV=1	0,511
E9PZF0	Nucleoside diphosphate kinase OS=Mus musculus GN=Gm20390 PE=3 SV=1	0,51
A6ZI44	Fructose-bisphosphate aldolase OS=Mus musculus GN=Aldoa PE=1 SV=1	0,507
Q3U2G2	Heat shock 70 kDa protein 4 OS=Mus musculus GN=Hspa4 PE=1 SV=1	0,505
P09405	Nucleolin OS=Mus musculus GN=Ncl PE=1 SV=2	0,504
P61922	4-aminobutyrate aminotransferase, mitochondrial OS=Mus musculus GN=Abat PE=1 SV=1	0,498
Q9Z2D6-2	Isoform B of Methyl-CpG-binding protein 2 OS=Mus musculus GN=Mecp2	0,496
P80313	T-complex protein 1 subunit eta OS=Mus musculus GN=Cct7 PE=1 SV=1	0,496
Q149Z9	Histone cluster 1, H1d OS=Mus musculus GN=Hist1h1d PE=2 SV=1	0,492
P17751	Triosephosphate isomerase OS=Mus musculus GN=Tpi1 PE=1 SV=4	0,492
Q9R0P9	Ubiquitin carboxyl-terminal hydrolase isozyme L1 OS=Mus musculus GN=Uchl1 PE=1 SV=1	0,489
Q9EQU5-2	Isoform 2 of Protein SET OS=Mus musculus GN=Set	0,486
Q8C2Q7	Heterogeneous nuclear ribonucleoprotein H OS=Mus musculus GN=Hnrnph1 PE=1 SV=1	0,483
Q9JJV2	Profilin-2 OS=Mus musculus GN=Pfn2 PE=1 SV=3	0,483
P68372	Tubulin beta-4B chain OS=Mus musculus GN=Tubb4b PE=1 SV=1	0,48
Q60668	Heterogeneous nuclear ribonucleoprotein D0 OS=Mus musculus GN=Hnrnpd PE=1 SV=2	0,479
Q8BVI4	Dihydropteridine reductase OS=Mus musculus GN=Qdpr PE=1 SV=2	0,478
Q543Y7	Putative uncharacterized protein OS=Mus musculus GN=Pacsin1 PE=2 SV=1	0,471
P28474	Alcohol dehydrogenase class-3 OS=Mus musculus GN=Adh5 PE=1 SV=3	0,465
P14869	60S acidic ribosomal protein P0 OS=Mus musculus GN=Rplp0 PE=1 SV=3	0,464
P61979	Heterogeneous nuclear ribonucleoprotein K OS=Mus musculus GN=Hnrnpk PE=1 SV=1	0,463
Q6GT24	Peroxiredoxin 6 OS=Mus musculus GN=Prdx6 PE=1 SV=1	0,462
P26883	Peptidyl-prolyl cis-trans isomerase FKBP1A OS=Mus musculus GN=Fkbp1a PE=1 SV=2	0,461
P84086	Complexin-2 OS=Mus musculus GN=Cplx2 PE=1 SV=1	0,459
O88569	Heterogeneous nuclear ribonucleoproteins A2/B1 OS=Mus musculus GN=Hnrnpa2b1 PE=1 SV=2	0,457
Q921M7	Protein FAM49B OS=Mus musculus GN=Fam49b PE=2 SV=1	0,456
P20029	78 kDa glucose-regulated protein OS=Mus musculus GN=Hspa5 PE=1 SV=3	0,454
Q9CZC8	Secernin-1 OS=Mus musculus GN=Scrn1 PE=1 SV=1	0,452
P99024	Tubulin beta-5 chain OS=Mus musculus GN=Tubb5 PE=1 SV=1	0,45
P42669	Transcriptional activator protein Pur-alpha OS=Mus musculus GN=Pura PE=1 SV=1	0,45
P68510	14-3-3 protein eta OS=Mus musculus GN=Ywhah PE=1 SV=2	0,447
B2RTK3	Histone H2B OS=Mus musculus GN=Hist1h2bm PE=2 SV=1	0,445
A0A0A0MQF6	Glyceraldehyde-3-phosphate dehydrogenase OS=Mus musculus GN=Gapdh PE=1 SV=1	0,443
Q99PU5	Long-chain-fatty-acid--CoA ligase ACSBG1 OS=Mus musculus GN=Acsbg1 PE=1 SV=1	0,442
O08539	Myc box-dependent-interacting protein 1 OS=Mus musculus GN=Bin1 PE=1 SV=1	0,439

P19157	Glutathione S-transferase P 1 OS=Mus musculus GN=Gstp1 PE=1 SV=2	0,438
Q9CZ13	Cytochrome b-c1 complex subunit 1, mitochondrial OS=Mus musculus GN=Uqcrc1 PE=1 SV=2	0,438
Q9QYC0	Alpha-adducin OS=Mus musculus GN=Add1 PE=1 SV=2	0,437
A2AWN8	YTH domain family 1, isoform CRA_a OS=Mus musculus GN=Ythdf1 PE=1 SV=1	0,434
Q9WTT4	V-type proton ATPase subunit G 2 OS=Mus musculus GN=Atp6v1g2 PE=3 SV=1	0,432
Q61598	Rab GDP dissociation inhibitor beta OS=Mus musculus GN=Gdi2 PE=1 SV=1	0,432
P50518	V-type proton ATPase subunit E 1 OS=Mus musculus GN=Atp6v1e1 PE=1 SV=2	0,428
P12658	Calbindin OS=Mus musculus GN=Calb1 PE=1 SV=2	0,427
P14152	Malate dehydrogenase, cytoplasmic OS=Mus musculus GN=Mdh1 PE=1 SV=3	0,419
B2RSH2	Guanine nucleotide-binding protein G(i) subunit alpha-1 OS=Mus musculus GN=Gnai1 PE=1 SV=1	0,419
Q922J6	Tetraspanin-2 OS=Mus musculus GN=Tspan2 PE=1 SV=1	0,417
P48722	Heat shock 70 kDa protein 4L OS=Mus musculus GN=Hspa4l PE=1 SV=2	0,417
Q60631	Growth factor receptor-bound protein 2 OS=Mus musculus GN=Grb2 PE=1 SV=1	0,409
A0A076FRG6	KCC2a variant 1 OS=Mus musculus GN=Slc12a5 PE=2 SV=1	0,407
Q80TL4	PHD finger protein 24 OS=Mus musculus GN=Phf24 PE=1 SV=2	0,403
Q7TQI3	Ubiquitin thioesterase OTUB1 OS=Mus musculus GN=Otub1 PE=1 SV=2	0,394
P63038	60 kDa heat shock protein, mitochondrial OS=Mus musculus GN=Hspd1 PE=1 SV=1	0,393
P06837	Neuromodulin OS=Mus musculus GN=Gap43 PE=1 SV=1	0,381
P62774	Myotrophin OS=Mus musculus GN=Mtpn PE=1 SV=2	0,379
A0A0G2JFT8	Protein RUFY3 OS=Mus musculus GN=Rufy3 PE=1 SV=1	0,372
Q9CPW4	Actin-related protein 2/3 complex subunit 5 OS=Mus musculus GN=Arpc5 PE=2 SV=3	0,371
Q68FL4	Putative adenosylhomocysteinase 3 OS=Mus musculus GN=Ahcyl2 PE=1 SV=1	0,368
Q6IRU5	Clathrin light chain B OS=Mus musculus GN=Cltb PE=1 SV=1	0,366
P31650	Sodium- and chloride-dependent GABA transporter 3 OS=Mus musculus GN=Slc6a11 PE=1 SV=2	0,366
P60761	Neurogranin OS=Mus musculus GN=Nrgn PE=1 SV=1	0,364
O08749	Dihydrolipoyl dehydrogenase, mitochondrial OS=Mus musculus GN=Dld PE=1 SV=2	0,362
P99027	60S acidic ribosomal protein P2 OS=Mus musculus GN=Rplp2 PE=1 SV=3	0,355
P08228	Superoxide dismutase [Cu-Zn] OS=Mus musculus GN=Sod1 PE=1 SV=2	0,346
Q9JKD3	Secretory carrier-associated membrane protein 5 OS=Mus musculus GN=Scamp5 PE=1 SV=1	0,34
P48036	Annexin A5 OS=Mus musculus GN=Anxa5 PE=1 SV=1	0,339
Q9CX86	Heterogeneous nuclear ribonucleoprotein A0 OS=Mus musculus GN=Hnrnpa0 PE=1 SV=1	0,338
Q63810	Calcineurin subunit B type 1 OS=Mus musculus GN=Ppp3r1 PE=1 SV=3	0,337
P63040	Complexin-1 OS=Mus musculus GN=Cplx1 PE=1 SV=1	0,335
P32848	Parvalbumin alpha OS=Mus musculus GN=Pvalb PE=1 SV=3	0,327
Q4VWZ5	Acyl-CoA-binding protein OS=Mus musculus GN=Dbi PE=1 SV=1	0,324
F6VPT0	Protein Ccdc163 (Fragment) OS=Mus musculus GN=Ccdc163 PE=4 SV=1	0,323
P02802	Metallothionein-1 OS=Mus musculus GN=Mt1 PE=1 SV=1	0,322
P62204	Calmodulin OS=Mus musculus GN=Calm1 PE=1 SV=2	0,313
D3YXH0	Immunoglobulin superfamily member 5 OS=Mus musculus GN=Igsf5 PE=4 SV=1	0,311
Q9D3D9	ATP synthase subunit delta, mitochondrial OS=Mus musculus GN=Atp5d PE=1 SV=1	0,297
Q91XV3	Brain acid soluble protein 1 OS=Mus musculus GN=Basp1 PE=1 SV=3	0,284
Q9CRB6	Tubulin polymerization-promoting protein family member 3 OS=Mus musculus GN=Tppp3 PE=1 SV=1	0,274

P26645	Myristoylated alanine-rich C-kinase substrate OS=Mus musculus GN=Marcks PE=1 SV=2	0,273
Q9WV69	Dematin OS=Mus musculus GN=Dmtn PE=1 SV=1	0,269
Q9JKC6	Cell cycle exit and neuronal differentiation protein 1 OS=Mus musculus GN=Cend1 PE=1 SV=1	0,269
P43274	Histone H1.4 OS=Mus musculus GN=Hist1h1e PE=1 SV=2	0,256
B1AWD9	Clathrin light chain A OS=Mus musculus GN=Clta PE=1 SV=1	0,255
Q8CI43	Myosin light chain 6B OS=Mus musculus GN=Myl6b PE=2 SV=1	0,252
P61089	Ubiquitin-conjugating enzyme E2 N OS=Mus musculus GN=Ube2n PE=1 SV=1	0,249
G5E8N5	L-lactate dehydrogenase OS=Mus musculus GN=Ldha PE=1 SV=1	0,248
Q6ZWX2	Thymosin, beta 4, X chromosome OS=Mus musculus GN=Tmsb4x PE=2 SV=1	0,239
P13595	Neural cell adhesion molecule 1 OS=Mus musculus GN=Ncam1 PE=1 SV=3	0,224
E9PYN1	Cell adhesion molecule 1 OS=Mus musculus GN=Cadm1 PE=1 SV=1	0,212
P28663	Beta-soluble NSF attachment protein OS=Mus musculus GN=Napb PE=1 SV=2	0,21
P20065	Thymosin beta-4 OS=Mus musculus GN=Tmsb4x PE=1 SV=1	0,207
P60904	DnaJ homolog subfamily C member 5 OS=Mus musculus GN=Dnajc5 PE=1 SV=1	0,204

DATA FILE S1

REGULATED PROTEINS TG: 24 vs. 3 months

Accession	Description	Abundance Ratio: (TG24) / (TG3)
P43276	Histone H1.5 OS=Mus musculus GN=Hist1h1b PE=1 SV=2	16,605
Q9Z331	Keratin, type II cytoskeletal 6B OS=Mus musculus GN=Krt6b PE=1 SV=3	11,79
Q5SZA3	Histone cluster 1, H1c OS=Mus musculus GN=Hist1h1c PE=2 SV=1	10,817
P12023	Amyloid beta A4 protein OS=Mus musculus GN=App PE=1 SV=3	10,645
Q3SYP5	Keratin 16 OS=Mus musculus GN=Krt16 PE=2 SV=1	8,456
Q8R1B4	Eukaryotic translation initiation factor 3 subunit C OS=Mus musculus GN=Eif3c PE=1 SV=1	8,243
Q02105	Complement C1q subcomponent subunit C OS=Mus musculus GN=C1qc PE=2 SV=2	8,076
Q04690	Neurofibromin OS=Mus musculus GN=Nf1 PE=1 SV=1	7,567
Q3TXU4	Apolipoprotein E, isoform CRA_h OS=Mus musculus GN=Apoe PE=2 SV=1	7,512
P14106	Complement C1q subcomponent subunit B OS=Mus musculus GN=C1qb PE=1 SV=2	6,261
P01592	Immunoglobulin J chain OS=Mus musculus GN=Igj PE=2 SV=4	5,777
J3QMG3	Voltage-dependent anion-selective channel protein 3 OS=Mus musculus GN=Vdac3 PE=1 SV=1	5,506
Q9WTL4	Insulin receptor-related protein OS=Mus musculus GN=Insrr PE=1 SV=2	5,505
P28651	Carbonic anhydrase-related protein OS=Mus musculus GN=Ca8 PE=1 SV=5	5,411
Q3U7E0	Putative uncharacterized protein OS=Mus musculus GN=Atp6v1g1 PE=2 SV=1	5,379
Q61782	Type I epidermal keratin mRNA, 3'end (Fragment) OS=Mus musculus PE=2 SV=1	5,352
Q9ESM3	Hyaluronan and proteoglycan link protein 2 OS=Mus musculus GN=Hapln2 PE=1 SV=1	5,11
Q9QWL7	Keratin, type I cytoskeletal 17 OS=Mus musculus GN=Krt17 PE=1 SV=3	4,988
Q8BGT8	Phytanoyl-CoA hydroxylase-interacting protein-like OS=Mus musculus GN=Phyhipl PE=2 SV=1	4,932
P10637-3	Isoform Tau-B of Microtubule-associated protein tau OS=Mus musculus GN=Mapt	4,524
E9Q7Q3	Tropomyosin alpha-3 chain OS=Mus musculus GN=Tpm3 PE=1 SV=1	4,331
A6H611	Mitochondrial intermediate peptidase OS=Mus musculus GN=Mipep PE=1 SV=1	4,243
P21460	Cystatin-C OS=Mus musculus GN=Cst3 PE=1 SV=2	4,101
Q61282	Aggrecan core protein OS=Mus musculus GN=Acan PE=1 SV=2	4,049
Q9JM93	ADP-ribosylation factor-like protein 6-interacting protein 4 OS=Mus musculus GN=Arl6ip4 PE=1 SV=1	4,046
Q9QUP5	Hyaluronan and proteoglycan link protein 1 OS=Mus musculus GN=Hapln1 PE=1 SV=1	3,997
E9PYH0	Versican core protein OS=Mus musculus GN=Vcan PE=1 SV=1	3,976
F6YVP7	Protein Gm10260 OS=Mus musculus GN=Gm10260 PE=3 SV=2	3,763
Q9D3D9	ATP synthase subunit delta, mitochondrial OS=Mus musculus GN=Atp5d PE=1 SV=1	3,747
P11983	T-complex protein 1 subunit alpha OS=Mus musculus GN=Tcp1 PE=1 SV=3	3,73
P10922	Histone H1.0 OS=Mus musculus GN=H1f0 PE=2 SV=4	3,51
P28663	Beta-soluble NSF attachment protein OS=Mus musculus GN=Napb PE=1 SV=2	3,483
P28184	Metallothionein-3 OS=Mus musculus GN=Mt3 PE=1 SV=1	3,433
Q99MN9	Propionyl-CoA carboxylase beta chain, mitochondrial OS=Mus musculus GN=Pccb PE=1 SV=2	3,239
E9Q035	Protein Gm20425 OS=Mus musculus GN=Gm20425 PE=4 SV=1	3,214
Q8BMS1	Trifunctional enzyme subunit alpha, mitochondrial OS=Mus musculus GN=Hadha PE=1 SV=1	3,211
P17156	Heat shock-related 70 kDa protein 2 OS=Mus musculus GN=Hspa2 PE=1 SV=2	3,206
Q564G0	Guanylate kinase OS=Mus musculus GN=Guk1 PE=1 SV=1	3,184
P55066	Neurocan core protein OS=Mus musculus GN=Ncan PE=2 SV=1	3,037
P19001	Keratin, type I cytoskeletal 19 OS=Mus musculus GN=Krt19 PE=1 SV=1	3,026

P00920	Carbonic anhydrase 2 OS=Mus musculus GN=Ca2 PE=1 SV=4	3,003
Q9QYC0	Alpha-adducin OS=Mus musculus GN=Add1 PE=1 SV=2	2,926
Q9DCD0	6-phosphogluconate dehydrogenase, decarboxylating OS=Mus musculus GN=Pgd PE=1 SV=3	2,894
Q58EA6	MCG10725, isoform CRA_a OS=Mus musculus GN=Rps25 PE=2 SV=1	2,884
P26883	Peptidyl-prolyl cis-trans isomerase FKBP1A OS=Mus musculus GN=Fkbp1a PE=1 SV=2	2,87
P63040	Complexin-1 OS=Mus musculus GN=Cplx1 PE=1 SV=1	2,867
Q9CXS4	Centromere protein V OS=Mus musculus GN=Cenpv PE=1 SV=2	2,808
Q3UNV7	Putative uncharacterized protein OS=Mus musculus GN=Mlf2 PE=2 SV=1	2,778
P70441	Na(+)/H(+) exchange regulatory cofactor NHE-RF1 OS=Mus musculus GN=Slc9a3r1 PE=1 SV=3	2,718
Q61781	Keratin, type I cytoskeletal 14 OS=Mus musculus GN=Krt14 PE=1 SV=2	2,655
B9EIC7	MCG3853 OS=Mus musculus GN=Phyhip PE=2 SV=1	2,637
Q4FJX9	Superoxide dismutase OS=Mus musculus GN=Sod2 PE=2 SV=1	2,609
P26645	Myristoylated alanine-rich C-kinase substrate OS=Mus musculus GN=Marcks PE=1 SV=2	2,609
Q60829	Protein phosphatase 1 regulatory subunit 1B OS=Mus musculus GN=Ppp1r1b PE=2 SV=2	2,584
A0A075B6A0	Ig mu chain C region (Fragment) OS=Mus musculus GN=Ighm PE=1 SV=2	2,575
A0A0G2JEG8	Amphiphysin OS=Mus musculus GN=Amph PE=1 SV=1	2,566
Q8BVI4	Dihydropteridine reductase OS=Mus musculus GN=Qdpr PE=1 SV=2	2,536
A2CEK3	Phosphoglucomutase-2 OS=Mus musculus GN=Pgm2 PE=1 SV=1	2,509
A0A075B5P2	Protein Igkc (Fragment) OS=Mus musculus GN=Igkc PE=1 SV=1	2,469
B2RXY7	Carbonyl reductase 1 OS=Mus musculus GN=Cbr1 PE=2 SV=1	2,462
P61089	Ubiquitin-conjugating enzyme E2 N OS=Mus musculus GN=Ube2n PE=1 SV=1	2,452
Q543Y7	Putative uncharacterized protein OS=Mus musculus GN=Pacsin1 PE=2 SV=1	2,44
Q9CZU6	Citrate synthase, mitochondrial OS=Mus musculus GN=Cs PE=1 SV=1	2,434
P62827	GTP-binding nuclear protein Ran OS=Mus musculus GN=Ran PE=1 SV=3	2,381
Q6IFX2	Keratin, type I cytoskeletal 42 OS=Mus musculus GN=Krt42 PE=1 SV=1	2,371
Q9Z2T6	Keratin, type II cuticular Hb5 OS=Mus musculus GN=Krt85 PE=2 SV=2	2,37
Q60692	Proteasome subunit beta type-6 OS=Mus musculus GN=Psmb6 PE=1 SV=3	2,359
Q9CPW4	Actin-related protein 2/3 complex subunit 5 OS=Mus musculus GN=Arpc5 PE=2 SV=3	2,339
Q9CZY3	Ubiquitin-conjugating enzyme E2 variant 1 OS=Mus musculus GN=Ube2v1 PE=1 SV=1	2,33
P12382	ATP-dependent 6-phosphofructokinase, liver type OS=Mus musculus GN=Pfkl PE=1 SV=4	2,313
Q9R062	Glycogenin-1 OS=Mus musculus GN=Gyg1 PE=1 SV=3	2,31
E9PYN1	Cell adhesion molecule 1 OS=Mus musculus GN=Cadm1 PE=1 SV=1	2,307
Q9JKD3	Secretory carrier-associated membrane protein 5 OS=Mus musculus GN=Scamp5 PE=1 SV=1	2,286
Q7M6W1	Reticulon OS=Mus musculus GN=Rtn1 PE=1 SV=1	2,246
P43274	Histone H1.4 OS=Mus musculus GN=Hist1h1e PE=1 SV=2	2,24
Q9Z204	Heterogeneous nuclear ribonucleoproteins C1/C2 OS=Mus musculus GN=Hnrnpc PE=1 SV=1	2,235
P12787	Cytochrome c oxidase subunit 5A, mitochondrial OS=Mus musculus GN=Cox5a PE=1 SV=2	2,222
P62774	Myotrophin OS=Mus musculus GN=Mtpn PE=1 SV=2	2,201
P05201	Aspartate aminotransferase, cytoplasmic OS=Mus musculus GN=Got1 PE=1 SV=3	2,188
Q9JIS5	Synaptic vesicle glycoprotein 2A OS=Mus musculus GN=Sv2a PE=1 SV=1	2,175
Q8R0Y6	Cytosolic 10-formyltetrahydrofolate dehydrogenase OS=Mus musculus GN=Aldh1l1 PE=1 SV=1	2,174
P13707	Glycerol-3-phosphate dehydrogenase [NAD(+)], cytoplasmic OS=Mus musculus GN=Gpd1 PE=1 SV=3	2,173
A0A087WQN2	Prothymosin alpha (Fragment) OS=Mus musculus GN=Ptma PE=1 SV=1	2,163
Q8BVE3	V-type proton ATPase subunit H OS=Mus musculus GN=Atp6v1h PE=1 SV=1	2,138

Q91VE0	Long-chain fatty acid transport protein 4 OS=Mus musculus GN=Slc27a4 PE=1 SV=1	2,134
O35955	Proteasome subunit beta type-10 OS=Mus musculus GN=Psmb10 PE=1 SV=1	2,112
A0A097PUG4	Anti-lox-1 15C4 light chain OS=Mus musculus PE=2 SV=1	2,103
P19783	Cytochrome c oxidase subunit 4 isoform 1, mitochondrial OS=Mus musculus GN=Cox4i1 PE=1 SV=2	2,101
Q9QZQ8	Core histone macro-H2A.1 OS=Mus musculus GN=H2afy PE=1 SV=3	2,087
A0A075B5P3	Protein Ighg2b (Fragment) OS=Mus musculus GN=Ighg2b PE=1 SV=1	2,086
Q78ZJ8	MCG22989, isoform CRA_b OS=Mus musculus GN=Rab11b PE=2 SV=1	2,07
Q9Z0E0	Neurochondrin OS=Mus musculus GN=Ncdn PE=1 SV=1	2,07
B1AQW2	Microtubule-associated protein OS=Mus musculus GN=Mapt PE=1 SV=1	2,064
O55091	Protein IMPACT OS=Mus musculus GN=Impact PE=1 SV=2	2,043
P08228	Superoxide dismutase [Cu-Zn] OS=Mus musculus GN=Sod1 PE=1 SV=2	2,017
P62305	Small nuclear ribonucleoprotein E OS=Mus musculus GN=Snrpe PE=1 SV=1	2,004
P61979	Heterogeneous nuclear ribonucleoprotein K OS=Mus musculus GN=Hnrnpk PE=1 SV=1	2,001
Q8BWF0	Succinate-semialdehyde dehydrogenase, mitochondrial OS=Mus musculus GN=Aldh5a1 PE=1 SV=1	1,992
Q9QXS1	Plectin OS=Mus musculus GN=Plec PE=1 SV=3	1,992
Q3TQ70	Beta1 subnuit of GTP-binding protein OS=Mus musculus GN=Gnb1 PE=2 SV=1	1,987
Q8BTI8	Serine/arginine repetitive matrix protein 2 OS=Mus musculus GN=Srrm2 PE=1 SV=3	1,98
P56399	Ubiquitin carboxyl-terminal hydrolase 5 OS=Mus musculus GN=Usp5 PE=1 SV=1	1,973
E9Q557	Desmoplakin OS=Mus musculus GN=Dsp PE=1 SV=1	1,968
P68040	Receptor of activated protein C kinase 1 OS=Mus musculus GN=Rack1 PE=1 SV=3	1,968
Q9WUB3	Glycogen phosphorylase, muscle form OS=Mus musculus GN=Pygm PE=1 SV=3	1,957
Q9QYX7	Protein piccolo OS=Mus musculus GN=Pclo PE=1 SV=4	1,957
D3Z722	40S ribosomal protein S19 OS=Mus musculus GN=Rps19 PE=1 SV=1	1,947
Q9Z1G4	V-type proton ATPase 116 kDa subunit a isoform 1 OS=Mus musculus GN=Atp6v0a1 PE=1 SV=3	1,947
Q9Z0H4	CUGBP Elav-like family member 2 OS=Mus musculus GN=Celf2 PE=1 SV=1	1,944
P62715	Serine/threonine-protein phosphatase 2A catalytic subunit beta isoform OS=Mus musculus GN=Ppp2cb PE=1 SV=1	1,938
Q3ULD5	Methylcrotonoyl-CoA carboxylase beta chain, mitochondrial OS=Mus musculus GN=Mccc2 PE=1 SV=1	1,928
P46460	Vesicle-fusing ATPase OS=Mus musculus GN=Nsf PE=1 SV=2	1,902
Q9QXV0	ProSAAS OS=Mus musculus GN=Pcsk1n PE=1 SV=2	1,901
Q61838	Alpha-2-macroglobulin OS=Mus musculus GN=A2m PE=1 SV=3	1,893
E9PUA3	IQ motif and SEC7 domain-containing protein 1 OS=Mus musculus GN=Iqsec1 PE=1 SV=1	1,891
Q3UYK6	Amino acid transporter OS=Mus musculus GN=Slc1a2 PE=2 SV=1	1,89
P97300	Neuroplastin OS=Mus musculus GN=Nptn PE=1 SV=3	1,882
Q6GT24	Peroxiredoxin 6 OS=Mus musculus GN=Prdx6 PE=1 SV=1	1,877
Q9D0M5	Dynein light chain 2, cytoplasmic OS=Mus musculus GN=Dynll2 PE=1 SV=1	1,875
Q549A5	Clusterin OS=Mus musculus GN=Clu PE=2 SV=1	1,869
P62814	V-type proton ATPase subunit B, brain isoform OS=Mus musculus GN=Atp6v1b2 PE=1 SV=1	1,852
Q4FJX4	Csrp1 protein OS=Mus musculus GN=Csrp1 PE=2 SV=1	1,851
Q8R001	Microtubule-associated protein RP/EB family member 2 OS=Mus musculus GN=Mapre2 PE=1 SV=1	1,846
Q3UY21	Myelin-oligodendrocyte glycoprotein OS=Mus musculus GN=Mog PE=1 SV=1	1,821
P63276	40S ribosomal protein S17 OS=Mus musculus GN=Rps17 PE=1 SV=2	1,818
Q9D2G2	Dihydrolipoyllysine-residue succinyltransferase component of 2-oxoglutarate dehydrogenase complex, mitochondrial OS=Mus musculus GN=Dlst PE=1 SV=1	1,81
Q9Z1G3	V-type proton ATPase subunit C 1 OS=Mus musculus GN=Atp6v1c1 PE=1 SV=4	1,805
Q3TVK3	Aspartyl aminopeptidase OS=Mus musculus GN=Dnpep PE=1 SV=1	1,8

P48036	Annexin A5 OS=Mus musculus GN=Anxa5 PE=1 SV=1	1,795
P62858	40S ribosomal protein S28 OS=Mus musculus GN=Rps28 PE=1 SV=1	1,794
Q9Z2D6-2	Isoform B of Methyl-CpG-binding protein 2 OS=Mus musculus GN=Mecp2	1,784
F6VPT0	Protein Ccdc163 (Fragment) OS=Mus musculus GN=Ccdc163 PE=4 SV=1	1,783
E9PZF0	Nucleoside diphosphate kinase OS=Mus musculus GN=Gm20390 PE=3 SV=1	1,782
E9Q455	Tropomyosin alpha-1 chain OS=Mus musculus GN=Tpm1 PE=1 SV=1	1,78
Q8BG05	Heterogeneous nuclear ribonucleoprotein A3 OS=Mus musculus GN=Hnrnpa3 PE=1 SV=1	1,78
Q7TSJ2	Microtubule-associated protein 6 OS=Mus musculus GN=Map6 PE=1 SV=2	1,776
P11881	Inositol 1,4,5-trisphosphate receptor type 1 OS=Mus musculus GN=Itpr1 PE=1 SV=2	1,774
P05202	Aspartate aminotransferase, mitochondrial OS=Mus musculus GN=Got2 PE=1 SV=1	1,772
Q9D0M3	Cytochrome c1, heme protein, mitochondrial OS=Mus musculus GN=Cyc1 PE=1 SV=1	1,764
Q8C605	ATP-dependent 6-phosphofructokinase OS=Mus musculus GN=Pfkp PE=1 SV=1	1,751
Q99PT1	Rho GDP-dissociation inhibitor 1 OS=Mus musculus GN=Arhgdia PE=1 SV=3	1,738
P47857	ATP-dependent 6-phosphofructokinase, muscle type OS=Mus musculus GN=Pfkm PE=1 SV=3	1,736
Q9JLZ3	Methylglutaconyl-CoA hydratase, mitochondrial OS=Mus musculus GN=Auh PE=1 SV=1	1,714
Q8BYI9	Tenascin-R OS=Mus musculus GN=Tnr PE=1 SV=2	1,703
Q9Z2I9	Succinate--CoA ligase [ADP-forming] subunit beta, mitochondrial OS=Mus musculus GN=Sucla2 PE=1 SV=2	1,691
Q6ZWX2	Thymosin, beta 4, X chromosome OS=Mus musculus GN=Tmsb4x PE=2 SV=1	1,688
O55143	Sarcoplasmic/endoplasmic reticulum calcium ATPase 2 OS=Mus musculus GN=Atp2a2 PE=1 SV=2	1,68
P57780	Alpha-actinin-4 OS=Mus musculus GN=Actn4 PE=1 SV=1	1,674
Q0VF55	Calcium-transporting ATPase OS=Mus musculus GN=Atp2b3 PE=1 SV=1	1,674
Q9CPU0	Lactoylglutathione lyase OS=Mus musculus GN=Glo1 PE=1 SV=3	1,664
B2RTL5	Aldehyde dehydrogenase family 1, subfamily A7 OS=Mus musculus GN=Aldh1a7 PE=2 SV=1	1,663
Q3UMU9	Hepatoma-derived growth factor-related protein 2 OS=Mus musculus GN=Hdgfrp2 PE=1 SV=1	1,66
Q3V0Q1	Dynein heavy chain 12, axonemal OS=Mus musculus GN=Dnah12 PE=1 SV=2	1,655
Q9DBG3	AP-2 complex subunit beta OS=Mus musculus GN=Ap2b1 PE=1 SV=1	1,651
P47757	F-actin-capping protein subunit beta OS=Mus musculus GN=Capzb PE=1 SV=3	1,641
Q8R016	Bleomycin hydrolase OS=Mus musculus GN=Blmh PE=1 SV=1	1,639
G5E924	Heterogeneous nuclear ribonucleoprotein L (Fragment) OS=Mus musculus GN=Hnrnpl PE=1 SV=1	1,636
P14211	Calreticulin OS=Mus musculus GN=Calr PE=1 SV=1	1,616
P80316	T-complex protein 1 subunit epsilon OS=Mus musculus GN=Cct5 PE=1 SV=1	1,613
P31324	cAMP-dependent protein kinase type II-beta regulatory subunit OS=Mus musculus GN=Prkar2b PE=1 SV=3	1,608
H3BKH6	S-formylglutathione hydrolase OS=Mus musculus GN=Esd PE=1 SV=1	1,605
P61922	4-aminobutyrate aminotransferase, mitochondrial OS=Mus musculus GN=Abat PE=1 SV=1	1,589
Q99KI0	Aconitate hydratase, mitochondrial OS=Mus musculus GN=Aco2 PE=1 SV=1	1,588
Q99M71	Mammalian ependymin-related protein 1 OS=Mus musculus GN=Epdr1 PE=2 SV=1	1,587
Q61598	Rab GDP dissociation inhibitor beta OS=Mus musculus GN=Gdi2 PE=1 SV=1	1,586
Q542X7	Chaperonin subunit 2 (Beta), isoform CRA_a OS=Mus musculus GN=Cct2 PE=2 SV=1	1,584
P70168	Importin subunit beta-1 OS=Mus musculus GN=Kpnb1 PE=1 SV=2	1,574
Q8K2C9	Very-long-chain (3R)-3-hydroxyacyl-CoA dehydratase 3 OS=Mus musculus GN=Hacd3 PE=1 SV=2	1,574
Q8BMF4	Dihydrolipoyllysine-residue acetyltransferase component of pyruvate dehydrogenase complex, mitochondrial OS=Mus musculus GN=Dlat PE=1 SV=2	1,574
P48771	Cytochrome c oxidase subunit 7A2, mitochondrial OS=Mus musculus GN=Cox7a2 PE=1 SV=2	1,573
E0CYV0	Protein-L-isoaspartate O-methyltransferase OS=Mus musculus GN=Pcmt1 PE=1 SV=1	1,568
P08249	Malate dehydrogenase, mitochondrial OS=Mus musculus GN=Mdh2 PE=1 SV=3	1,566

Q3TGU7	Proliferation-associated 2G4 OS=Mus musculus GN=Pa2g4 PE=2 SV=1	1,565
P63011	Ras-related protein Rab-3A OS=Mus musculus GN=Rab3a PE=1 SV=1	1,565
P40336	Vacuolar protein sorting-associated protein 26A OS=Mus musculus GN=Vps26a PE=1 SV=1	1,562
Q99PU5	Long-chain-fatty-acid--CoA ligase ACSBG1 OS=Mus musculus GN=Acsbg1 PE=1 SV=1	1,561
Q9D8B3	Charged multivesicular body protein 4b OS=Mus musculus GN=Chmp4b PE=1 SV=2	1,557
A2AWN8	YTH domain family 1, isoform CRA_a OS=Mus musculus GN=Ythdf1 PE=1 SV=1	1,554
Q544E3	Phosphatidylinositol-4-phosphate 5-kinase, type II, alpha OS=Mus musculus GN=Pip4k2a PE=2 SV=1	1,552
Q61361	Brevican core protein OS=Mus musculus GN=Bcan PE=1 SV=2	1,544
P60335	Poly(rC)-binding protein 1 OS=Mus musculus GN=Pcbp1 PE=1 SV=1	1,542
E9Q8N8	Anion exchange protein OS=Mus musculus GN=Slc4a4 PE=1 SV=1	1,539
Q3U1N0	Coronin OS=Mus musculus GN=Coro1a PE=2 SV=1	1,538
Q5BLK0	MCG18564, isoform CRA_a OS=Mus musculus GN=Rpl12 PE=2 SV=1	1,528
Q61990	Poly(rC)-binding protein 2 OS=Mus musculus GN=Pcbp2 PE=1 SV=1	1,52
P20357	Microtubule-associated protein 2 OS=Mus musculus GN=Map2 PE=1 SV=2	1,508
Q3U4U6	T-complex protein 1 subunit gamma OS=Mus musculus GN=Cct3 PE=2 SV=1	1,508
P50396	Rab GDP dissociation inhibitor alpha OS=Mus musculus GN=Gdi1 PE=1 SV=3	1,501
P14148	60S ribosomal protein L7 OS=Mus musculus GN=Rpl7 PE=1 SV=2	1,5
Q01853	Transitional endoplasmic reticulum ATPase OS=Mus musculus GN=Vcp PE=1 SV=4	1,493
Q91ZU6	Dystonin OS=Mus musculus GN=Dst PE=1 SV=2	1,493
P05063	Fructose-bisphosphate aldolase C OS=Mus musculus GN=Aldoc PE=1 SV=4	1,492
Q68FL4	Putative adenosylhomocysteinase 3 OS=Mus musculus GN=Ahcyl2 PE=1 SV=1	1,485
P35235	Tyrosine-protein phosphatase non-receptor type 11 OS=Mus musculus GN=Ptpn11 PE=1 SV=2	1,484
Q61171	Peroxiredoxin-2 OS=Mus musculus GN=Prdx2 PE=1 SV=3	1,483
P51150	Ras-related protein Rab-7a OS=Mus musculus GN=Rab7a PE=1 SV=2	1,473
Q80YX1	Tenascin OS=Mus musculus GN=Tnc PE=1 SV=1	1,473
Q2PFD7	PH and SEC7 domain-containing protein 3 OS=Mus musculus GN=Psd3 PE=1 SV=2	1,473
Q91ZZ3	Beta-synuclein OS=Mus musculus GN=Sncb PE=1 SV=1	1,469
Q7TQD2	Tubulin polymerization-promoting protein OS=Mus musculus GN=Tppp PE=1 SV=1	1,468
Q9JKC6	Cell cycle exit and neuronal differentiation protein 1 OS=Mus musculus GN=Cend1 PE=1 SV=1	1,468
B2RRX2	Serine/threonine-protein phosphatase OS=Mus musculus GN=Ppp3ca PE=2 SV=1	1,464
Q3UAD6	Heat shock protein 90kDa beta (Grp94), member 1 OS=Mus musculus GN=Hsp90b1 PE=2 SV=1	1,462
Q5M9J8	MCG13936 OS=Mus musculus GN=Rpl28 PE=2 SV=1	1,46
Q52KC1	Eukaryotic translation initiation factor 4A2 OS=Mus musculus GN=Eif4a2 PE=2 SV=1	1,458
P60761	Neurogranin OS=Mus musculus GN=Nrgn PE=1 SV=1	1,457
P20152	Vimentin OS=Mus musculus GN=Vim PE=1 SV=3	1,454
Q5DQJ3	Capping protein (Actin filament) muscle Z-line, alpha 2, isoform CRA_c OS=Mus musculus GN=Capza2 PE=2 SV=1	1,45
P52760	Ribonuclease UK114 OS=Mus musculus GN=Hrsp12 PE=1 SV=3	1,449
P63085	Mitogen-activated protein kinase 1 OS=Mus musculus GN=Mapk1 PE=1 SV=3	1,448
F8WHB1	Calcium-transporting ATPase OS=Mus musculus GN=Atp2b2 PE=1 SV=1	1,441
P27661	Histone H2AX OS=Mus musculus GN=H2afx PE=1 SV=2	1,438
Q9DAK9	14 kDa phosphohistidine phosphatase OS=Mus musculus GN=Phpt1 PE=1 SV=1	1,437
P60710	Actin, cytoplasmic 1 OS=Mus musculus GN=Actb PE=1 SV=1	1,43
P70349	Histidine triad nucleotide-binding protein 1 OS=Mus musculus GN=Hint1 PE=1 SV=3	1,429
Q9CPX4	Ferritin OS=Mus musculus GN=Ftl1 PE=1 SV=1	1,423

P31650	Sodium- and chloride-dependent GABA transporter 3 OS=Mus musculus GN=Slc6a11 PE=1 SV=2	1,42
O08749	Dihydrolipoyl dehydrogenase, mitochondrial OS=Mus musculus GN=Dld PE=1 SV=2	1,419
Q80TL4	PHD finger protein 24 OS=Mus musculus GN=Phf24 PE=1 SV=2	1,417
P61264	Syntaxin-1B OS=Mus musculus GN=Stx1b PE=1 SV=1	1,414
B9EHN0	Ubiquitin-activating enzyme E1, Chr X OS=Mus musculus GN=Uba1 PE=2 SV=1	1,398
P15105	Glutamine synthetase OS=Mus musculus GN=Glul PE=1 SV=6	1,392
Q9R1P0	Proteasome subunit alpha type-4 OS=Mus musculus GN=Psma4 PE=1 SV=1	1,392
Q8VCE0	Sodium/potassium-transporting ATPase subunit alpha OS=Mus musculus GN=Atp1a3 PE=1 SV=1	1,39
Q8CI94	Glycogen phosphorylase, brain form OS=Mus musculus GN=Pygb PE=1 SV=3	1,385
O88342	WD repeat-containing protein 1 OS=Mus musculus GN=Wdr1 PE=1 SV=3	1,383
P68369	Tubulin alpha-1A chain OS=Mus musculus GN=Tuba1a PE=1 SV=1	1,378
Q8VDN2	Sodium/potassium-transporting ATPase subunit alpha-1 OS=Mus musculus GN=Atp1a1 PE=1 SV=1	1,377
A2ARP8	Microtubule-associated protein 1A OS=Mus musculus GN=Map1a PE=1 SV=1	1,372
Q8VEK3	Heterogeneous nuclear ribonucleoprotein U OS=Mus musculus GN=Hnrnpu PE=1 SV=1	1,37
Q91ZX7	Prolow-density lipoprotein receptor-related protein 1 OS=Mus musculus GN=Lrp1 PE=1 SV=1	1,368
P58252	Elongation factor 2 OS=Mus musculus GN=Eef2 PE=1 SV=2	1,364
Q9CZ13	Cytochrome b-c1 complex subunit 1, mitochondrial OS=Mus musculus GN=Uqcrc1 PE=1 SV=2	1,363
A0A0A0MQA5	Tubulin alpha chain (Fragment) OS=Mus musculus GN=Tuba4a PE=1 SV=1	1,353
P84078	ADP-ribosylation factor 1 OS=Mus musculus GN=Arf1 PE=1 SV=2	1,352
P08752	Guanine nucleotide-binding protein G(i) subunit alpha-2 OS=Mus musculus GN=Gnai2 PE=1 SV=5	1,35
Q9D051	Pyruvate dehydrogenase E1 component subunit beta, mitochondrial OS=Mus musculus GN=Pdhb PE=1 SV=1	1,345
Q9WTT4	V-type proton ATPase subunit G 2 OS=Mus musculus GN=Atp6v1g2 PE=3 SV=1	1,344
G5E902	MCG10343, isoform CRA_b OS=Mus musculus GN=Slc25a3 PE=1 SV=1	1,338
P62317	Small nuclear ribonucleoprotein Sm D2 OS=Mus musculus GN=Snrpd2 PE=3 SV=1	1,331
A0A0G2JFT8	Protein RUFY3 OS=Mus musculus GN=Rufy3 PE=1 SV=1	1,328
F6RSK3	Protein Gm17430 OS=Mus musculus GN=Gm17430 PE=4 SV=1	1,325
P55088	Aquaporin-4 OS=Mus musculus GN=Aqp4 PE=1 SV=2	1,323
P11031	Activated RNA polymerase II transcriptional coactivator p15 OS=Mus musculus GN=Sub1 PE=1 SV=3	1,321
Q8C522	Endonuclease domain-containing 1 protein OS=Mus musculus GN=Endod1 PE=1 SV=2	1,321
Q8K0T0	Reticulon-1 OS=Mus musculus GN=Rtn1 PE=1 SV=1	1,308
A8IP69	14-3-3 protein gamma subtype OS=Mus musculus GN=Ywhag PE=2 SV=1	1,307
P63318	Protein kinase C gamma type OS=Mus musculus GN=Prkcg PE=1 SV=1	1,304
Q60668	Heterogeneous nuclear ribonucleoprotein D0 OS=Mus musculus GN=Hnrnpd PE=1 SV=2	1,303
Q9R1P4	Proteasome subunit alpha type-1 OS=Mus musculus GN=Psma1 PE=1 SV=1	1,301
Q546G4	Albumin 1 OS=Mus musculus GN=Alb PE=2 SV=1	0,775
P47915	60S ribosomal protein L29 OS=Mus musculus GN=Rpl29 PE=2 SV=2	0,76
Q9CU62	Structural maintenance of chromosomes protein 1A OS=Mus musculus GN=Smc1a PE=1 SV=4	0,757
P62855	40S ribosomal protein S26 OS=Mus musculus GN=Rps26 PE=1 SV=3	0,752
Q3TT94	Serine/threonine-protein phosphatase 2A 55 kDa regulatory subunit B OS=Mus musculus GN=Ppp2r2a PE=2 SV=1	0,751
P01831	Thy-1 membrane glycoprotein OS=Mus musculus GN=Thy1 PE=1 SV=1	0,75
P83882	60S ribosomal protein L36a OS=Mus musculus GN=Rpl36a PE=1 SV=2	0,744
P62996	Transformer-2 protein homolog beta OS=Mus musculus GN=Tra2b PE=1 SV=1	0,744
Q91VB8	Alpha globin 1 OS=Mus musculus GN=haemaglobin alpha 2 PE=1 SV=1	0,733
D3Z4B2	Gamma-soluble NSF attachment protein (Fragment) OS=Mus musculus GN=Napg PE=1 SV=1	0,726

O08539	Myc box-dependent-interacting protein 1 OS=Mus musculus GN=Bin1 PE=1 SV=1	0,711
Q99PV0	Pre-mRNA-processing-splicing factor 8 OS=Mus musculus GN=Prpf8 PE=1 SV=2	0,71
P18872	Guanine nucleotide-binding protein G(o) subunit alpha OS=Mus musculus GN=Gnao1 PE=1 SV=3	0,709
D0VYV6	Erythrocyte protein band 4.1-like 3 isoform B OS=Mus musculus GN=Epb4.1l3 PE=2 SV=1	0,708
Q9WUM5	Succinyl-CoA ligase [ADP/GDP-forming] subunit alpha, mitochondrial OS=Mus musculus GN=Suclg1 PE=1 SV=4	0,705
Q3TLP8	RAS-related C3 botulinum substrate 1, isoform CRA_a OS=Mus musculus GN=Rac1 PE=1 SV=1	0,693
P02802	Metallothionein-1 OS=Mus musculus GN=Mt1 PE=1 SV=1	0,689
P63038	60 kDa heat shock protein, mitochondrial OS=Mus musculus GN=Hspd1 PE=1 SV=1	0,688
P17742	Peptidyl-prolyl cis-trans isomerase A OS=Mus musculus GN=Ppia PE=1 SV=2	0,681
P12970	60S ribosomal protein L7a OS=Mus musculus GN=Rpl7a PE=1 SV=2	0,68
P62204	Calmodulin OS=Mus musculus GN=Calm1 PE=1 SV=2	0,679
B1AQZ0	Septin-8 OS=Mus musculus GN=Sept8 PE=1 SV=1	0,678
P68510	14-3-3 protein eta OS=Mus musculus GN=Ywhah PE=1 SV=2	0,677
Q9CVB6	Actin-related protein 2/3 complex subunit 2 OS=Mus musculus GN=Arpc2 PE=1 SV=3	0,665
P08551	Neurofilament light polypeptide OS=Mus musculus GN=Nefl PE=1 SV=5	0,66
P99024	Tubulin beta-5 chain OS=Mus musculus GN=Tubb5 PE=1 SV=1	0,659
O09167	60S ribosomal protein L21 OS=Mus musculus GN=Rpl21 PE=1 SV=3	0,659
Q6IRU5	Clathrin light chain B OS=Mus musculus GN=Cltb PE=1 SV=1	0,657
E9Q0J5	Kinesin-like protein KIF21A OS=Mus musculus GN=Kif21a PE=1 SV=2	0,657
P20065	Thymosin beta-4 OS=Mus musculus GN=Tmsb4x PE=1 SV=1	0,656
Q548L4	Glutamate decarboxylase OS=Mus musculus GN=Gad2 PE=2 SV=1	0,655
F8WGL3	Cofilin-1 OS=Mus musculus GN=Cfl1 PE=1 SV=1	0,651
Q8BKZ9	Pyruvate dehydrogenase protein X component, mitochondrial OS=Mus musculus GN=Pdhx PE=1 SV=1	0,643
Q8C2Q7	Heterogeneous nuclear ribonucleoprotein H OS=Mus musculus GN=Hnrnph1 PE=1 SV=1	0,627
Q5M9M5	MCG10806 OS=Mus musculus GN=Rpl23a PE=2 SV=1	0,624
P99028	Cytochrome b-c1 complex subunit 6, mitochondrial OS=Mus musculus GN=Uqcrh PE=1 SV=2	0,622
P99027	60S acidic ribosomal protein P2 OS=Mus musculus GN=Rplp2 PE=1 SV=3	0,62
P63163	Small nuclear ribonucleoprotein-associated protein N OS=Mus musculus GN=Snrpn PE=2 SV=1	0,612
Q9CZC8	Secernin-1 OS=Mus musculus GN=Scrn1 PE=1 SV=1	0,61
P63017	Heat shock cognate 71 kDa protein OS=Mus musculus GN=Hspa8 PE=1 SV=1	0,61
Q921M7	Protein FAM49B OS=Mus musculus GN=Fam49b PE=2 SV=1	0,61
P27659	60S ribosomal protein L3 OS=Mus musculus GN=Rpl3 PE=1 SV=3	0,606
O08599	Syntaxin-binding protein 1 OS=Mus musculus GN=Stxbp1 PE=1 SV=2	0,606
P08553	Neurofilament medium polypeptide OS=Mus musculus GN=Nefm PE=1 SV=4	0,604
Q8R366	Immunoglobulin superfamily member 8 OS=Mus musculus GN=Igsf8 PE=1 SV=2	0,592
Q80YN3	Breast carcinoma-amplified sequence 1 homolog OS=Mus musculus GN=Bcas1 PE=1 SV=3	0,59
F6RT34	Myelin basic protein (Fragment) OS=Mus musculus GN=Mbp PE=1 SV=1	0,58
P06837	Neuromodulin OS=Mus musculus GN=Gap43 PE=1 SV=1	0,58
Q99104	Unconventional myosin-Va OS=Mus musculus GN=Myo5a PE=1 SV=2	0,58
Q3UR55	ATPase, Na+/K+ transporting, beta 2 polypeptide, isoform CRA_b OS=Mus musculus GN=Atp1b2 PE=2 SV=1	0,573
Q548F2	Guanine deaminase OS=Mus musculus GN=Gda PE=2 SV=1	0,567
Q6ZWV7	60S ribosomal protein L35 OS=Mus musculus GN=Rpl35 PE=1 SV=1	0,561
Q923T9	Calcium/calmodulin-dependent protein kinase type II subunit gamma OS=Mus musculus GN=Camk2g PE=1 SV=1	0,556
Q60631	Growth factor receptor-bound protein 2 OS=Mus musculus GN=Grb2 PE=1 SV=1	0,553

Q08331	Calretinin OS=Mus musculus GN=Calb2 PE=1 SV=3	0,551
P62267	40S ribosomal protein S23 OS=Mus musculus GN=Rps23 PE=1 SV=3	0,549
P68433	Histone H3.1 OS=Mus musculus GN=Hist1h3a PE=1 SV=2	0,544
G5E866	Splicing factor 3B subunit 1 OS=Mus musculus GN=Sf3b1 PE=1 SV=1	0,533
P12658	Calbindin OS=Mus musculus GN=Calb1 PE=1 SV=2	0,525
Q9EQK5	Major vault protein OS=Mus musculus GN=Mvp PE=1 SV=4	0,525
Q9WV69	Dematin OS=Mus musculus GN=Dmtn PE=1 SV=1	0,524
P29341	Polyadenylate-binding protein 1 OS=Mus musculus GN=Pabpc1 PE=1 SV=2	0,522
Q9CR57	60S ribosomal protein L14 OS=Mus musculus GN=Rpl14 PE=1 SV=3	0,52
Q3UH59	Myosin-10 OS=Mus musculus GN=Myh10 PE=1 SV=1	0,519
P62307	Small nuclear ribonucleoprotein F OS=Mus musculus GN=Snrpf PE=1 SV=1	0,519
Q5SS83	Flotillin 2, isoform CRA_a OS=Mus musculus GN=Flot2 PE=1 SV=1	0,519
P62911	60S ribosomal protein L32 OS=Mus musculus GN=Rpl32 PE=1 SV=2	0,506
Q5I0T8	Ribosomal protein L19 OS=Mus musculus GN=Rpl19 PE=2 SV=1	0,506
Q9CRB6	Tubulin polymerization-promoting protein family member 3 OS=Mus musculus GN=Tppp3 PE=1 SV=1	0,5
P97499	Telomerase protein component 1 OS=Mus musculus GN=Tep1 PE=1 SV=1	0,499
Q9R1T4	Septin-6 OS=Mus musculus GN=Sept6 PE=1 SV=4	0,493
Q8BL66	Early endosome antigen 1 OS=Mus musculus GN=Eea1 PE=1 SV=2	0,487
Q3TYV5	Cyclic nucleotide phosphodiesterase 1, isoform CRA_b OS=Mus musculus GN=Cnp PE=2 SV=1	0,487
Q9CYR0	Single-stranded DNA-binding protein, mitochondrial OS=Mus musculus GN=Ssbp1 PE=1 SV=1	0,487
P20029	78 kDa glucose-regulated protein OS=Mus musculus GN=Hspa5 PE=1 SV=3	0,48
Q4VWZ5	Acyl-CoA-binding protein OS=Mus musculus GN=Dbi PE=1 SV=1	0,461
Q497E9	40S ribosomal protein S8 OS=Mus musculus GN=Rps8 PE=2 SV=1	0,457
P63101	14-3-3 protein zeta/delta OS=Mus musculus GN=Ywhaz PE=1 SV=1	0,456
Q505A8	MCG17585 OS=Mus musculus GN=Rpl39 PE=2 SV=1	0,456
Q7TQI3	Ubiquitin thioesterase OTUB1 OS=Mus musculus GN=Otub1 PE=1 SV=2	0,452
P47911	60S ribosomal protein L6 OS=Mus musculus GN=Rpl6 PE=1 SV=3	0,452
Q8VDD5	Myosin-9 OS=Mus musculus GN=Myh9 PE=1 SV=4	0,451
Q60864	Stress-induced-phosphoprotein 1 OS=Mus musculus GN=Stip1 PE=1 SV=1	0,448
E9QAZ2	Ribosomal protein L15 OS=Mus musculus GN=Gm10020 PE=3 SV=1	0,447
P14869	60S acidic ribosomal protein P0 OS=Mus musculus GN=Rplp0 PE=1 SV=3	0,438
Q564E8	Ribosomal protein L4 OS=Mus musculus GN=Rpl4 PE=2 SV=1	0,437
P32067	Lupus La protein homolog OS=Mus musculus GN=Ssb PE=1 SV=1	0,425
P47963	60S ribosomal protein L13 OS=Mus musculus GN=Rpl13 PE=1 SV=3	0,414
Q3UBP6	Putative uncharacterized protein OS=Mus musculus GN=Actb PE=2 SV=1	0,407
P62264	40S ribosomal protein S14 OS=Mus musculus GN=Rps14 PE=1 SV=3	0,399
P63005	Platelet-activating factor acetylhydrolase IB subunit alpha OS=Mus musculus GN=Pafah1b1 PE=1 SV=2	0,396
Q8CI43	Myosin light chain 6B OS=Mus musculus GN=Myl6b PE=2 SV=1	0,388
B2RSH2	Guanine nucleotide-binding protein G(i) subunit alpha-1 OS=Mus musculus GN=Gnai1 PE=1 SV=1	0,382
Q5SVJ0	Calcium/calmodulin-dependent protein kinase II, beta, isoform CRA_b OS=Mus musculus GN=Camk2b PE=1 SV=1	0,37
B1AQ77	Keratin 15, isoform CRA_a OS=Mus musculus GN=Krt15 PE=1 SV=1	0,367
Q5XJF6	Ribosomal protein OS=Mus musculus GN=Rpl10a PE=1 SV=1	0,367
P62320	Small nuclear ribonucleoprotein Sm D3 OS=Mus musculus GN=Snrpd3 PE=1 SV=1	0,36
Q9D1R9	60S ribosomal protein L34 OS=Mus musculus GN=Rpl34 PE=1 SV=2	0,347

P14115	60S ribosomal protein L27a OS=Mus musculus GN=Rpl27a PE=2 SV=5	0,344
Z4YL23	Fer-1-like protein 4 OS=Mus musculus GN=Fer1l4 PE=4 SV=1	0,336
P62889	60S ribosomal protein L30 OS=Mus musculus GN=Rpl30 PE=1 SV=2	0,319
P62918	60S ribosomal protein L8 OS=Mus musculus GN=Rpl8 PE=1 SV=2	0,311
Q5BLK1	40S ribosomal protein S6 OS=Mus musculus GN=Rps6 PE=2 SV=1	0,298
Q8CAK3	UPF0515 protein C19orf66 homolog OS=Mus musculus PE=2 SV=1	0,292
P62315	Small nuclear ribonucleoprotein Sm D1 OS=Mus musculus GN=Snrpd1 PE=1 SV=1	0,275
P62717	60S ribosomal protein L18a OS=Mus musculus GN=Rpl18a PE=1 SV=1	0,245
P60904	DnaJ homolog subfamily C member 5 OS=Mus musculus GN=Dnajc5 PE=1 SV=1	0,231
Q8C1Y8	Vacuolar fusion protein CCZ1 homolog OS=Mus musculus GN=Ccz1 PE=1 SV=1	0,217
P47962	60S ribosomal protein L5 OS=Mus musculus GN=Rpl5 PE=1 SV=3	0,203
Q3V117	ATP-citrate synthase OS=Mus musculus GN=Acly PE=1 SV=1	0,173

DATA FILE S1

REGULATED PROTEINS WT: 24 vs. 3 months

Accession	Description	Abundance Ratio: (WT24) / (WT3)
P28663	Beta-soluble NSF attachment protein OS=Mus musculus GN=Napb PE=1 SV=2	17,199
Q6ZWX2	Thymosin, beta 4, X chromosome OS=Mus musculus GN=Tmsb4x PE=2 SV=1	12,952
E9PYN1	Cell adhesion molecule 1 OS=Mus musculus GN=Cadm1 PE=1 SV=1	11,645
Q9D3D9	ATP synthase subunit delta, mitochondrial OS=Mus musculus GN=Atp5d PE=1 SV=1	10,358
P28651	Carbonic anhydrase-related protein OS=Mus musculus GN=Ca8 PE=1 SV=5	9,736
P61089	Ubiquitin-conjugating enzyme E2 N OS=Mus musculus GN=Ube2n PE=1 SV=1	9,43
Q5SZA3	Histone cluster 1, H1c OS=Mus musculus GN=Hist1h1c PE=2 SV=1	8,966
Q9JKD3	Secretory carrier-associated membrane protein 5 OS=Mus musculus GN=Scamp5 PE=1 SV=1	7,509
P63040	Complexin-1 OS=Mus musculus GN=Cplx1 PE=1 SV=1	6,894
Q9CPW4	Actin-related protein 2/3 complex subunit 5 OS=Mus musculus GN=Arpc5 PE=2 SV=3	6,543
P26645	Myristoylated alanine-rich C-kinase substrate OS=Mus musculus GN=Marcks PE=1 SV=2	6,515
B1AWD9	Clathrin light chain A OS=Mus musculus GN=Clta PE=1 SV=1	6,296
D3YXH0	Immunoglobulin superfamily member 5 OS=Mus musculus GN=Igsf5 PE=4 SV=1	6,247
P43274	Histone H1.4 OS=Mus musculus GN=Hist1h1e PE=1 SV=2	6,212
P20065	Thymosin beta-4 OS=Mus musculus GN=Tmsb4x PE=1 SV=1	5,338
P08228	Superoxide dismutase [Cu-Zn] OS=Mus musculus GN=Sod1 PE=1 SV=2	5,303
P43276	Histone H1.5 OS=Mus musculus GN=Hist1h1b PE=1 SV=2	5,115
P62774	Myotrophin OS=Mus musculus GN=Mtpn PE=1 SV=2	5,082
P60761	Neurogranin OS=Mus musculus GN=Nrgn PE=1 SV=1	4,696
P26883	Peptidyl-prolyl cis-trans isomerase FKBP1A OS=Mus musculus GN=Fkbp1a PE=1 SV=2	4,695
Q149Z9	Histone cluster 1, H1d OS=Mus musculus GN=Hist1h1d PE=2 SV=1	4,689
P84086	Complexin-2 OS=Mus musculus GN=Cplx2 PE=1 SV=1	4,52
Q60829	Protein phosphatase 1 regulatory subunit 1B OS=Mus musculus GN=Ppp1r1b PE=2 SV=2	4,487
Q6GT24	Peroxiredoxin 6 OS=Mus musculus GN=Prdx6 PE=1 SV=1	4,479
P13595	Neural cell adhesion molecule 1 OS=Mus musculus GN=Ncam1 PE=1 SV=3	4,18
O08749	Dihydrolipoyl dehydrogenase, mitochondrial OS=Mus musculus GN=Dld PE=1 SV=2	4,18
P61979	Heterogeneous nuclear ribonucleoprotein K OS=Mus musculus GN=Hnrnpk PE=1 SV=1	4,093
Q9JKC6	Cell cycle exit and neuronal differentiation protein 1 OS=Mus musculus GN=Cend1 PE=1 SV=1	3,964
P02802	Metallothionein-1 OS=Mus musculus GN=Mt1 PE=1 SV=1	3,841

Q63810	Calcineurin subunit B type 1 OS=Mus musculus GN=Ppp3r1 PE=1 SV=3	3,837
Q8BVI4	Dihydropteridine reductase OS=Mus musculus GN=Qdpr PE=1 SV=2	3,815
Q9QYC0	Alpha-adducin OS=Mus musculus GN=Add1 PE=1 SV=2	3,773
G5E902	MCG10343, isoform CRA_b OS=Mus musculus GN=Slc25a3 PE=1 SV=1	3,754
P32848	Parvalbumin alpha OS=Mus musculus GN=Pvalb PE=1 SV=3	3,748
P28184	Metallothionein-3 OS=Mus musculus GN=Mt3 PE=1 SV=1	3,637
P62204	Calmodulin OS=Mus musculus GN=Calm1 PE=1 SV=2	3,634
Q543Y7	Putative uncharacterized protein OS=Mus musculus GN=Pacsin1 PE=2 SV=1	3,629
Q9Z2D6-2	Isoform B of Methyl-CpG-binding protein 2 OS=Mus musculus GN=Mecp2	3,602
G5E8N5	L-lactate dehydrogenase OS=Mus musculus GN=Ldha PE=1 SV=1	3,561
Q9WTT4	V-type proton ATPase subunit G 2 OS=Mus musculus GN=Atp6v1g2 PE=3 SV=1	3,54
A0A087WQN2	Prothymosin alpha (Fragment) OS=Mus musculus GN=Ptma PE=1 SV=1	3,536
Q61361	Brevican core protein OS=Mus musculus GN=Bcan PE=1 SV=2	3,507
P19157	Glutathione S-transferase P 1 OS=Mus musculus GN=Gstp1 PE=1 SV=2	3,447
Q4VWZ5	Acyl-CoA-binding protein OS=Mus musculus GN=Dbi PE=1 SV=1	3,436
Q3TTY5	Keratin, type II cytoskeletal 2 epidermal OS=Mus musculus GN=Krt2 PE=1 SV=1	3,424
O08539	Myc box-dependent-interacting protein 1 OS=Mus musculus GN=Bin1 PE=1 SV=1	3,412
P10922	Histone H1.0 OS=Mus musculus GN=H1f0 PE=2 SV=4	3,345
P08249	Malate dehydrogenase, mitochondrial OS=Mus musculus GN=Mdh2 PE=1 SV=3	3,329
Q91XV3	Brain acid soluble protein 1 OS=Mus musculus GN=Basp1 PE=1 SV=3	3,237
A0A075B5P2	Protein Igkc (Fragment) OS=Mus musculus GN=Igkc PE=1 SV=1	3,216
E9Q035	Protein Gm20425 OS=Mus musculus GN=Gm20425 PE=4 SV=1	3,149
Q99PT1	Rho GDP-dissociation inhibitor 1 OS=Mus musculus GN=Arhgdia PE=1 SV=3	3,105
E9PZF0	Nucleoside diphosphate kinase OS=Mus musculus GN=Gm20390 PE=3 SV=1	3,097
P52760	Ribonuclease UK114 OS=Mus musculus GN=Hrsp12 PE=1 SV=3	3,075
Q9WV69	Dematin OS=Mus musculus GN=Dmtn PE=1 SV=1	3,036
P48036	Annexin A5 OS=Mus musculus GN=Anxa5 PE=1 SV=1	3,036
Q02105	Complement C1q subcomponent subunit C OS=Mus musculus GN=C1qc PE=2 SV=2	3,033
O88569	Heterogeneous nuclear ribonucleoproteins A2/B1 OS=Mus musculus GN=Hnrnpa2b1 PE=1 SV=2	2,987
P27661	Histone H2AX OS=Mus musculus GN=H2afx PE=1 SV=2	2,98
Q9DBJ1	Phosphoglycerate mutase 1 OS=Mus musculus GN=Pgam1 PE=1 SV=3	2,963
Q9ESM3	Hyaluronan and proteoglycan link protein 2 OS=Mus musculus GN=Hapln2 PE=1 SV=1	2,956
Q9Z204	Heterogeneous nuclear ribonucleoproteins C1/C2 OS=Mus musculus GN=Hnrnpc PE=1 SV=1	2,944

P61922	4-aminobutyrate aminotransferase, mitochondrial OS=Mus musculus GN=Abat PE=1 SV=1	2,942
P17751	Triosephosphate isomerase OS=Mus musculus GN=Tpi1 PE=1 SV=4	2,933
Q9DBG3	AP-2 complex subunit beta OS=Mus musculus GN=Ap2b1 PE=1 SV=1	2,896
Q61598	Rab GDP dissociation inhibitor beta OS=Mus musculus GN=Gdi2 PE=1 SV=1	2,888
A0A075B6A0	Ig mu chain C region (Fragment) OS=Mus musculus GN=Ighm PE=1 SV=2	2,831
P05063	Fructose-bisphosphate aldolase C OS=Mus musculus GN=Aldoc PE=1 SV=4	2,804
P21460	Cystatin-C OS=Mus musculus GN=Cst3 PE=1 SV=2	2,769
P50518	V-type proton ATPase subunit E 1 OS=Mus musculus GN=Atp6v1e1 PE=1 SV=2	2,751
E9Q7Q3	Tropomyosin alpha-3 chain OS=Mus musculus GN=Tpm3 PE=1 SV=1	2,751
Q61782	Type I epidermal keratin mRNA, 3'end (Fragment) OS=Mus musculus PE=2 SV=1	2,733
Q8CI43	Myosin light chain 6B OS=Mus musculus GN=Myl6b PE=2 SV=1	2,729
Q9Z2T6	Keratin, type II cuticular Hb5 OS=Mus musculus GN=Krt85 PE=2 SV=2	2,725
A0A0G2JEG8	Amphiphysin OS=Mus musculus GN=Amph PE=1 SV=1	2,701
Q9R0P9	Ubiquitin carboxyl-terminal hydrolase isozyme L1 OS=Mus musculus GN=Uchl1 PE=1 SV=1	2,671
P98086	Complement C1q subcomponent subunit A OS=Mus musculus GN=C1qa PE=1 SV=2	2,655
Q8BWF0	Succinate-semialdehyde dehydrogenase, mitochondrial OS=Mus musculus GN=Aldh5a1 PE=1 SV=1	2,651
P99027	60S acidic ribosomal protein P2 OS=Mus musculus GN=Rplp2 PE=1 SV=3	2,65
Q60668	Heterogeneous nuclear ribonucleoprotein D0 OS=Mus musculus GN=Hnrnpd PE=1 SV=2	2,639
Q9EQU5-2	Isoform 2 of Protein SET OS=Mus musculus GN=Set	2,585
Q91VB8	Alpha globin 1 OS=Mus musculus GN=haemaglobin alpha 2 PE=1 SV=1	2,527
P14152	Malate dehydrogenase, cytoplasmic OS=Mus musculus GN=Mdh1 PE=1 SV=3	2,513
P99024	Tubulin beta-5 chain OS=Mus musculus GN=Tubb5 PE=1 SV=1	2,508
Q68FL4	Putative adenosylhomocysteinase 3 OS=Mus musculus GN=Ahcyl2 PE=1 SV=1	2,494
Q04690	Neurofibromin OS=Mus musculus GN=Nf1 PE=1 SV=1	2,489
D3Z722	40S ribosomal protein S19 OS=Mus musculus GN=Rps19 PE=1 SV=1	2,476
Q9DCD0	6-phosphogluconate dehydrogenase, decarboxylating OS=Mus musculus GN=Pgd PE=1 SV=3	2,476
P28474	Alcohol dehydrogenase class-3 OS=Mus musculus GN=Adh5 PE=1 SV=3	2,453
B2RTK3	Histone H2B OS=Mus musculus GN=Hist1h2bm PE=2 SV=1	2,451
Q3UY00	Protein S100 OS=Mus musculus GN=S100b PE=2 SV=1	2,441
Q6W8Q3	Purkinje cell protein 4-like protein 1 OS=Mus musculus GN=Pcp4l1 PE=1 SV=1	2,407
P62259	14-3-3 protein epsilon OS=Mus musculus GN=Ywhae PE=1 SV=1	2,399
A8DUK4	Beta-globin OS=Mus musculus GN=Hbbt1 PE=1 SV=1	2,39
H3BKH6	S-formylglutathione hydrolase OS=Mus musculus GN=Esd PE=1 SV=1	2,378

J3QMG3	Voltage-dependent anion-selective channel protein 3 OS=Mus musculus GN=Vdac3 PE=1 SV=1	2,378
Q9CZ13	Cytochrome b-c1 complex subunit 1, mitochondrial OS=Mus musculus GN=Uqcrc1 PE=1 SV=2	2,378
A0A0G2JFT8	Protein RUFY3 OS=Mus musculus GN=Rufy3 PE=1 SV=1	2,374
Q4FJX9	Superoxide dismutase OS=Mus musculus GN=Sod2 PE=2 SV=1	2,373
P62858	40S ribosomal protein S28 OS=Mus musculus GN=Rps28 PE=1 SV=1	2,364
P09405	Nucleolin OS=Mus musculus GN=Ncl PE=1 SV=2	2,353
Q91ZZ3	Beta-synuclein OS=Mus musculus GN=Sncb PE=1 SV=1	2,347
Q3ULD5	Methylcrotonoyl-CoA carboxylase beta chain, mitochondrial OS=Mus musculus GN=Mccc2 PE=1 SV=1	2,338
Q3U1N0	Coronin OS=Mus musculus GN=Coro1a PE=2 SV=1	2,33
Q545B6	Stathmin OS=Mus musculus GN=Stmn1 PE=2 SV=1	2,29
Q5EBQ2	MCG7941, isoform CRA_f OS=Mus musculus GN=Pebp1 PE=2 SV=1	2,28
E9PYH0	Versican core protein OS=Mus musculus GN=Vcan PE=1 SV=1	2,276
Q6IRU5	Clathrin light chain B OS=Mus musculus GN=Cltb PE=1 SV=1	2,269
Q61282	Aggrecan core protein OS=Mus musculus GN=Acan PE=1 SV=2	2,244
P05201	Aspartate aminotransferase, cytoplasmic OS=Mus musculus GN=Got1 PE=1 SV=3	2,22
P20357	Microtubule-associated protein 2 OS=Mus musculus GN=Map2 PE=1 SV=2	2,209
A0A0A0MQF6	Glyceraldehyde-3-phosphate dehydrogenase OS=Mus musculus GN=Gapdh PE=1 SV=1	2,205
P10649	Glutathione S-transferase Mu 1 OS=Mus musculus GN=Gstm1 PE=1 SV=2	2,176
P31650	Sodium- and chloride-dependent GABA transporter 3 OS=Mus musculus GN=Slc6a11 PE=1 SV=2	2,176
P60710	Actin, cytoplasmic 1 OS=Mus musculus GN=Actb PE=1 SV=1	2,161
Q99KI0	Aconitate hydratase, mitochondrial OS=Mus musculus GN=Aco2 PE=1 SV=1	2,121
P14873	Microtubule-associated protein 1B OS=Mus musculus GN=Map1b PE=1 SV=2	2,117
P68510	14-3-3 protein eta OS=Mus musculus GN=Ywhah PE=1 SV=2	2,114
P01592	Immunoglobulin J chain OS=Mus musculus GN=Igj PE=2 SV=4	2,078
Q9CX86	Heterogeneous nuclear ribonucleoprotein A0 OS=Mus musculus GN=Hnrnpa0 PE=1 SV=1	2,055
P60335	Poly(rC)-binding protein 1 OS=Mus musculus GN=Pcbp1 PE=1 SV=1	2,049
P51863	V-type proton ATPase subunit d 1 OS=Mus musculus GN=Atp6v0d1 PE=1 SV=2	2,047
Q9Z1G3	V-type proton ATPase subunit C 1 OS=Mus musculus GN=Atp6v1c1 PE=1 SV=4	2,041
Q9CRB6	Tubulin polymerization-promoting protein family member 3 OS=Mus musculus GN=Tppp3 PE=1 SV=1	2,031
P50396	Rab GDP dissociation inhibitor alpha OS=Mus musculus GN=Gdi1 PE=1 SV=3	2,031
Q7TQD2	Tubulin polymerization-promoting protein OS=Mus musculus GN=Tppp PE=1 SV=1	2,02
Q9CPU0	Lactoylglutathione lyase OS=Mus musculus GN=Glo1 PE=1 SV=3	2,019
Q810U4	Neuronal cell adhesion molecule OS=Mus musculus GN=Nrcam PE=1 SV=2	2,014

Q9Z1G4	V-type proton ATPase 116 kDa subunit a isoform 1 OS=Mus musculus GN=Atp6v0a1 PE=1 SV=3	2,005
Q9JJV2	Profilin-2 OS=Mus musculus GN=Pfn2 PE=1 SV=3	1,989
P17156	Heat shock-related 70 kDa protein 2 OS=Mus musculus GN=Hspa2 PE=1 SV=2	1,973
P06745	Glucose-6-phosphate isomerase OS=Mus musculus GN=Gpi PE=1 SV=4	1,963
Q01853	Transitional endoplasmic reticulum ATPase OS=Mus musculus GN=Vcp PE=1 SV=4	1,962
P68372	Tubulin beta-4B chain OS=Mus musculus GN=Tubb4b PE=1 SV=1	1,96
Q3UL22	Chaperonin subunit 8 (Theta), isoform CRA_a OS=Mus musculus GN=Cct8 PE=2 SV=1	1,946
A6ZI44	Fructose-bisphosphate aldolase OS=Mus musculus GN=Aldoa PE=1 SV=1	1,942
P57780	Alpha-actinin-4 OS=Mus musculus GN=Actn4 PE=1 SV=1	1,93
Q9R0Y5	Adenylate kinase isoenzyme 1 OS=Mus musculus GN=Ak1 PE=1 SV=1	1,925
P13707	Glycerol-3-phosphate dehydrogenase [NAD(+)], cytoplasmic OS=Mus musculus GN=Gpd1 PE=1 SV=3	1,92
Q548F2	Guanine deaminase OS=Mus musculus GN=Gda PE=2 SV=1	1,919
Q9CZC8	Secernin-1 OS=Mus musculus GN=Scrn1 PE=1 SV=1	1,909
P35700	Peroxiredoxin-1 OS=Mus musculus GN=Prdx1 PE=1 SV=1	1,904
P05202	Aspartate aminotransferase, mitochondrial OS=Mus musculus GN=Got2 PE=1 SV=1	1,903
P16125	L-lactate dehydrogenase B chain OS=Mus musculus GN=Ldhb PE=1 SV=2	1,882
P14106	Complement C1q subcomponent subunit B OS=Mus musculus GN=C1qb PE=1 SV=2	1,876
Q76MZ3	Serine/threonine-protein phosphatase 2A 65 kDa regulatory subunit A alpha isoform OS=Mus musculı	1,875
Q7M6W1	Reticulon OS=Mus musculus GN=Rtn1 PE=1 SV=1	1,87
Q546G4	Albumin 1 OS=Mus musculus GN=Alb PE=2 SV=1	1,863
F6VW30	14-3-3 protein theta (Fragment) OS=Mus musculus GN=Ywhaq PE=1 SV=1	1,861
Q9QUP5	Hyaluronan and proteoglycan link protein 1 OS=Mus musculus GN=Hapln1 PE=1 SV=1	1,85
Q99PU5	Long-chain-fatty-acid--CoA ligase ACSBG1 OS=Mus musculus GN=Acsbg1 PE=1 SV=1	1,847
P00920	Carbonic anhydrase 2 OS=Mus musculus GN=Ca2 PE=1 SV=4	1,834
P58252	Elongation factor 2 OS=Mus musculus GN=Eef2 PE=1 SV=2	1,833
Q80TL4	PHD finger protein 24 OS=Mus musculus GN=Phf24 PE=1 SV=2	1,832
P46460	Vesicle-fusing ATPase OS=Mus musculus GN=Nsf PE=1 SV=2	1,825
D3Z4B2	Gamma-soluble NSF attachment protein (Fragment) OS=Mus musculus GN=Napg PE=1 SV=1	1,823
Q8C2Q7	Heterogeneous nuclear ribonucleoprotein H OS=Mus musculus GN=Hnrnph1 PE=1 SV=1	1,819
Q642L7	MCG13441 OS=Mus musculus GN=Rps27a PE=2 SV=1	1,815
Q5FW97	Enolase 1, alpha non-neuron OS=Mus musculus GN=EG433182 PE=2 SV=1	1,814
P63038	60 kDa heat shock protein, mitochondrial OS=Mus musculus GN=Hspd1 PE=1 SV=1	1,812
Q3U2G2	Heat shock 70 kDa protein 4 OS=Mus musculus GN=Hspa4 PE=1 SV=1	1,806

A6H611	Mitochondrial intermediate peptidase OS=Mus musculus GN=Mipep PE=1 SV=1	1,805
B2RXY7	Carbonyl reductase 1 OS=Mus musculus GN=Cbr1 PE=2 SV=1	1,802
A2ALV3	Endophilin-A1 OS=Mus musculus GN=Sh3gl2 PE=1 SV=1	1,796
P11031	Activated RNA polymerase II transcriptional coactivator p15 OS=Mus musculus GN=Sub1 PE=1 SV=3	1,789
B1AQW2	Microtubule-associated protein OS=Mus musculus GN=Mapt PE=1 SV=1	1,773
Q8K183	Pyridoxal kinase OS=Mus musculus GN=Pdxk PE=1 SV=1	1,772
B0QZN5	Vesicle-associated membrane protein 2 OS=Mus musculus GN=Vamp2 PE=1 SV=1	1,764
P26443	Glutamate dehydrogenase 1, mitochondrial OS=Mus musculus GN=Glud1 PE=1 SV=1	1,759
Q9CZU6	Citrate synthase, mitochondrial OS=Mus musculus GN=Cs PE=1 SV=1	1,753
Q78ZJ8	MCG22989, isoform CRA_b OS=Mus musculus GN=Rab11b PE=2 SV=1	1,747
O55091	Protein IMPACT OS=Mus musculus GN=Impact PE=1 SV=2	1,74
A0A097PUG4	Anti-lox-1 15C4 light chain OS=Mus musculus PE=2 SV=1	1,734
Q3U7E0	Putative uncharacterized protein OS=Mus musculus GN=Atp6v1g1 PE=2 SV=1	1,72
Q3UV17	Keratin, type II cytoskeletal 2 oral OS=Mus musculus GN=Krt76 PE=2 SV=1	1,71
Q9QYX7	Protein piccolo OS=Mus musculus GN=Pclo PE=1 SV=4	1,702
B9EKR1	Receptor-type tyrosine-protein phosphatase zeta OS=Mus musculus GN=Ptprz1 PE=1 SV=1	1,7
P70349	Histidine triad nucleotide-binding protein 1 OS=Mus musculus GN=Hint1 PE=1 SV=3	1,687
A2ARP8	Microtubule-associated protein 1A OS=Mus musculus GN=Map1a PE=1 SV=1	1,683
Q9JLZ3	Methylglutaconyl-CoA hydratase, mitochondrial OS=Mus musculus GN=Auh PE=1 SV=1	1,669
P68369	Tubulin alpha-1A chain OS=Mus musculus GN=Tuba1a PE=1 SV=1	1,656
A0A087WP80	Limbic system-associated membrane protein OS=Mus musculus GN=Lsamp PE=1 SV=1	1,649
Q922J6	Tetraspanin-2 OS=Mus musculus GN=Tspan2 PE=1 SV=1	1,635
Q9D6F9	Tubulin beta-4A chain OS=Mus musculus GN=Tubb4a PE=1 SV=3	1,627
P17742	Peptidyl-prolyl cis-trans isomerase A OS=Mus musculus GN=Ppia PE=1 SV=2	1,624
Q3UMU9	Hepatoma-derived growth factor-related protein 2 OS=Mus musculus GN=Hdgfrp2 PE=1 SV=1	1,622
A2AWN8	YTH domain family 1, isoform CRA_a OS=Mus musculus GN=Ythdf1 PE=1 SV=1	1,601
Q9QXV0	ProSAAS OS=Mus musculus GN=Pcsk1n PE=1 SV=2	1,6
Q7TSJ2	Microtubule-associated protein 6 OS=Mus musculus GN=Map6 PE=1 SV=2	1,596
F8WGL3	Cofilin-1 OS=Mus musculus GN=Cfl1 PE=1 SV=1	1,593
F6RSK3	Protein Gm17430 OS=Mus musculus GN=Gm17430 PE=4 SV=1	1,587
P56399	Ubiquitin carboxyl-terminal hydrolase 5 OS=Mus musculus GN=Usp5 PE=1 SV=1	1,586
P55066	Neurocan core protein OS=Mus musculus GN=Ncan PE=2 SV=1	1,586
A0A075B5P3	Protein Ighg2b (Fragment) OS=Mus musculus GN=Ighg2b PE=1 SV=1	1,58

P14211	Calreticulin OS=Mus musculus GN=Calr PE=1 SV=1	1,577
Q04447	Creatine kinase B-type OS=Mus musculus GN=Ckb PE=1 SV=1	1,576
F6VPT0	Protein Ccdc163 (Fragment) OS=Mus musculus GN=Ccdc163 PE=4 SV=1	1,571
Q61171	Peroxiredoxin-2 OS=Mus musculus GN=Prdx2 PE=1 SV=3	1,57
P05132	cAMP-dependent protein kinase catalytic subunit alpha OS=Mus musculus GN=Prkaca PE=1 SV=3	1,568
P62137	Serine/threonine-protein phosphatase PP1-alpha catalytic subunit OS=Mus musculus GN=Ppp1ca PE=	1,565
P12658	Calbindin OS=Mus musculus GN=Calb1 PE=1 SV=2	1,561
B9EHN0	Ubiquitin-activating enzyme E1, Chr X OS=Mus musculus GN=Uba1 PE=2 SV=1	1,554
Q08331	Calretinin OS=Mus musculus GN=Calb2 PE=1 SV=3	1,545
A8IP69	14-3-3 protein gamma subtype OS=Mus musculus GN=Ywhag PE=2 SV=1	1,537
P80316	T-complex protein 1 subunit epsilon OS=Mus musculus GN=Cct5 PE=1 SV=1	1,536
F6YVP7	Protein Gm10260 OS=Mus musculus GN=Gm10260 PE=3 SV=2	1,53
P63276	40S ribosomal protein S17 OS=Mus musculus GN=Rps17 PE=1 SV=2	1,523
P09411	Phosphoglycerate kinase 1 OS=Mus musculus GN=Pgk1 PE=1 SV=4	1,521
Q3U4U6	T-complex protein 1 subunit gamma OS=Mus musculus GN=Cct3 PE=2 SV=1	1,52
P47857	ATP-dependent 6-phosphofructokinase, muscle type OS=Mus musculus GN=Pfkm PE=1 SV=3	1,517
Q5SXR6	Clathrin heavy chain OS=Mus musculus GN=Cltc PE=1 SV=1	1,512
E0CYV0	Protein-L-isoaspartate O-methyltransferase OS=Mus musculus GN=Pcmt1 PE=1 SV=1	1,491
P14869	60S acidic ribosomal protein P0 OS=Mus musculus GN=Rplp0 PE=1 SV=3	1,486
O55042	Alpha-synuclein OS=Mus musculus GN=Snca PE=1 SV=2	1,486
P01787	Ig heavy chain V regions TEPC 15/S107/HPCM1/HPCM2/HPCM3 OS=Mus musculus PE=1 SV=1	1,482
Q8BGT8	Phytanoyl-CoA hydroxylase-interacting protein-like OS=Mus musculus GN=Phyhipl PE=2 SV=1	1,481
P40142	Transketolase OS=Mus musculus GN=Tkt PE=1 SV=1	1,476
Q3UYK6	Amino acid transporter OS=Mus musculus GN=Slc1a2 PE=2 SV=1	1,465
Q8C1B7	Septin-11 OS=Mus musculus GN=Sept11 PE=1 SV=4	1,454
P19783	Cytochrome c oxidase subunit 4 isoform 1, mitochondrial OS=Mus musculus GN=Cox4i1 PE=1 SV=2	1,454
A0A0A6YXW6	Protein Igha (Fragment) OS=Mus musculus GN=Igha PE=1 SV=1	1,442
O88342	WD repeat-containing protein 1 OS=Mus musculus GN=Wdr1 PE=1 SV=3	1,437
Q3V117	ATP-citrate synthase OS=Mus musculus GN=Acly PE=1 SV=1	1,434
Q9Z2I9	Succinate--CoA ligase [ADP-forming] subunit beta, mitochondrial OS=Mus musculus GN=Sucla2 PE=1 S	1,429
P52480	Pyruvate kinase PKM OS=Mus musculus GN=Pkm PE=1 SV=4	1,422
Q921M7	Protein FAM49B OS=Mus musculus GN=Fam49b PE=2 SV=1	1,415
Q8BMS1	Trifunctional enzyme subunit alpha, mitochondrial OS=Mus musculus GN=Hadha PE=1 SV=1	1,406

Q8K0T0	Reticulon-1 OS=Mus musculus GN=Rtn1 PE=1 SV=1	1,403
P70168	Importin subunit beta-1 OS=Mus musculus GN=Kpnb1 PE=1 SV=2	1,402
Q545V3	Enolase 2, gamma neuronal, isoform CRA_a OS=Mus musculus GN=Eno2 PE=2 SV=1	1,399
P62631	Elongation factor 1-alpha 2 OS=Mus musculus GN=Eef1a2 PE=1 SV=1	1,398
Q56A15	Cytochrome c OS=Mus musculus GN=Cycs PE=2 SV=1	1,378
P17710	Hexokinase-1 OS=Mus musculus GN=Hk1 PE=1 SV=3	1,369
Q3TXU4	Apolipoprotein E, isoform CRA_h OS=Mus musculus GN=Apoe PE=2 SV=1	1,369
Q3UNV7	Putative uncharacterized protein OS=Mus musculus GN=Mlf2 PE=2 SV=1	1,367
Q9ERD7	Tubulin beta-3 chain OS=Mus musculus GN=Tubb3 PE=1 SV=1	1,361
Q9D6R2	Isocitrate dehydrogenase [NAD] subunit alpha, mitochondrial OS=Mus musculus GN=Idh3a PE=1 SV=1	1,355
Q542X7	Chaperonin subunit 2 (Beta), isoform CRA_a OS=Mus musculus GN=Cct2 PE=2 SV=1	1,355
P40336	Vacuolar protein sorting-associated protein 26A OS=Mus musculus GN=Vps26a PE=1 SV=1	1,348
Q58E64	Elongation factor 1-alpha OS=Mus musculus GN=Eef1a1 PE=2 SV=1	1,342
P48722	Heat shock 70 kDa protein 4L OS=Mus musculus GN=Hspa4l PE=1 SV=2	1,338
O08553	Dihydropyrimidinase-related protein 2 OS=Mus musculus GN=Dpysl2 PE=1 SV=2	1,333
A0A076FRG6	KCC2a variant 1 OS=Mus musculus GN=Slc12a5 PE=2 SV=1	1,332
Q5YLW3	Ribosomal protein S3 OS=Mus musculus GN=Rps3 PE=2 SV=1	1,322
Q3UY21	Myelin-oligodendrocyte glycoprotein OS=Mus musculus GN=Mog PE=1 SV=1	1,309
P97300	Neuroplastin OS=Mus musculus GN=Nptn PE=1 SV=3	1,309
P63005	Platelet-activating factor acetylhydrolase IB subunit alpha OS=Mus musculus GN=Pafah1b1 PE=1 SV=2	1,308
P63101	14-3-3 protein zeta/delta OS=Mus musculus GN=Ywhaz PE=1 SV=1	1,308
Q9DCW4	Electron transfer flavoprotein subunit beta OS=Mus musculus GN=Etfb PE=1 SV=3	1,303
Q61990	Poly(rC)-binding protein 2 OS=Mus musculus GN=Pcbp2 PE=1 SV=1	1,303
P06837	Neuromodulin OS=Mus musculus GN=Gap43 PE=1 SV=1	1,302
P60766	Cell division control protein 42 homolog OS=Mus musculus GN=Cdc42 PE=1 SV=2	1,3
P62880	Guanine nucleotide-binding protein G(I)/G(S)/G(T) subunit beta-2 OS=Mus musculus GN=Gnb2 PE=1 S	0,749
P46097	Synaptotagmin-2 OS=Mus musculus GN=Syt2 PE=1 SV=1	0,746
P97427	Dihydropyrimidinase-related protein 1 OS=Mus musculus GN=Crmp1 PE=1 SV=1	0,743
Q3TQ70	Beta1 subnuit of GTP-binding protein OS=Mus musculus GN=Gnb1 PE=2 SV=1	0,743
A2AQR0	Glycerol-3-phosphate dehydrogenase OS=Mus musculus GN=Gpd2 PE=1 SV=1	0,738
D3Z656	Synaptojanin-1 OS=Mus musculus GN=Synj1 PE=1 SV=1	0,733
Q9CVB6	Actin-related protein 2/3 complex subunit 2 OS=Mus musculus GN=Arpc2 PE=1 SV=3	0,732
Q9WTL4	Insulin receptor-related protein OS=Mus musculus GN=Insrr PE=1 SV=2	0,731

Q9QZQ8	Core histone macro-H2A.1 OS=Mus musculus GN=H2afy PE=1 SV=3	0,724
P52480-2	Isoform M1 of Pyruvate kinase PKM OS=Mus musculus GN=Pkm	0,719
P47963	60S ribosomal protein L13 OS=Mus musculus GN=Rpl13 PE=1 SV=3	0,716
O54962	Barrier-to-autointegration factor OS=Mus musculus GN=Banf1 PE=1 SV=1	0,715
Q91ZU6	Dystonin OS=Mus musculus GN=Dst PE=1 SV=2	0,714
Q99M71	Mammalian ependymin-related protein 1 OS=Mus musculus GN=Epdr1 PE=2 SV=1	0,712
Q9CXS4	Centromere protein V OS=Mus musculus GN=Cenpv PE=1 SV=2	0,711
P12787	Cytochrome c oxidase subunit 5A, mitochondrial OS=Mus musculus GN=Cox5a PE=1 SV=2	0,709
P08752	Guanine nucleotide-binding protein G(i) subunit alpha-2 OS=Mus musculus GN=Gnai2 PE=1 SV=5	0,707
P35235	Tyrosine-protein phosphatase non-receptor type 11 OS=Mus musculus GN=Ptpn11 PE=1 SV=2	0,707
Q8R1B4	Eukaryotic translation initiation factor 3 subunit C OS=Mus musculus GN=Eif3c PE=1 SV=1	0,706
Q9EQF6	Dihydropyrimidinase-related protein 5 OS=Mus musculus GN=Dpysl5 PE=1 SV=1	0,703
Q9WV34	MAGUK p55 subfamily member 2 OS=Mus musculus GN=Mpp2 PE=1 SV=1	0,698
P14148	60S ribosomal protein L7 OS=Mus musculus GN=Rpl7 PE=1 SV=2	0,697
P19096	Fatty acid synthase OS=Mus musculus GN=Fasn PE=1 SV=2	0,69
Q9R1P1	Proteasome subunit beta type-3 OS=Mus musculus GN=Psmb3 PE=1 SV=1	0,685
E9PUA3	IQ motif and SEC7 domain-containing protein 1 OS=Mus musculus GN=Iqsec1 PE=1 SV=1	0,684
Q8BFZ9	Erlin-2 OS=Mus musculus GN=Erlin2 PE=1 SV=1	0,681
Q8VEK3	Heterogeneous nuclear ribonucleoprotein U OS=Mus musculus GN=Hnrnpu PE=1 SV=1	0,679
Q6ZWN5	40S ribosomal protein S9 OS=Mus musculus GN=Rps9 PE=1 SV=3	0,677
Q6IFX2	Keratin, type I cytoskeletal 42 OS=Mus musculus GN=Krt42 PE=1 SV=1	0,667
Q9WUM5	Succinyl-CoA ligase [ADP/GDP-forming] subunit alpha, mitochondrial OS=Mus musculus GN=Suclg1 PE	0,663
Q9R1P4	Proteasome subunit alpha type-1 OS=Mus musculus GN=Psma1 PE=1 SV=1	0,662
S4R249	Ankyrin-2 OS=Mus musculus GN=Ank2 PE=1 SV=1	0,66
E9QAX2	Unconventional myosin-XVIIIa OS=Mus musculus GN=Myo18a PE=1 SV=1	0,66
Q9Z1B3	1-phosphatidylinositol 4,5-bisphosphate phosphodiesterase beta-1 OS=Mus musculus GN=Plcb1 PE=1	0,659
Q548L4	Glutamate decarboxylase OS=Mus musculus GN=Gad2 PE=2 SV=1	0,652
P47915	60S ribosomal protein L29 OS=Mus musculus GN=Rpl29 PE=2 SV=2	0,646
A2CEK3	Phosphoglucomutase-2 OS=Mus musculus GN=Pgm2 PE=1 SV=1	0,646
A0A0G2JGS4	Calcium/calmodulin-dependent protein kinase type II subunit delta OS=Mus musculus GN=Camk2d PE	0,645
P14115	60S ribosomal protein L27a OS=Mus musculus GN=Rpl27a PE=2 SV=5	0,641
G5E866	Splicing factor 3B subunit 1 OS=Mus musculus GN=Sf3b1 PE=1 SV=1	0,641
O09061	Proteasome subunit beta type-1 OS=Mus musculus GN=Psmb1 PE=1 SV=1	0,641

Q5M9M5	MCG10806 OS=Mus musculus GN=Rpl23a PE=2 SV=1	0,639
P11798	Calcium/calmodulin-dependent protein kinase type II subunit alpha OS=Mus musculus GN=Camk2a PE	0,633
P11881	Inositol 1,4,5-trisphosphate receptor type 1 OS=Mus musculus GN=Itpr1 PE=1 SV=2	0,633
Q99JB2	Stomatin-like protein 2, mitochondrial OS=Mus musculus GN=Stoml2 PE=1 SV=1	0,632
Q99PV0	Pre-mRNA-processing-splicing factor 8 OS=Mus musculus GN=Prpf8 PE=1 SV=2	0,629
Q91ZX7	Prolow-density lipoprotein receptor-related protein 1 OS=Mus musculus GN=Lrp1 PE=1 SV=1	0,627
P63318	Protein kinase C gamma type OS=Mus musculus GN=Prkcg PE=1 SV=1	0,624
S4R1P5	Dystonin OS=Mus musculus GN=Dst PE=1 SV=1	0,621
Q8CCK0	Core histone macro-H2A.2 OS=Mus musculus GN=H2afy2 PE=1 SV=3	0,619
A0A0A0MQA5	Tubulin alpha chain (Fragment) OS=Mus musculus GN=Tuba4a PE=1 SV=1	0,619
B1AQZ0	Septin-8 OS=Mus musculus GN=Sept8 PE=1 SV=1	0,614
Q5XJF6	Ribosomal protein OS=Mus musculus GN=Rpl10a PE=1 SV=1	0,611
Q3UHL1	CaM kinase-like vesicle-associated protein OS=Mus musculus GN=Camkv PE=1 SV=2	0,609
Q2PFD7	PH and SEC7 domain-containing protein 3 OS=Mus musculus GN=Psd3 PE=1 SV=2	0,609
P62889	60S ribosomal protein L30 OS=Mus musculus GN=Rpl30 PE=1 SV=2	0,604
P12970	60S ribosomal protein L7a OS=Mus musculus GN=Rpl7a PE=1 SV=2	0,597
O08788	Dynactin subunit 1 OS=Mus musculus GN=Dctn1 PE=1 SV=3	0,592
Q9WV92	Band 4.1-like protein 3 OS=Mus musculus GN=Epb41l3 PE=1 SV=1	0,59
P61514	60S ribosomal protein L37a OS=Mus musculus GN=Rpl37a PE=3 SV=2	0,584
P03995	Glial fibrillary acidic protein OS=Mus musculus GN=Gfap PE=1 SV=4	0,583
E9Q0J5	Kinesin-like protein KIF21A OS=Mus musculus GN=Kif21a PE=1 SV=2	0,582
Q6DFW4	Nucleolar protein 58 OS=Mus musculus GN=Nop58 PE=1 SV=1	0,582
P27773	Protein disulfide-isomerase A3 OS=Mus musculus GN=Pdia3 PE=1 SV=2	0,573
P86048	60S ribosomal protein L10-like OS=Mus musculus GN=Rpl10l PE=2 SV=1	0,572
Q9CPX4	Ferritin OS=Mus musculus GN=Ftl1 PE=1 SV=1	0,571
P08551	Neurofilament light polypeptide OS=Mus musculus GN=Nefl PE=1 SV=5	0,569
Q0VF55	Calcium-transporting ATPase OS=Mus musculus GN=Atp2b3 PE=1 SV=1	0,567
P17426	AP-2 complex subunit alpha-1 OS=Mus musculus GN=Ap2a1 PE=1 SV=1	0,566
Q3UGC8	Propionyl-Coenzyme A carboxylase, alpha polypeptide, isoform CRA_b OS=Mus musculus GN=Pcca PE	0,566
P19001	Keratin, type I cytoskeletal 19 OS=Mus musculus GN=Krt19 PE=1 SV=1	0,565
Q6ZWV7	60S ribosomal protein L35 OS=Mus musculus GN=Rpl35 PE=1 SV=1	0,563
Q3TYV5	Cyclic nucleotide phosphodiesterase 1, isoform CRA_b OS=Mus musculus GN=Cnp PE=2 SV=1	0,559
P62996	Transformer-2 protein homolog beta OS=Mus musculus GN=Tra2b PE=1 SV=1	0,557

Q3TVK3	Aspartyl aminopeptidase OS=Mus musculus GN=Dnpep PE=1 SV=1	0,555
Q3TLP8	RAS-related C3 botulinum substrate 1, isoform CRA_a OS=Mus musculus GN=Rac1 PE=1 SV=1	0,552
D0VYV6	Erythrocyte protein band 4.1-like 3 isoform B OS=Mus musculus GN=Epb4.1l3 PE=2 SV=1	0,532
Q545X8	40S ribosomal protein S4 OS=Mus musculus GN=Rps4x PE=2 SV=1	0,527
Q9R1T4	Septin-6 OS=Mus musculus GN=Sept6 PE=1 SV=4	0,526
P60879	Synaptosomal-associated protein 25 OS=Mus musculus GN=Snap25 PE=1 SV=1	0,525
Q9QWI6	SRC kinase signaling inhibitor 1 OS=Mus musculus GN=Srcin1 PE=1 SV=2	0,522
P62264	40S ribosomal protein S14 OS=Mus musculus GN=Rps14 PE=1 SV=3	0,521
Q9QXS1	Plectin OS=Mus musculus GN=Plec PE=1 SV=3	0,521
P47911	60S ribosomal protein L6 OS=Mus musculus GN=Rpl6 PE=1 SV=3	0,52
P63085	Mitogen-activated protein kinase 1 OS=Mus musculus GN=Mapk1 PE=1 SV=3	0,516
Q3UH59	Myosin-10 OS=Mus musculus GN=Myh10 PE=1 SV=1	0,514
Q9QUM9	Proteasome subunit alpha type-6 OS=Mus musculus GN=Psma6 PE=1 SV=1	0,514
O08599	Syntaxin-binding protein 1 OS=Mus musculus GN=Stxbp1 PE=1 SV=2	0,513
Q9Z2U1	Proteasome subunit alpha type-5 OS=Mus musculus GN=Psma5 PE=1 SV=1	0,507
P19246	Neurofilament heavy polypeptide OS=Mus musculus GN=Nefh PE=1 SV=3	0,505
O09167	60S ribosomal protein L21 OS=Mus musculus GN=Rpl21 PE=1 SV=3	0,504
Q8VDD5	Myosin-9 OS=Mus musculus GN=Myh9 PE=1 SV=4	0,498
E9QAZ2	Ribosomal protein L15 OS=Mus musculus GN=Gm10020 PE=3 SV=1	0,497
Q3TI05	Chaperonin containing Tcp1, subunit 6a (Zeta) OS=Mus musculus GN=Cct6a PE=2 SV=1	0,491
A0A140T8K6	60S ribosomal protein L36 OS=Mus musculus GN=Rpl36-ps3 PE=3 SV=1	0,49
P99026	Proteasome subunit beta type-4 OS=Mus musculus GN=Psmb4 PE=1 SV=1	0,49
P27659	60S ribosomal protein L3 OS=Mus musculus GN=Rpl3 PE=1 SV=3	0,485
P31938	Dual specificity mitogen-activated protein kinase kinase 1 OS=Mus musculus GN=Map2k1 PE=1 SV=2	0,484
P53395	Lipoamide acyltransferase component of branched-chain alpha-keto acid dehydrogenase complex, mi	0,477
Q9JHU4	Cytoplasmic dynein 1 heavy chain 1 OS=Mus musculus GN=Dync1h1 PE=1 SV=2	0,475
Q8C522	Endonuclease domain-containing 1 protein OS=Mus musculus GN=Endod1 PE=1 SV=2	0,474
O70318	Band 4.1-like protein 2 OS=Mus musculus GN=Epb41l2 PE=1 SV=2	0,474
P47962	60S ribosomal protein L5 OS=Mus musculus GN=Rpl5 PE=1 SV=3	0,471
E9Q401	Ryanodine receptor 2 OS=Mus musculus GN=Ryr2 PE=1 SV=1	0,466
Q5I0T8	Ribosomal protein L19 OS=Mus musculus GN=Rpl19 PE=2 SV=1	0,447
Q9Z2U0	Proteasome subunit alpha type-7 OS=Mus musculus GN=Psma7 PE=1 SV=1	0,441
Q5BLK0	MCG18564, isoform CRA_a OS=Mus musculus GN=Rpl12 PE=2 SV=1	0,44

P62911	60S ribosomal protein L32 OS=Mus musculus GN=Rpl32 PE=1 SV=2	0,439
E9PYK3	Poly [ADP-ribose] polymerase OS=Mus musculus GN=Parp4 PE=1 SV=1	0,439
Q4VAG4	MCG12304 OS=Mus musculus GN=Rpl22 PE=2 SV=1	0,439
P12023	Amyloid beta A4 protein OS=Mus musculus GN=App PE=1 SV=3	0,432
Q9D8B3	Charged multivesicular body protein 4b OS=Mus musculus GN=Chmp4b PE=1 SV=2	0,431
P49722	Proteasome subunit alpha type-2 OS=Mus musculus GN=Psma2 PE=1 SV=3	0,425
Q9CZY3	Ubiquitin-conjugating enzyme E2 variant 1 OS=Mus musculus GN=Ube2v1 PE=1 SV=1	0,423
Q9D0M3	Cytochrome c1, heme protein, mitochondrial OS=Mus musculus GN=Cyc1 PE=1 SV=1	0,421
Q9R1P3	Proteasome subunit beta type-2 OS=Mus musculus GN=Psmb2 PE=1 SV=1	0,419
Q58EW0	60S ribosomal protein L18 OS=Mus musculus GN=Rpl18 PE=2 SV=1	0,416
Q9Z0H4	CUGBP Elav-like family member 2 OS=Mus musculus GN=Celf2 PE=1 SV=1	0,416
Q5BLJ9	60S ribosomal protein L27 OS=Mus musculus GN=Rpl27 PE=2 SV=1	0,414
Q497E9	40S ribosomal protein S8 OS=Mus musculus GN=Rps8 PE=2 SV=1	0,412
Q80YX1	Tenascin OS=Mus musculus GN=Tnc PE=1 SV=1	0,412
Q5BLK1	40S ribosomal protein S6 OS=Mus musculus GN=Rps6 PE=2 SV=1	0,411
Z4YL23	Fer-1-like protein 4 OS=Mus musculus GN=Fer1l4 PE=4 SV=1	0,399
Q923T9	Calcium/calmodulin-dependent protein kinase type II subunit gamma OS=Mus musculus GN=Camk2g	0,399
O08917	Flotillin-1 OS=Mus musculus GN=Flot1 PE=1 SV=1	0,399
Q91VE0	Long-chain fatty acid transport protein 4 OS=Mus musculus GN=Slc27a4 PE=1 SV=1	0,392
Q505A8	MCG17585 OS=Mus musculus GN=Rpl39 PE=2 SV=1	0,389
P46660	Alpha-internexin OS=Mus musculus GN=Ina PE=1 SV=3	0,389
Q5SVJ0	Calcium/calmodulin-dependent protein kinase II, beta, isoform CRA_b OS=Mus musculus GN=Camk2b	0,386
P62267	40S ribosomal protein S23 OS=Mus musculus GN=Rps23 PE=1 SV=3	0,383
P29341	Polyadenylate-binding protein 1 OS=Mus musculus GN=Pabpc1 PE=1 SV=2	0,38
P08553	Neurofilament medium polypeptide OS=Mus musculus GN=Nefm PE=1 SV=4	0,377
Q9CU62	Structural maintenance of chromosomes protein 1A OS=Mus musculus GN=Smc1a PE=1 SV=4	0,376
O55234	Proteasome subunit beta type-5 OS=Mus musculus GN=Psmb5 PE=1 SV=3	0,376
P17427	AP-2 complex subunit alpha-2 OS=Mus musculus GN=Ap2a2 PE=1 SV=2	0,371
Q9D1R9	60S ribosomal protein L34 OS=Mus musculus GN=Rpl34 PE=1 SV=2	0,37
P09528	Ferritin heavy chain OS=Mus musculus GN=Fth1 PE=1 SV=2	0,369
Q564E8	Ribosomal protein L4 OS=Mus musculus GN=Rpl4 PE=2 SV=1	0,367
P14685	26S proteasome non-ATPase regulatory subunit 3 OS=Mus musculus GN=Psmd3 PE=1 SV=3	0,367
Q8BKZ9	Pyruvate dehydrogenase protein X component, mitochondrial OS=Mus musculus GN=Pdhx PE=1 SV=1	0,362

P32067	Lupus La protein homolog OS=Mus musculus GN=Ssb PE=1 SV=1	0,358
Q58EV4	Proteasome subunit alpha type OS=Mus musculus GN=Psma3 PE=2 SV=1	0,353
Q8BMF4	Dihydrolipoyllysine-residue acetyltransferase component of pyruvate dehydrogenase complex, mitocl	0,345
P62715	Serine/threonine-protein phosphatase 2A catalytic subunit beta isoform OS=Mus musculus GN=Ppp2c	0,344
Q99104	Unconventional myosin-Va OS=Mus musculus GN=Myo5a PE=1 SV=2	0,337
F6TYB7	Myelin basic protein (Fragment) OS=Mus musculus GN=Mbp PE=1 SV=1	0,334
Q9JLM8	Serine/threonine-protein kinase DCLK1 OS=Mus musculus GN=Dclk1 PE=1 SV=1	0,321
P62855	40S ribosomal protein S26 OS=Mus musculus GN=Rps26 PE=1 SV=3	0,316
Q9CR57	60S ribosomal protein L14 OS=Mus musculus GN=Rpl14 PE=1 SV=3	0,313
P70195	Proteasome subunit beta type-7 OS=Mus musculus GN=Psmb7 PE=1 SV=1	0,31
Q9D823	60S ribosomal protein L37 OS=Mus musculus GN=Rpl37 PE=3 SV=3	0,305
Q9EQK5	Major vault protein OS=Mus musculus GN=Mvp PE=1 SV=4	0,292
Q5SQX6	Cytoplasmic FMR1-interacting protein 2 OS=Mus musculus GN=Cyfip2 PE=1 SV=2	0,291
V9GX76	Unconventional myosin-VI OS=Mus musculus GN=Myo6 PE=1 SV=1	0,285
P97499	Telomerase protein component 1 OS=Mus musculus GN=Tep1 PE=1 SV=1	0,273
Q9JM93	ADP-ribosylation factor-like protein 6-interacting protein 4 OS=Mus musculus GN=Arl6ip4 PE=1 SV=1	0,251
Q5SS83	Flotillin 2, isoform CRA_a OS=Mus musculus GN=Flot2 PE=1 SV=1	0,25
P62918	60S ribosomal protein L8 OS=Mus musculus GN=Rpl8 PE=1 SV=2	0,244
P63163	Small nuclear ribonucleoprotein-associated protein N OS=Mus musculus GN=Snrpn PE=2 SV=1	0,241
Q8R366	Immunoglobulin superfamily member 8 OS=Mus musculus GN=Igsf8 PE=1 SV=2	0,234
Q8CAK3	UPF0515 protein C19orf66 homolog OS=Mus musculus PE=2 SV=1	0,229
Q9CYR0	Single-stranded DNA-binding protein, mitochondrial OS=Mus musculus GN=Ssbp1 PE=1 SV=1	0,205
P62320	Small nuclear ribonucleoprotein Sm D3 OS=Mus musculus GN=Snrpd3 PE=1 SV=1	0,204
P62315	Small nuclear ribonucleoprotein Sm D1 OS=Mus musculus GN=Snrpd1 PE=1 SV=1	0,203
P62717	60S ribosomal protein L18a OS=Mus musculus GN=Rpl18a PE=1 SV=1	0,193
Q99MN9	Propionyl-CoA carboxylase beta chain, mitochondrial OS=Mus musculus GN=Pccb PE=1 SV=2	0,187
Q3V0Q1	Dynein heavy chain 12, axonemal OS=Mus musculus GN=Dnah12 PE=1 SV=2	0,149
P62307	Small nuclear ribonucleoprotein F OS=Mus musculus GN=Snrpf PE=1 SV=1	0,146
Q8C1Y8	Vacuolar fusion protein CCZ1 homolog OS=Mus musculus GN=Ccz1 PE=1 SV=1	0,126

DATA FILE S1

REGULATED PROTEINS AD vs. non-AD

Accession	Description	Abundance Ratio: (AD) / (non-AD)
P10636-6	Isoform of P10636, Isoform Tau-D of Microtubule-associated protein tau OS=Homo sapiens GN=MAPT	60,425
P10636-4	Isoform of P10636, Isoform Tau-B of Microtubule-associated protein tau OS=Homo sapiens GN=MAPT	43,146
A0A0G2JMX7	Microtubule-associated protein OS=Homo sapiens GN=MAPT PE=1 SV=1	37,151
P62979	Ubiquitin-40S ribosomal protein S27a OS=Homo sapiens GN=RPS27A PE=1 SV=2	8,079
Q13867	Bleomycin hydrolase OS=Homo sapiens GN=BLMH PE=1 SV=1	7,447
Q7Z7K6	Centromere protein V OS=Homo sapiens GN=CENPV PE=1 SV=1	5,332
P63244	Receptor of activated protein C kinase 1 OS=Homo sapiens GN=RACK1 PE=1 SV=3	4,905
P08670	Vimentin OS=Homo sapiens GN=VIM PE=1 SV=4	4,749
Q99747	Gamma-soluble NSF attachment protein OS=Homo sapiens GN=NAPG PE=1 SV=1	4,461
A0A087WV75	Isoform of P13591, Neural cell adhesion molecule 1 OS=Homo sapiens GN=NCAM1 PE=1 SV=1	4,26
P11182	Lipoamide acyltransferase component of branched-chain alpha-keto acid dehydrogenase complex, mi	3,851
B7Z6Z4	Isoform of P60660, Myosin light polypeptide 6 OS=Homo sapiens GN=MYL6 PE=1 SV=1	3,766
Q9UBB6	Neurochondrin OS=Homo sapiens GN=NCDN PE=1 SV=1	3,646
A0A087X165	Isoform of Q9C0H9, SRC kinase-signaling inhibitor 1 OS=Homo sapiens GN=SRCIN1 PE=1 SV=1	3,564
P05067	Amyloid beta A4 protein OS=Homo sapiens GN=APP PE=1 SV=3	2,998
P61927	60S ribosomal protein L37 OS=Homo sapiens GN=RPL37 PE=1 SV=2	2,831
Q01813	ATP-dependent 6-phosphofructokinase, platelet type OS=Homo sapiens GN=PFKP PE=1 SV=2	2,762
Q13509	Tubulin beta-3 chain OS=Homo sapiens GN=TUBB3 PE=1 SV=2	2,732
P11021	78 kDa glucose-regulated protein OS=Homo sapiens GN=HSPA5 PE=1 SV=2	2,656
P0DME0	Protein SETSIP OS=Homo sapiens GN=SETSIP PE=1 SV=1	2,477
G8JLB6	Heterogeneous nuclear ribonucleoprotein H OS=Homo sapiens GN=HNRNPH1 PE=1 SV=1	2,471
P02144	Myoglobin OS=Homo sapiens GN=MB PE=1 SV=2	2,414
P30044	Peroxiredoxin-5, mitochondrial OS=Homo sapiens GN=PRDX5 PE=1 SV=4	2,327
P52306	Rap1 GTPase-GDP dissociation stimulator 1 OS=Homo sapiens GN=RAP1GDS1 PE=1 SV=3	2,291
P19338	Nucleolin OS=Homo sapiens GN=NCL PE=1 SV=3	1,952
P62888	60S ribosomal protein L30 OS=Homo sapiens GN=RPL30 PE=1 SV=2	1,935
P0C0S5	Histone H2A.Z OS=Homo sapiens GN=H2AFZ PE=1 SV=2	1,784
Q00839	Heterogeneous nuclear ribonucleoprotein U OS=Homo sapiens GN=HNRNPU PE=1 SV=6	1,71
Q9UQ80	Proliferation-associated protein 2G4 OS=Homo sapiens GN=PA2G4 PE=1 SV=3	1,702

P50990	T-complex protein 1 subunit theta OS=Homo sapiens GN=CCT8 PE=1 SV=4	1,702
P61513	60S ribosomal protein L37a OS=Homo sapiens GN=RPL37A PE=1 SV=2	1,693
P62266	40S ribosomal protein S23 OS=Homo sapiens GN=RPS23 PE=1 SV=3	1,689
P02792	Ferritin light chain OS=Homo sapiens GN=FTL PE=1 SV=2	1,674
Q13243	Serine/arginine-rich splicing factor 5 OS=Homo sapiens GN=SRSF5 PE=1 SV=1	1,643
Q07954	Prolow-density lipoprotein receptor-related protein 1 OS=Homo sapiens GN=LRP1 PE=1 SV=2	1,633
P07737	Profilin-1 OS=Homo sapiens GN=PFN1 PE=1 SV=2	1,567
P62318	Small nuclear ribonucleoprotein Sm D3 OS=Homo sapiens GN=SNRPD3 PE=1 SV=1	1,522
P15531	Nucleoside diphosphate kinase A OS=Homo sapiens GN=NME1 PE=1 SV=1	1,504
Q9NQ66	1-phosphatidylinositol 4,5-bisphosphate phosphodiesterase beta-1 OS=Homo sapiens GN=PLCB1 PE=1	1,499
P39019	40S ribosomal protein S19 OS=Homo sapiens GN=RPS19 PE=1 SV=2	1,495
P04899	Guanine nucleotide-binding protein G(i) subunit alpha-2 OS=Homo sapiens GN=GNAI2 PE=1 SV=3	1,493
A0A0J9YXJ0	Isoform of O95319, CUGBP Elav-like family member 2 OS=Homo sapiens GN=CELF2 PE=1 SV=1	1,488
H0YKD8	Isoform of P46779, 60S ribosomal protein L28 OS=Homo sapiens GN=RPL28 PE=1 SV=1	1,469
P06454	Prothymosin alpha OS=Homo sapiens GN=PTMA PE=1 SV=2	1,456
P31146	Coronin-1A OS=Homo sapiens GN=CORO1A PE=1 SV=4	1,451
O00499	Myc box-dependent-interacting protein 1 OS=Homo sapiens GN=BIN1 PE=1 SV=1	1,439
A0A075B767	Peptidyl-prolyl cis-trans isomerase OS=Homo sapiens GN=LOC105371242 PE=3 SV=1	1,439
P21291	Cysteine and glycine-rich protein 1 OS=Homo sapiens GN=CSRP1 PE=1 SV=3	1,437
Q01484	Ankyrin-2 OS=Homo sapiens GN=ANK2 PE=1 SV=4	1,429
O60636	Tetraspanin-2 OS=Homo sapiens GN=TSPAN2 PE=1 SV=2	1,427
P78386	Keratin, type II cuticular Hb5 OS=Homo sapiens GN=KRT85 PE=1 SV=1	1,404
P14678	Small nuclear ribonucleoprotein-associated proteins B and B' OS=Homo sapiens GN=SNRPB PE=1 SV=2	1,403
P39023	60S ribosomal protein L3 OS=Homo sapiens GN=RPL3 PE=1 SV=2	1,389
U3KQK0	Isoform of Q99877, Histone H2B OS=Homo sapiens GN=HIST1H2BN PE=1 SV=1	1,376
P18621-3	Isoform of P18621, Isoform 3 of 60S ribosomal protein L17 OS=Homo sapiens GN=RPL17	1,375
Q9UQ35	Serine/arginine repetitive matrix protein 2 OS=Homo sapiens GN=SRRM2 PE=1 SV=2	1,366
Q9ULV4	Coronin-1C OS=Homo sapiens GN=CORO1C PE=1 SV=1	1,36
Q92599	Septin-8 OS=Homo sapiens GN=SEPT8 PE=1 SV=4	1,359
P53396	ATP-citrate synthase OS=Homo sapiens GN=ACLY PE=1 SV=3	1,344
P61254	60S ribosomal protein L26 OS=Homo sapiens GN=RPL26 PE=1 SV=1	1,343
P51991	Heterogeneous nuclear ribonucleoprotein A3 OS=Homo sapiens GN=HNRNPA3 PE=1 SV=2	1,332
P35080	Profilin-2 OS=Homo sapiens GN=PFN2 PE=1 SV=3	0,774

P55072	Transitional endoplasmic reticulum ATPase OS=Homo sapiens GN=VCP PE=1 SV=4	0,771
P62195	26S protease regulatory subunit 8 OS=Homo sapiens GN=PSMC5 PE=1 SV=1	0,767
P48426	Phosphatidylinositol 5-phosphate 4-kinase type-2 alpha OS=Homo sapiens GN=PIP4K2A PE=1 SV=2	0,755
P12277	Creatine kinase B-type OS=Homo sapiens GN=CKB PE=1 SV=1	0,751
P14625	Endoplasmin OS=Homo sapiens GN=HSP90B1 PE=1 SV=1	0,748
A0A0U1RRH7	Histone H2A OS=Homo sapiens PE=3 SV=1	0,746
Q86YZ3	Hornerin OS=Homo sapiens GN=HRNR PE=1 SV=2	0,746
P16615	Sarcoplasmic/endoplasmic reticulum calcium ATPase 2 OS=Homo sapiens GN=ATP2A2 PE=1 SV=1	0,738
A0A087WUS0	40S ribosomal protein S24 OS=Homo sapiens GN=RPS24 PE=1 SV=1	0,734
P53597	Succinate--CoA ligase [ADP/GDP-forming] subunit alpha, mitochondrial OS=Homo sapiens GN=SUCLG1	0,733
P00558	Phosphoglycerate kinase 1 OS=Homo sapiens GN=PGK1 PE=1 SV=3	0,733
P35219	Carbonic anhydrase-related protein OS=Homo sapiens GN=CA8 PE=1 SV=3	0,731
P63151	Serine/threonine-protein phosphatase 2A 55 kDa regulatory subunit B alpha isoform OS=Homo sapien	0,729
Q08554	Desmocollin-1 OS=Homo sapiens GN=DSC1 PE=1 SV=2	0,725
P17600	Synapsin-1 OS=Homo sapiens GN=SYN1 PE=1 SV=3	0,719
Q15366	Poly(rC)-binding protein 2 OS=Homo sapiens GN=PCBP2 PE=1 SV=1	0,719
P08621	U1 small nuclear ribonucleoprotein 70 kDa OS=Homo sapiens GN=SNRNP70 PE=1 SV=2	0,716
P23528	Cofilin-1 OS=Homo sapiens GN=CFL1 PE=1 SV=3	0,714
P60709	Actin, cytoplasmic 1 OS=Homo sapiens GN=ACTB PE=1 SV=1	0,709
P13797	Plastin-3 OS=Homo sapiens GN=PLS3 PE=1 SV=4	0,707
P62937	Peptidyl-prolyl cis-trans isomerase A OS=Homo sapiens GN=PPIA PE=1 SV=2	0,707
P61764	Syntaxin-binding protein 1 OS=Homo sapiens GN=STXBP1 PE=1 SV=1	0,703
Q16143	Beta-synuclein OS=Homo sapiens GN=SNCB PE=1 SV=1	0,701
Q8TAC9	Secretory carrier-associated membrane protein 5 OS=Homo sapiens GN=SCAMP5 PE=1 SV=1	0,698
Q5JXB2	Putative ubiquitin-conjugating enzyme E2 N-like OS=Homo sapiens GN=UBE2NL PE=1 SV=1	0,692
P40925	Malate dehydrogenase, cytoplasmic OS=Homo sapiens GN=MDH1 PE=1 SV=4	0,692
P20336	Ras-related protein Rab-3A OS=Homo sapiens GN=RAB3A PE=1 SV=1	0,691
P40227	T-complex protein 1 subunit zeta OS=Homo sapiens GN=CCT6A PE=1 SV=3	0,691
Q16629	Serine/arginine-rich splicing factor 7 OS=Homo sapiens GN=SRSF7 PE=1 SV=1	0,687
P11766	Alcohol dehydrogenase class-3 OS=Homo sapiens GN=ADH5 PE=1 SV=4	0,683
P05771	Protein kinase C beta type OS=Homo sapiens GN=PRKCB PE=1 SV=4	0,68
P07900	Heat shock protein HSP 90-alpha OS=Homo sapiens GN=HSP90AA1 PE=1 SV=5	0,679
Q9Y2J2	Band 4.1-like protein 3 OS=Homo sapiens GN=EPB41L3 PE=1 SV=2	0,678

Q04837	Single-stranded DNA-binding protein, mitochondrial OS=Homo sapiens GN=SSBP1 PE=1 SV=1	0,674
P06576	ATP synthase subunit beta, mitochondrial OS=Homo sapiens GN=ATP5B PE=1 SV=3	0,674
Q8NCB2	CaM kinase-like vesicle-associated protein OS=Homo sapiens GN=CAMKV PE=2 SV=2	0,672
Q02413	Desmoglein-1 OS=Homo sapiens GN=DSG1 PE=1 SV=2	0,671
Q14982	Opioid-binding protein/cell adhesion molecule OS=Homo sapiens GN=OPCML PE=1 SV=1	0,671
P21579	Synaptotagmin-1 OS=Homo sapiens GN=SYT1 PE=1 SV=1	0,669
P19367	Hexokinase-1 OS=Homo sapiens GN=HK1 PE=1 SV=3	0,667
P10412	Histone H1.4 OS=Homo sapiens GN=HIST1H1E PE=1 SV=2	0,666
P02768	Serum albumin OS=Homo sapiens GN=ALB PE=1 SV=2	0,665
P18669	Phosphoglycerate mutase 1 OS=Homo sapiens GN=PGAM1 PE=1 SV=2	0,663
Q05639	Elongation factor 1-alpha 2 OS=Homo sapiens GN=EEF1A2 PE=1 SV=1	0,662
Q7Z4S6	Kinesin-like protein KIF21A OS=Homo sapiens GN=KIF21A PE=1 SV=2	0,662
P18124	60S ribosomal protein L7 OS=Homo sapiens GN=RPL7 PE=1 SV=1	0,661
P61981	14-3-3 protein gamma OS=Homo sapiens GN=YWHAG PE=1 SV=2	0,655
Q92598	Heat shock protein 105 kDa OS=Homo sapiens GN=HSPH1 PE=1 SV=1	0,655
Q9UJZ1	Stomatin-like protein 2, mitochondrial OS=Homo sapiens GN=STOML2 PE=1 SV=1	0,654
A0A1B0GTW6	Isoform of Q9H4G0, Band 4.1-like protein 1 (Fragment) OS=Homo sapiens GN=EPB41L1 PE=1 SV=1	0,65
P17858	ATP-dependent 6-phosphofructokinase, liver type OS=Homo sapiens GN=PFKL PE=1 SV=6	0,65
P49720	Proteasome subunit beta type-3 OS=Homo sapiens GN=PSMB3 PE=1 SV=2	0,648
P46777	60S ribosomal protein L5 OS=Homo sapiens GN=RPL5 PE=1 SV=3	0,641
Q14141	Septin-6 OS=Homo sapiens GN=SEPT6 PE=1 SV=4	0,639
O15075	Serine/threonine-protein kinase DCLK1 OS=Homo sapiens GN=DCLK1 PE=1 SV=2	0,631
E7EQ64	Isoform of P07477, Trypsin-1 OS=Homo sapiens GN=PRSS1 PE=1 SV=1	0,63
Q9Y277	Voltage-dependent anion-selective channel protein 3 OS=Homo sapiens GN=VDAC3 PE=1 SV=1	0,628
H3BR70	Isoform of P14618, Pyruvate kinase OS=Homo sapiens GN=PKM PE=1 SV=1	0,627
P35908	Keratin, type II cytoskeletal 2 epidermal OS=Homo sapiens GN=KRT2 PE=1 SV=2	0,625
Q15773	Myeloid leukemia factor 2 OS=Homo sapiens GN=MLF2 PE=1 SV=1	0,623
A0A0B4J2C3	Translationally-controlled tumor protein OS=Homo sapiens GN=TPT1 PE=1 SV=1	0,622
Q6ZN40	Tropomyosin 1 (Alpha), isoform CRA_f OS=Homo sapiens GN=TPM1 PE=1 SV=1	0,621
Q6PUV4	Complexin-2 OS=Homo sapiens GN=CPLX2 PE=2 SV=2	0,621
P60201	Myelin proteolipid protein OS=Homo sapiens GN=PLP1 PE=1 SV=2	0,614
Q15365	Poly(rC)-binding protein 1 OS=Homo sapiens GN=PCBP1 PE=1 SV=2	0,612
P28070	Proteasome subunit beta type-4 OS=Homo sapiens GN=PSMB4 PE=1 SV=4	0,61

A0A024RA52	Proteasome subunit alpha type OS=Homo sapiens GN=PSMA2 PE=1 SV=1	0,61
P13929	Beta-enolase OS=Homo sapiens GN=ENO3 PE=1 SV=5	0,609
O14818	Proteasome subunit alpha type-7 OS=Homo sapiens GN=PSMA7 PE=1 SV=1	0,607
P62316	Small nuclear ribonucleoprotein Sm D2 OS=Homo sapiens GN=SNRPD2 PE=1 SV=1	0,606
P07195	L-lactate dehydrogenase B chain OS=Homo sapiens GN=LDHB PE=1 SV=2	0,603
Q14683	Structural maintenance of chromosomes protein 1A OS=Homo sapiens GN=SMC1A PE=1 SV=2	0,602
P13647	Keratin, type II cytoskeletal 5 OS=Homo sapiens GN=KRT5 PE=1 SV=3	0,601
P28066	Proteasome subunit alpha type-5 OS=Homo sapiens GN=PSMA5 PE=1 SV=3	0,6
P09471	Guanine nucleotide-binding protein G(o) subunit alpha OS=Homo sapiens GN=GNAO1 PE=1 SV=4	0,6
P58546	Myotrophin OS=Homo sapiens GN=MTPN PE=1 SV=2	0,598
Q92752	Tenascin-R OS=Homo sapiens GN=TNR PE=1 SV=3	0,596
P13645	Keratin, type I cytoskeletal 10 OS=Homo sapiens GN=KRT10 PE=1 SV=6	0,594
P20930	Filaggrin OS=Homo sapiens GN=FLG PE=1 SV=3	0,593
Q9BPU6	Dihydropyrimidinase-related protein 5 OS=Homo sapiens GN=DPYSL5 PE=1 SV=1	0,592
P62750	60S ribosomal protein L23a OS=Homo sapiens GN=RPL23A PE=1 SV=1	0,59
P51149	Ras-related protein Rab-7a OS=Homo sapiens GN=RAB7A PE=1 SV=1	0,588
Q9Y639	Neuroplastin OS=Homo sapiens GN=NPTN PE=1 SV=2	0,587
P02538	Keratin, type II cytoskeletal 6A OS=Homo sapiens GN=KRT6A PE=1 SV=3	0,586
O00330	Pyruvate dehydrogenase protein X component, mitochondrial OS=Homo sapiens GN=PDHX PE=1 SV=3	0,585
P50395	Rab GDP dissociation inhibitor beta OS=Homo sapiens GN=GDI2 PE=1 SV=2	0,579
P07910	Heterogeneous nuclear ribonucleoproteins C1/C2 OS=Homo sapiens GN=HNRNPC PE=1 SV=4	0,578
P21796	Voltage-dependent anion-selective channel protein 1 OS=Homo sapiens GN=VDAC1 PE=1 SV=2	0,575
E7EMK3	Isoform of Q14254, Flotillin-2 OS=Homo sapiens GN=FLOT2 PE=1 SV=1	0,575
P25705	ATP synthase subunit alpha, mitochondrial OS=Homo sapiens GN=ATP5A1 PE=1 SV=1	0,574
F5GYJ8	Isoform of Q96FW1, Ubiquitin thioesterase OTUB1 OS=Homo sapiens GN=OTUB1 PE=1 SV=1	0,57
P07437	Tubulin beta chain OS=Homo sapiens GN=TUBB PE=1 SV=2	0,569
P05388	60S acidic ribosomal protein P0 OS=Homo sapiens GN=RPLP0 PE=1 SV=1	0,569
P22676	Calretinin OS=Homo sapiens GN=CALB2 PE=2 SV=2	0,569
P07305	Histone H1.0 OS=Homo sapiens GN=H1F0 PE=1 SV=3	0,565
O76013	Keratin, type I cuticular Ha6 OS=Homo sapiens GN=KRT36 PE=2 SV=1	0,564
O75390	Citrate synthase, mitochondrial OS=Homo sapiens GN=CS PE=1 SV=2	0,563
Q9Y2T3	Guanine deaminase OS=Homo sapiens GN=GDA PE=1 SV=1	0,563
P04350	Tubulin beta-4A chain OS=Homo sapiens GN=TUBB4A PE=1 SV=2	0,562

P30153	Serine/threonine-protein phosphatase 2A 65 kDa regulatory subunit A alpha isoform OS=Homo sapier	0,561
Q7L0J3	Synaptic vesicle glycoprotein 2A OS=Homo sapiens GN=SV2A PE=1 SV=1	0,559
F8WF69	Isoform of P09496, Clathrin light chain A OS=Homo sapiens GN=CLTA PE=1 SV=1	0,559
H7BY58	Isoform of P22061, Protein-L-isoaspartate O-methyltransferase OS=Homo sapiens GN=PCMT1 PE=1 S'	0,559
Q04695	Keratin, type I cytoskeletal 17 OS=Homo sapiens GN=KRT17 PE=1 SV=2	0,555
P06702	Protein S100-A9 OS=Homo sapiens GN=S100A9 PE=1 SV=1	0,554
P05387	60S acidic ribosomal protein P2 OS=Homo sapiens GN=RPLP2 PE=1 SV=1	0,552
P28072	Proteasome subunit beta type-6 OS=Homo sapiens GN=PSMB6 PE=1 SV=4	0,55
A0A1C7CYX9	Dihydropyrimidinase-related protein 2 OS=Homo sapiens GN=DPYSL2 PE=1 SV=1	0,548
P31946	14-3-3 protein beta/alpha OS=Homo sapiens GN=YWHAB PE=1 SV=3	0,545
P46459	Vesicle-fusing ATPase OS=Homo sapiens GN=NSF PE=1 SV=3	0,544
Q9UPV7	PHD finger protein 24 OS=Homo sapiens GN=PHF24 PE=1 SV=2	0,539
A0A0B4J231	Isoform of B9A064, Immunoglobulin lambda-like polypeptide 5 OS=Homo sapiens GN=IGLL5 PE=1 SV=	0,531
P46821	Microtubule-associated protein 1B OS=Homo sapiens GN=MAP1B PE=1 SV=2	0,529
E7EPK1	Isoform of Q16181, Septin-7 OS=Homo sapiens GN=SEPT7 PE=1 SV=2	0,525
P09936	Ubiquitin carboxyl-terminal hydrolase isozyme L1 OS=Homo sapiens GN=UCHL1 PE=1 SV=2	0,525
P61266	Syntaxin-1B OS=Homo sapiens GN=STX1B PE=1 SV=1	0,52
P62701	40S ribosomal protein S4, X isoform OS=Homo sapiens GN=RPS4X PE=1 SV=2	0,52
P21281	V-type proton ATPase subunit B, brain isoform OS=Homo sapiens GN=ATP6V1B2 PE=1 SV=3	0,514
P17987	T-complex protein 1 subunit alpha OS=Homo sapiens GN=TCP1 PE=1 SV=1	0,512
P08779	Keratin, type I cytoskeletal 16 OS=Homo sapiens GN=KRT16 PE=1 SV=4	0,51
Q14194	Dihydropyrimidinase-related protein 1 OS=Homo sapiens GN=CRMP1 PE=1 SV=1	0,509
Q12860	Contactin-1 OS=Homo sapiens GN=CNTN1 PE=1 SV=1	0,503
P40926	Malate dehydrogenase, mitochondrial OS=Homo sapiens GN=MDH2 PE=1 SV=3	0,502
Q9NZT1	Calmodulin-like protein 5 OS=Homo sapiens GN=CALML5 PE=1 SV=2	0,501
P23396	40S ribosomal protein S3 OS=Homo sapiens GN=RPS3 PE=1 SV=2	0,501
P02533	Keratin, type I cytoskeletal 14 OS=Homo sapiens GN=KRT14 PE=1 SV=4	0,493
Q9BY11	Protein kinase C and casein kinase substrate in neurons protein 1 OS=Homo sapiens GN=PACSIN1 PE=	0,489
P11142	Heat shock cognate 71 kDa protein OS=Homo sapiens GN=HSPA8 PE=1 SV=1	0,487
Q16720	Plasma membrane calcium-transporting ATPase 3 OS=Homo sapiens GN=ATP2B3 PE=1 SV=3	0,483
P04264	Keratin, type II cytoskeletal 1 OS=Homo sapiens GN=KRT1 PE=1 SV=6	0,481
P31944	Caspase-14 OS=Homo sapiens GN=CASP14 PE=1 SV=2	0,48
P81605	Dermcidin OS=Homo sapiens GN=DCD PE=1 SV=2	0,479

P04075	Fructose-bisphosphate aldolase A OS=Homo sapiens GN=ALDOA PE=1 SV=2	0,478
P63104	14-3-3 protein zeta/delta OS=Homo sapiens GN=YWHAZ PE=1 SV=1	0,474
P04259	Keratin, type II cytoskeletal 6B OS=Homo sapiens GN=KRT6B PE=1 SV=5	0,473
A0A0A0MT26	Isoform of P13637, Sodium/potassium-transporting ATPase subunit alpha-3 OS=Homo sapiens GN=AT	0,472
P30101	Protein disulfide-isomerase A3 OS=Homo sapiens GN=PDIA3 PE=1 SV=4	0,472
P32119	Peroxiredoxin-2 OS=Homo sapiens GN=PRDX2 PE=1 SV=5	0,467
P14136	Glial fibrillary acidic protein OS=Homo sapiens GN=GFAP PE=1 SV=1	0,466
P13646	Keratin, type I cytoskeletal 13 OS=Homo sapiens GN=KRT13 PE=1 SV=4	0,461
P69905	Hemoglobin subunit alpha OS=Homo sapiens GN=HBA1 PE=1 SV=2	0,46
P68366	Tubulin alpha-4A chain OS=Homo sapiens GN=TUBA4A PE=1 SV=1	0,457
P27797	Calreticulin OS=Homo sapiens GN=CALR PE=1 SV=1	0,454
P35527	Keratin, type I cytoskeletal 9 OS=Homo sapiens GN=KRT9 PE=1 SV=3	0,452
D6RER5	Isoform of Q9NVA2, Septin-11 OS=Homo sapiens GN=SEPT11 PE=1 SV=1	0,452
P27348	14-3-3 protein theta OS=Homo sapiens GN=YWHAQ PE=1 SV=1	0,451
Q04917	14-3-3 protein eta OS=Homo sapiens GN=YWHAH PE=1 SV=4	0,45
Q14103	Heterogeneous nuclear ribonucleoprotein D0 OS=Homo sapiens GN=HNRNPD PE=1 SV=1	0,443
P20618	Proteasome subunit beta type-1 OS=Homo sapiens GN=PSMB1 PE=1 SV=2	0,441
P34932	Heat shock 70 kDa protein 4 OS=Homo sapiens GN=HSPA4 PE=1 SV=4	0,434
V9GZ17	Isoform of Q9NY65, Tubulin alpha-8 chain (Fragment) OS=Homo sapiens GN=TUBA8 PE=1 SV=1	0,431
P43004	Excitatory amino acid transporter 2 OS=Homo sapiens GN=SLC1A2 PE=1 SV=2	0,429
P61978	Heterogeneous nuclear ribonucleoprotein K OS=Homo sapiens GN=HNRNPK PE=1 SV=1	0,425
P47914	60S ribosomal protein L29 OS=Homo sapiens GN=RPL29 PE=1 SV=2	0,424
G3V5Z7	Isoform of P60900, Proteasome subunit alpha type OS=Homo sapiens GN=PSMA6 PE=1 SV=1	0,422
Q99436	Proteasome subunit beta type-7 OS=Homo sapiens GN=PSMB7 PE=1 SV=1	0,417
Q96JE9	Microtubule-associated protein 6 OS=Homo sapiens GN=MAP6 PE=1 SV=2	0,412
Q13825	Methylglutaconyl-CoA hydratase, mitochondrial OS=Homo sapiens GN=AUH PE=1 SV=1	0,406
P00918	Carbonic anhydrase 2 OS=Homo sapiens GN=CA2 PE=1 SV=2	0,403
P45880	Voltage-dependent anion-selective channel protein 2 OS=Homo sapiens GN=VDAC2 PE=1 SV=2	0,403
P54652	Heat shock-related 70 kDa protein 2 OS=Homo sapiens GN=HSPA2 PE=1 SV=1	0,403
Q9H3Z4	DnaJ homolog subfamily C member 5 OS=Homo sapiens GN=DNAJC5 PE=1 SV=1	0,399
P61313	60S ribosomal protein L15 OS=Homo sapiens GN=RPL15 PE=1 SV=2	0,396
Q96FJ2	Dynein light chain 2, cytoplasmic OS=Homo sapiens GN=DYNLL2 PE=1 SV=1	0,395
O14594	Neurocan core protein OS=Homo sapiens GN=NCAN PE=1 SV=3	0,38

P55087	Aquaporin-4 OS=Homo sapiens GN=AQP4 PE=1 SV=2	0,379
P68871	Hemoglobin subunit beta OS=Homo sapiens GN=HBB PE=1 SV=2	0,378
O75822	Eukaryotic translation initiation factor 3 subunit J OS=Homo sapiens GN=EIF3J PE=1 SV=2	0,375
A0A0D9SGF6	Isoform of Q13813, Spectrin alpha chain, non-erythrocytic 1 OS=Homo sapiens GN=SPTAN1 PE=1 SV=	0,371
Q96HN2	Adenosylhomocysteinase 3 OS=Homo sapiens GN=AHCYL2 PE=1 SV=1	0,367
P49721	Proteasome subunit beta type-2 OS=Homo sapiens GN=PSMB2 PE=1 SV=1	0,358
P36543	V-type proton ATPase subunit E 1 OS=Homo sapiens GN=ATP6V1E1 PE=1 SV=1	0,358
P46776	60S ribosomal protein L27a OS=Homo sapiens GN=RPL27A PE=1 SV=2	0,355
P36871	Phosphoglucomutase-1 OS=Homo sapiens GN=PGM1 PE=1 SV=3	0,353
A0A087WZQ7	Isoform of Q9H115, Beta-soluble NSF attachment protein OS=Homo sapiens GN=NAPB PE=1 SV=1	0,35
P21283	V-type proton ATPase subunit C 1 OS=Homo sapiens GN=ATP6V1C1 PE=1 SV=4	0,347
P15104	Glutamine synthetase OS=Homo sapiens GN=GLUL PE=1 SV=4	0,345
P04271	Protein S100-B OS=Homo sapiens GN=S100B PE=1 SV=2	0,344
P62942	Peptidyl-prolyl cis-trans isomerase FKBP1A OS=Homo sapiens GN=FKBP1A PE=1 SV=2	0,341
P78371	T-complex protein 1 subunit beta OS=Homo sapiens GN=CCT2 PE=1 SV=4	0,332
A0A087WUZ3	Spectrin beta chain OS=Homo sapiens GN=SPTBN1 PE=1 SV=1	0,326
Q93050	V-type proton ATPase 116 kDa subunit a isoform 1 OS=Homo sapiens GN=ATP6V0A1 PE=1 SV=3	0,314
O95670	V-type proton ATPase subunit G 2 OS=Homo sapiens GN=ATP6V1G2 PE=2 SV=1	0,313
P50993	Sodium/potassium-transporting ATPase subunit alpha-2 OS=Homo sapiens GN=ATP1A2 PE=1 SV=1	0,305
F5GYQ1	Isoform of P61421, V-type proton ATPase subunit d 1 OS=Homo sapiens GN=ATP6V0D1 PE=1 SV=1	0,304
H7BYR8	Isoform of P02686, Myelin basic protein OS=Homo sapiens GN=MBP PE=1 SV=1	0,299
P52209	6-phosphogluconate dehydrogenase, decarboxylating OS=Homo sapiens GN=PGD PE=1 SV=3	0,286
Q08380	Galectin-3-binding protein OS=Homo sapiens GN=LGALS3BP PE=1 SV=1	0,284
P02686	Myelin basic protein OS=Homo sapiens GN=MBP PE=1 SV=3	0,284
P80723	Brain acid soluble protein 1 OS=Homo sapiens GN=BASP1 PE=1 SV=2	0,271
P46976	Glycogenin-1 OS=Homo sapiens GN=GYG1 PE=1 SV=4	0,269
Q15907	Ras-related protein Rab-11B OS=Homo sapiens GN=RAB11B PE=1 SV=4	0,268
P05026	Sodium/potassium-transporting ATPase subunit beta-1 OS=Homo sapiens GN=ATP1B1 PE=1 SV=1	0,267
P62873	Guanine nucleotide-binding protein G(I)/G(S)/G(T) subunit beta-1 OS=Homo sapiens GN=GNB1 PE=1 S	0,267
H3BNQ7	Isoform of P80404, 4-aminobutyrate aminotransferase, mitochondrial OS=Homo sapiens GN=ABAT PE	0,266
P09543	2',3'-cyclic-nucleotide 3'-phosphodiesterase OS=Homo sapiens GN=CNP PE=1 SV=2	0,265
P30041	Peroxiredoxin-6 OS=Homo sapiens GN=PRDX6 PE=1 SV=3	0,263
E7EX88	Aggrecan core protein OS=Homo sapiens GN=ACAN PE=1 SV=2	0,257

Q96GW7	Brevican core protein OS=Homo sapiens GN=BCAN PE=1 SV=2	0,255
Q9Y2A7	Nck-associated protein 1 OS=Homo sapiens GN=NCKAP1 PE=1 SV=1	0,213
Q5D862	Filaggrin-2 OS=Homo sapiens GN=FLG2 PE=1 SV=1	0,209
Q9HCC0	Methylcrotonoyl-CoA carboxylase beta chain, mitochondrial OS=Homo sapiens GN=MCCC2 PE=1 SV=1	0,207
Q92747	Actin-related protein 2/3 complex subunit 1A OS=Homo sapiens GN=ARPC1A PE=1 SV=2	0,204
A0A0G2JHM8	Myelin-oligodendrocyte glycoprotein OS=Homo sapiens GN=MOG PE=1 SV=1	0,2
Q9GZV7	Hyaluronan and proteoglycan link protein 2 OS=Homo sapiens GN=HAPLN2 PE=2 SV=1	0,187
Q13404	Ubiquitin-conjugating enzyme E2 variant 1 OS=Homo sapiens GN=UBE2V1 PE=1 SV=2	0,178
P10915	Hyaluronan and proteoglycan link protein 1 OS=Homo sapiens GN=HAPLN1 PE=2 SV=2	0,155
H3BLU2	Limbic system-associated membrane protein (Fragment) OS=Homo sapiens GN=LSAMP PE=1 SV=1	0,15
P00441	Superoxide dismutase [Cu-Zn] OS=Homo sapiens GN=SOD1 PE=1 SV=2	0,146
P41222	Prostaglandin-H2 D-isomerase OS=Homo sapiens GN=PTGDS PE=1 SV=1	0,141
A0A075B6H6	Isoform of P01834, Ig kappa chain C region (Fragment) OS=Homo sapiens GN=IGKC PE=1 SV=1	0,125
P40306	Proteasome subunit beta type-10 OS=Homo sapiens GN=PSMB10 PE=1 SV=1	0,098
P00738	Haptoglobin OS=Homo sapiens GN=HP PE=1 SV=1	0,079
P13611	Versican core protein OS=Homo sapiens GN=VCAN PE=1 SV=3	0,075
A0A1B0GUU9	Isoform of P01871, Ig mu chain C region (Fragment) OS=Homo sapiens GN=IGHM PE=1 SV=1	0,06